ABSTRACT

Title of Document: DEVELOPMENT OF MECHANISTIC MODELS OF TRANSITION PERIODS BETWEEN LAG/EXPONENTIAL AND EXPONENTIAL/STATIONARY PHASES

Yangyang Wang, Doctor of Philosophy, 2016

Directed By: Professor, Robert L. Buchanan
Nutrition and Food Science Department, and
Director, Center for Food Safety and Security Systems

Nowadays, primary mathematical models are widely accepted as a tool for quantitative food microbiology. Such models are being used in conjunction with curve-fitting software to evaluate food-associated microbial growth. The three most commonly used models are Baranyi, Gompertz, and three-phase linear models. However, most of these models are not mechanistically-based and do not take into account the underlying physiological events. The ultimate goal of this study is to develop models that is more directly based on microbial physiological behavior and to better describe the transition periods of both lag/exponential and exponential/stationary phases.

In the study of lag/exponential transition, by using standard deviations from the trials, traditional smooth sigmoidal growth curve was obtainable through three-phase linear

model by Monte Carlo simulation. Moreover, by using nutritional-shift procedure, the time course of critical physiological events related to lactose metabolism were mapped.

While studying the transition period from exponential to stationary phase, both agitation rate and inoculum size were investigated for the potential impact of spatial nutrient depletion on the transition abruptness. While agitation rate had limited influence, inoculum size was proved to affect the shape of growth curve. Furthermore, combining the result of *rpoS* mRNA expression study, the time course of cell response to starvation was determined.

DEVELOPMENT OF MECHANISTIC MODELS OF TRANSITION PERIODS BETWEEN LAG/EXPONENTIAL AND EXPONENTIAL/STATIONARY PHASES

By

Yangyang Wang

Dissertation submitted to the Faculty of the Graduate School of the
University of Maryland, College Park, in partial fulfillment
of the requirements for the degree of
Doctor of Philosophy
2016

Advisory Committee:
Professor Robert L. Buchanan, Chair
Professor Jianghong Meng
Associate Professor Amy R. Sapkota
Assistant Professor Abani K Pradhan
Assistant Professor Shirley Micallef
Dr. Vijay K Juneja

© Copyright by
Yangyang Wang
2016

Acknowledgements

I would like to take this chance to express my appreciation to many people whoever helped me during this whole process. Without them, it won't be possible for me to complete my Ph.D. and also enjoy this wonderful journey.

My deepest gratitude goes to my advisor, Dr. Robert L. Buchanan. It was him who offered me an opportunity to pursue my dream in the U.S. I cannot express how grateful I am for all of his guidance, patience, encouragements, and supports through all these years. He helped me start my new career in food science area and also helped me build up my confidence in independent research. I would never forget the valuable knowledge and experiences he shared with me in both scientific area and wisdom of life. It is my great honor to have him as my research advisor in my life.

I would also like to express my sincere thanks to Dr. Vijay K Juneja, who accepted to serve on my committee and drove all the way down from Pennsylvania for my proposal meeting and defense. It is also my extreme pleasure to thank other members of my Ph.D. committee: Dr. Abani K Pradhan, Dr. Jianghong Meng, Dr. Shirley Micallef, and Dr. Amy R. Sapkota. Thanks for spending their precious time and sharing many insightful suggestions and critical comments with me.

I appreciate all the help and support I received from my amazing lab mates: Noelia, Ruth, Lucy, Asia, Mary, Mike, Ellen, and Kathleen. I would also like to acknowledge the support from the Department of Nutrition and Food Science faculty and staff.

Finally, and most importantly, I would like to thank my wonderful parents Changhua and Xiaoqin from the bottom of my heart. They are always there for me whenever and whatever. Their endless love and unconditional support made me strong enough

to overcome many difficulties. My appreciation also go to my parents-in-law for their understanding and support. Very special thanks to my wonderful husband Hao Pang, for all the things he did for me: cheer me up when I am depressed, help me out when I have doubts, and applause for me when I succeed. And I also thank my two lovely cats and also family members: Candy and Wukong. Their company is the best supports.

Table of Contents

List of Tables

List of Figures

Chapter 1: Introduction

1.1 Overview

Predictive microbiology has experienced great progress through the decades and it is now considered a sub-discipline of food microbiology (*111*). It greatly assists the implementation of HACCP (hazard analysis and critical control points) (*50*) and is a critical tool for the conduct of quantitative microbial risk assessment (QMRA) (*112*). A variety of predictive models have been developed to mathematically describe the behavior of microorganisms. Predictive microbiology models greatly assists with the hazard identification and safety plan formulation (*156*).

To build up a mathematical model, the first step is the identification of parameters that influence microbial behavior (e.g., growth, survival) in the system. Then an initial model structure is proposed which describes and predicts the possible effects of the parameters. The final step is to evaluate the effectiveness and validation by the actual experimental data and to improve the accuracy of the model (*5*, *162*).

Following these procedures, a number of models have been developed and widely applied nowadays, including primary, secondary, and tertiary models (*168*). To summarize, the primary models describe changes in microbial population with time; secondary models describe the changes of parameters in primary models under changing conditions; and the tertiary models are user-friendly software and expert systems. Some examples of primary models are the modified Gompertz model, Baranyi model, three-phase linear model, Huang model, logistic model, etc. It is usually very difficult to decide which model is more superior since they all have their own inherent limitations (*18*). The biggest and most common shortcoming is that the

models are empirical and do not take into account the physiological events underlying microbial behavior. This will be discussed in greater detail in the literature review. The lack of mechanistically-based models limits applications largely since interpolation and extrapolation of these models must be viewed with great caution.

Many researchers have attempted to overcome these inherent limitations by exploring means for incorporating physiological and molecular information in primary models (*143*, *161*, *164*). However, the predictive microbiology research still feels that mechanism-based modeling is critical to moving field to its next level of sophistication and utility. Despite the fact that understanding the bacterial growth curve is at the heart of all growth models, there is surprisingly little research focusing on modeling the physiological basis of the transition periods in classical growth curve, i.e., the lag phase to exponential phase transition and the exponential phase to stationary phase transition. Therefore, the overall goal of this research was to study aspects of both transition periods as a means to development of more mechanistically-based growth models based on an understanding of physiological and metabolic changes taking place during those transition periods.

1.2 Research Hypotheses

The major hypotheses of this research were:

- Lag to Exponential Phase Transition

1) The lag phase duration can be divided into two distinct components, namely, the adjustment period (t_a) and the metabolic period (t_m).
2) The curvilinear transition from lag phase to exponential phase represents the variability of t_a and t_m of individual bacterial cells.

- Exponential to Stationary Phase Transition

The transition from exponential to stationary phase primarily associated with spatial nutrient depletion where growth rates are increasingly dependent upon nutrient diffusion rates.

1.3 Study Approach

This study was conducted in four phases. The first phase focused on growth kinetics data collection during the lag phase and early exponential phase with a focus on measuring the variability in population behavior, and characterizing the impact of that variability through statistical analysis and simulation modeling. The second phase was characterizing that transition by monitoring selected enzyme activities to help define the timing of metabolic events during the lag to exponential transition. The third phase investigated the potential influence of nutrient diffusion rates during the transition from exponential to stationary phase. Lastly, the timing of mRNA expression for specific phase-dependent genes was studied to correlate the timing of gene expression with both the metabolic and phenotypic events observed during the first three phases of the study.

1.4 Potential Impact of Research

This study allows the development of more mechanistically-based primary model based on a better understanding of the transition periods between lag to exponential and exponential to stationary phases that take into account population variability and consideration of microenvironments surrounding individual cells. Further, it reinforces the concept that simple primary models such as three-phase linear model

which are based on microbial physiology can be augmented through inclusion of consideration of key microbiological physiology concepts.

Chapter 2: Literature Review

2.1 Microbial Growth: an Overview

2.1.1 Bacterial Growth

Individual Growth

In most prokaryotes and even some eukaryotes, the reproduction of individual cells occurs through an asexual process called “binary fission” (*33*). During binary fission, a parent cell divides into two separate daughter cells. If no mutational events take place, the parent cell and its daughter cells should be genetically identical.

Over 2000 chemical reactions are involved in this process. A complete cell cycle includes DNA replication, cell elongation, septum formation, formation of distinct walls, and eventually cell separation.

The time needed to complete a cell cycle varies depending on the type of microorganism and growth conditions. For instance, the average time for *Escherichia coli* to undergo a division is about 20 minutes under optimum environmental and nutritional conditions.

Population Growth

In addition to the replication of individual cells, the study of microbial growth kinetics must consider the growth and behavior of microbiological populations. During active growth, the total number of cells in the population doubles per unit of time during the exponential growth phase. The time it takes for a population to double is commonly referred to as the generation time. With generation time of 20 minutes, low contamination rates can become large populations in a relatively short period.

The mathematical relationship for exponential growth (*116*) is shown below in **Eq.1**:

$$N_t = N_o \times 2^n \quad (1)$$

Where: N_t is the cell number at time t; N_o is the initial cell number; n is the number of generations.

A logarithmic transformation is usually performed to make the calculation convenient and simple. In a semi-logarithmic graph, the number of cells is plotted on logarithmic scale [log (CFU/ml)], and time is presented arithmetically (h). This yields a linear relationship observed during exponential growth (*116*).

2.1.2 Growth Phases

When bacteria cells are inoculated into fresh medium and the growth is monitored over time, a typical growth curve can be obtained (**Figure 2.1**).

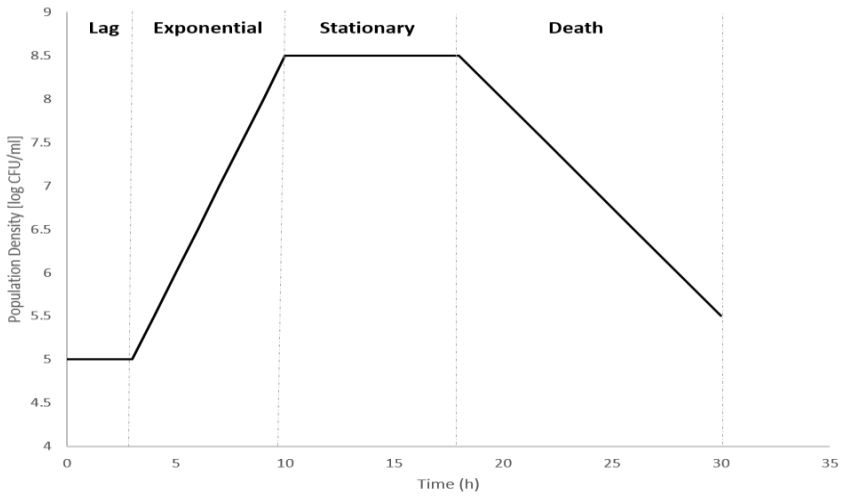

Figure 2.1 A classic growth curve for a bacterial population

This growth curve can be divided into four distinct phases: lag phase, exponential phase, stationary phase, and death phase.

Lag Phase

After inoculation, growth of bacteria cells generally does not begin immediately. A period without increase in population can be observed, and this period is referred to as the "lag phase". During lag phase, cells adapt to the new environment and prepare for the first division (*28*). The adaption includes a series of physiochemical changes in the cells such as the synthesis of critical enzymes and increasing metabolic activities. The length of lag phase duration is influenced by several factors, independently or synergistically. Depending on the previous culture history and environmental conditions, the length of lag phase varies from a few minutes to several hours or even days (*28*, *160*). More details will be covered in this chapter later. Generally speaking, the more drastic the shift is, the longer the expected lag phase.

Exponential (or log) Phase

As already mentioned before, the exponential phase displays a straight line if the growth curve is plotted on logarithmic scale. During exponential phase, cells divide at a constant rate which equals to the slope of the line. Similar to lag phase duration, the growth rate is mainly influenced by the type of microorganism and environmental conditions such as nutrient composition and incubation temperature.

Stationary Phase

The exponential growth cannot continue infinitely in a closed system. Ultimately the cells enter into the stationary phase. During this phase, the growth rate equals to the death rate, and no net increase of population is observed. The limiting factors could be either the depletion of essential nutrients or the accumulation of inhibitory waste. However, during this period, many cell functions still continue such as energy

metabolism and biosynthetic process (*125*). Typically, this process is controlled by specific regulatory genes and several complex global control mechanisms (*77*, *94*, *122*, *165*).

Death Phase

After the stationary phase, cells may enter into the death phase. During death phase, cell number decreases in an exponential manner. However, in most cases, the death rate is slower than the growth rate. In food microbiology, this period is often negligible as food at this point is seldom consumed due to unacceptable texture. Obvious exceptions are different types of fermented foods.

2.1.3 Factors Influence Microbial Growth

A variety of environmental conditions influence microbial growth, including both intrinsic (inherent to the food) and extrinsic (dependent of the environment in which the food is placed) factors. Understanding the effect and interactions among these factors is of great importance to the food industry since are often the basis for preventing or retarding the growth of target microorganisms. *Escherichia coli* is used as a major example of target microorganism in the following contents.

Intrinsic Factors

Intrinsic factors are those related to the food matrix itself, such as pH, water activity, redox potential, nutrient content, naturally occurring antimicrobials, and biological barriers.

1) pH

It has been well established that most organisms have a pH range within which growth is possible and an optimum pH at which the growth is maximal (*128*). For

instance, *E. coli* has a relatively wide pH range (from 4.4 to approximately 9.0) that can support growth, with optimum growth rates occurring at neutral pHs (6.5 to 7.5) (*134*). A number of studies have established the effect of pH on bacterial growth (*21*, *22*, *65*). Li et al. (*99*) demonstrated that the lag phase duration of *E. coli* O157:H7, as well as the standard deviations among the parallel trials, displayed a significant increase while the strains were exposed to mild acid stress. The underlying mechanism can be ascribed to the effect of pH on critical enzyme activities and transportation of essential nutrients.

2) Water Activity

Water activity (a_w) is another important factor affecting the growth of microorganisms in nature. One of the traditional methods of preserving food is by drying or desiccation which removes or binds available moisture. The minimum value of a_w for microbial growth differs depending on the type of microorganisms. In general, Gram-negative bacteria needs higher a_w than Gram-positive bacteria. A number of studies have confirmed the influence of a_w on bacterial growth kinetics including extending lag phase, decreasing growth rate and the maximum population density (*134*, *146*, *159*, *162*).

3) Redox Potential

Microorganisms have different degrees of sensitivity to the oxidation-reduction potential (O/R, Eh) in growth medium. Aerobic microorganisms require positive Eh while anaerobes need negative Eh for growth. When aerobic microorganism grows, Eh is decreased due to the depletion of oxygen. However, since the cells are able to

use oxygen-donating and hydrogen-accepting electrons in the medium, the growth is continued (*79*).

4) Nutrient Content

In order to grow and function normally, microorganisms need both carbon and nitrogen sources, specific minerals, and certain trace elements. Based on nutrient requirements, *E. coli* is classified as non-fastidious bacteria. In other words, it can grow on a wide variety of substrates. Li et al. (*99*) found considerable difference in lag phase duration among cells growing on glucose-free mineral medium (MOPS), Luria broth (LB) and tryptic soy broth (TSB).

Extrinsic Factors

Extrinsic factors refer to external environmental conditions including temperature, atmosphere, relative humidity, and competitive microorganisms.

1) Temperature

Similar as pH and water activity, temperature also have a range and an optimum value. Again take *E. coli* as an example, it can grow under a wide range of temperatures from 10^{o}C to 50^{o}C (*53*), with the optimum temperature for growth being 35^{o}C to 39^{o}C (*53*). Microorganisms are classified into three categories based on the temperatures under which they can grow: psychrophiles, mesophiles, and thermophiles. It has been widely accepted that temperature shifts play important roles in microbial growth kinetics (*55, 59, 74, 146*). As the temperature increases, both the chemical and enzymatic activities in the cells proceed much faster, resulting more rapid growth. However, when the temperature rises above a characteristic upper limit, key enzymes are denatured and growth ceases. At higher temperatures, proteins

become permanently denatured and biological structures such as cell membranes and ribosomes become damaged, the inactivation takes place (*36*).

2) Oxygen

Oxygen is another critical factor. Depending on the favorable concentration of oxygen, microorganisms fall into four groups: aerobes (require oxygen), anaerobes (require an absence of oxygen), facultative anaerobes (grow with or without oxygen), and microaerophile (require reduced levels of oxygen). *Escherichia coli* is a facultative anaerobe. While oxygen is present, aerobic respiration via the electron transport system will be the primary source of ATP. On the contrary, when oxygen is absent, facultative anaerobes shift to anaerobic metabolism. An exception is when preferred carbohydrate sources such as glucose are present. In this case the electron transport system is switched off and the cells rely on anaerobic metabolism. It is important to note that oxygen is poorly soluble in water (broth), and forced aeration may be required to maximize growth rates. It can be achieved either by agitation or continuous pumping of air.

2.1.4 Critical Growth Kinetics: Lag Phase Duration (λ)

Definition of Lag Phase

The history of lag phase can be traced back as early as 19th century, when Max Müller first noticed and proved the existence of lag phase (*120*). Later in 1914, Penfold (*172*) defined lag phase as the time interval between initial inoculation and the time point when cells reach the maximum growth rate. Monod (*116*) proposed that lag phase duration actually represented when a certain enzyme balance was achieved inside the cells, although the regulatory mechanism was not clear yet. The author also

mentioned the difficulties of determining the end of lag phase due to the sigmoidal shape of the growth curve. To solve this problem, Solberg and Nickerson (*157*) suggested to define lag phase as the time needed for a two-fold increase in population density. Nowadays, the most widely accepted definition of lag phase is derived from extrapolating the tangent at exponential phase to the initial population density at time zero (*160*), in other words, it is conveniently determined graphically. However, this is more based on mathematical method, not considering any underlying physiological or biochemical events that happened during the lag phase, which makes the current definition biologically questionable (*143*).

Quantifying Lag Phase

While dealing with food safety issues, one of the greatest challenges food microbiologists face is to confirm, identify, and quantify the microorganisms in food. One of the critical steps is to generate reliable data to describe the growth, survival, or inactivation of target microorganisms in food matrices. Many methods have been developed over the years, such as direct microscopic count, turbidity measurement, etc. Two prevailing techniques that are widely applied are the measurement based on absorbance or optical density (OD) and the traditional total viable counts based on colony forming units (CFU).

1) Absorbance (Optical density)

Based on Beer-Lambert law, the absorbance is proportional to the concentration of substances in the sample (*40*). Thus, it is reasonable to use OD measurements to represent the growth of microorganisms. One of the basic rules is to choose an

appropriate intensity of light scattering, namely, the wave length. For most growth studies, OD_{600} is used; however, OD_{540} is also widely employed.

2) Viable Counts

A conventional viable count method usually includes sampling, serial dilution, plating, incubation and enumeration. Either pour plating or surface plating methods are employed depending on the objective of the experiment and the nature of target microorganism. For example, by surface plating, not only the quantity but also the characteristics of microorganism can be determined. Surface plating is also preferential if the target microorganism is heat-sensitive to the point that it cannot tolerate the temperature of molten agar. With the development of newer technology, surface plating with a glass rod spreader is being replaced with automated spiral platers and electronic counters. These devices have improved the overall efficiency and accuracy of viable count methods.

Both the two aforementioned methods have been widely used in growth curve studies. However, they both have certain inherent limitations with applications. Compared to viable counts method, OD measurement is much more rapid and less labor-intensive. However, the major drawback of this method is the limited range of validity. According to Friedrich (*171*), the proportionality between OD and cell concentration only exists when $OD \leq 0.4$. Begot et al. (*19*) also similarly concluded that OD measurements produce misleading estimations of bacterial growth while the cell density $\geq 10^6$-10^7 bacteria/ml. Viable count method, on the other hand, is quite straightforward and accurate. However, its disadvantages are obvious: time-consuming and labor-intensive (*160*), and can be relatively expensive when one takes

into account the cost of the media and laboratory supplies needed. Usually, a substantial number of trials are necessary to obtain a relatively accurate estimation of growth kinetics. The reliability of growth kinetics studies is highly dependent on both the quantity and quality of the data (*18*, *24*, *132*). Studies on the transitions between growth phases typically require intense sampling before, during, and after the transition to achieve sufficient accuracy (*160*). While comparing the data obtained from the two methods, there always exist some discrepancies on lag time estimates. In some studies, it is found that lag time derived from OD measurement is constantly shorter than that from viable counts (*42*, *75*). One of the possible explanations might be the increase in cell sizes during lag phase (*75*). In general, viable counts method is more accurate and reliable than the OD measurement, especially when the culture enters into late exponential and stationary phases. However, Augustin et al. (*7*) also proposed the possibility to combine both the OD value and some viable data to obtain accurate estimates of growth kinetics.

3) Individual cell lag phase

The methods mentioned above are based on population level, however, in order to better understand the behavior of bacterial cells, lag time measurement of individual cells is also required (*133*). Many techniques have been developed with each has its own advantages and limitations. Some examples are Bioscreen® (*110*), direct microscopy (*174*), flow chamber, and flow cytometry (*155*).

Factors that Influence Lag Phase Duration

Typically, lag phase is induced by the change in the environment. The bacterial cells are first cultured in pre-culturing conditions: <ENV1>. Then at certain time point,

they are transferred to the post-incubation environment: <ENV2>. A delayed increase of microbial population can be anticipated since the cells need time to complete the modification and adapt to the new environment and reinitiate the growth again (*27*). Both past and present environments have influences on the length of lag phase duration. Generally speaking, the more drastic the change is, the longer the expected lag phase.

1) Temperature

Temperature is one of the most important factors that control the growth and survival of microorganisms. Numerous studies have been conducted to investigate the influence of temperature on growth kinetics. Despite differences in the objectives, these studies all concluded that temperature shifts play a critical role in lag phase duration (*1*, *54*, *55*, *142*).

The influence of temperature shift was evaluated for both the direction and intensity. For instance, Buchanan and Klawitter (*27*) pointed out that when *E. coli* O157:H7 cells were transferred from higher incubation temperature to a lower incubation temperature, the lag phase would have a marked increase. This conclusion is consistent with other studies using different bacterial strains (*1*, *113*). In general, within certain range, a negative temperature shift would always result in a longer lag phase duration compared to positive temperature shift, while the absolute difference is equivalent. This is partly because gene transcription and translation proceed more rapidly in higher temperatures. The magnitude of the shift also affects the degree of the response. Using *Aeromonas hydrophila*, Hudson (*74*) concluded that when the

pre- and post-incubation temperatures remained stable, the lag phase was minimum or could be ignored.

2) Type of medium

While the cells are transferred from one medium to a different medium, it is common to observe a prolonged lag phase. For instance, in order to investigate the effect of environmental stresses on individual cell lag time of *E. coli* O157:H7, Li et al. (*99*) designed a series of experiments to obtain starving cells by transferring cells that were previously cultured at optimum environment to poorer medium, including glucose-free mineral medium (MOPS), Luria Broth (LB), and tryptic soy broth (TSB). They found significant increase in both lag time and its standard deviations. The underlying mechanism is apparent. Most bacterial can grow on a variety of substrates. To take advantage of these substrates, the development and formation of specific enzymes is always necessary before the growth taking place (*116*). So during the lag time, the cells will synthesize new enzymes to utilize the new nutrients. One of studies in the current work was designed based on this concept and will be discussed in greater detail later.

3) Age of the inoculum

The effect of age (or stage, alternatively) of the inoculum has been investigated by several researchers. Similar experimental designs were employed: bacterial cells were first grown to different growth stages and then transferred to comparable conditions. A demonstration was made that exponentially grown cells have negligible lag phases, while the stationary phase cells showed extended lag phases (*170*). This phenomena is due to the depletion of essential constituents of cells and relatively lower metabolic

rates at stationary phase. Besides, exponentially grown cells seem to adapt to environmental changes more rapidly (*160*).

4) Inoculum size

The effect of inoculum size has been extensively investigated in numerous studies, most of which focused on the growth/no growth boundaries under stressed conditions. For example, Robinson et al. (*141*) observed an increasing variance of lag phase distributions of *Listeria monocytogenes* with increasing inoculum size under osmic stress. Equivalent results were reported by other scientists that the "power" of prevention from unfavorable conditions vary with inoculum size (*6*, *62*, *91*). This can be explained by the increasing variability of individual cells among a larger population (*6*). However, it seems that a critical threshold may exist. For small inoculum sizes, the influence is more apparent, while for large inoculum size, the effect is minimal (*116*).

2.1.5 Critical Growth Kinetics: Growth Rate (μ)

Definition and Calculation of Growth Rate

As mentioned before, if the microbial growth curve is plotted on a semi-logarithmic scale, then the exponential phase displays a straight line. Accordingly, the slope of this line is defined as the specific growth rate, abbreviated μ, means the increase of population per unit time.

$$\mu = \frac{logN_t - logN_o}{t} \quad (2)$$

Here t is the time elapse (h), and the unit of μ is log (CFU/ml)·h^{-1}. This is based on the assumption that during exponential phase, the growth rate remains stable and can be described by a constant (*116*). Alternative assumption proposed that other than a

constant, μ is increasing gradually from zero to its maximum. More details will be discussed in later this chapter.

Another critical metric in describing microbial growth is generation time (GT). It measures the time interval (h) between each division, which can be defined as below in **Eq.3** (*171*):

$$GT = \frac{t}{n} = \frac{t \times log2}{logN - logN_o} = \frac{0.301}{\mu} \quad (3)$$

Occasionally, the mean growth rate, *k*, is also described. This term represents the number of generations per unit time (h^{-1}).

Factors that Influence Growth Rate

While considering the exponential phase as a relatively steady state, the specific growth rate is controlled by a variety of factors (*7*, *42*, *114*). Similar to lag phase duration, nutrients, temperature, pH, oxygen, and other environmental conditions are all proven to have significant influences on the growth rate (*54*, *55*, *90*, *99*). Secondary models are developed to better estimate these effects (*46*). More details will be discussed in the next section.

2.1.6 Critical Growth Kinetics: Maximum Population Density (N_{max})

The maximum population density (N_{MAX}) is another critical kinetics in describing the shape of growth curve. During the growth of microorganisms, the metabolic activities of bacterial cells modified composition of medium in which they grow. On one hand, essential nutrients are depleted; on the other hand, metabolite products are generated including toxic compounds or organic acids which may lower the pH. All of these changes result in a decreased or complete cessation of growth. Eventually the cells enter into stationary phase. N_{MAX} is a critical parameter that represents the

characteristic of stationary phase and it reflects the whole capacity of the growth medium (*116*).

2.2 Predictive Microbiology

2.2.1 Brief Introduction of Predictive Microbiology

Food microbiology is now in a transition from being primarily qualitative to increasingly quantitative science. As mentioned before, the traditional methods for estimating the microbial growth in food are not only time consuming, but also labor intensive and expensive. Thus, there is an urgent need of novel approaches for providing accurate estimates of the behavior of target microorganisms in a timely manner (*9*). With the combined efforts of food scientists, engineers, and applied mathematicians, predictive microbiology is increasingly becoming a means for addressing these needs.

Predictive microbiology describes the behavior of microorganism under certain environmental conditions using mathematical models. Its history can be traced back to the early 1920s, with Esty and Meyer first use of a log-linear model to describe the thermal death rate of *Clostridium botulinum* (*51*). It was further advanced by Scott (*136*), who investigated the inactivation of microorganisms during thermal processing, and introduced "z-value" concepts. During the last three decades, this field of research has expanded greatly and significant progress has been made. A variety of models have been developed and applied to benefit food industries. This includes growth models, survival models, inactivation model, competition model, growth/no-growth models, etc. It is also the foundation on which quantitative microbiological risk assessment was built.

Early predictive microbiology started with empirical use of mathematical models without considering the underlying physiological factors that determine the behavior of the microorganisms. However, there has been long term goal to move to mechanistic models. It is of great importance to provide a sound scientific basis to make these models more convincible, reliable, and flexible (*13*, *112*).

The whole modeling system can be divided into three levels (*168*). To summarize, the primary models describe changes in microbial population with time under a single set of environmental conditions; secondary models describe the changes in the parameters of primary models that are needed to describe the effect of changes in the environmental conditions; and the last but not least, tertiary models are user-friendly software and expert systems that allow the primary and secondary models to be applied in food industries, government agencies, and research institutions.

2.2.2 Primary Models

Primary models are a set of time-dependent equations that describe the microbial population levels under specific environmental conditions (*112*, *147*, *169*). A number of mathematical models have been developed to describe the sigmoidal growth curve of microorganisms, including both linear and non-linear equations, such as Baranyi model, Gompertz model, three-phase linear model, logistic model, etc. Despite the diverse terms and parameters the various models employ to represent the growth kinetics, a typical growth curve usually contains a lag phase, an exponential phase, and a stationary phase. It is always difficult to decide which model is more superior without a defined situation. Parameters assessing the goodness-of-fit are used to evaluate and compare the effectiveness of different models, including root mean

square (RMS), bias factor (B), and accuracy factor (A) (*11*, *28*, *42*). Currently, the three most commonly used primary models are Baranyi model, modified Gompertz model, and the three-phase linear model, more details will be discussed below.

Baranyi model

Understanding the advantages and disadvantages of specific model requires understanding the reasoning process upon which the models is based.

Baranyi et al. (*10*) defined several new terms while developing their growth model. Their interactions are shown below in **Eq.4** and **Eq.5**

$$\alpha(t) = \frac{1+q(t)}{q(t)} \quad (4)$$

$$h(0) = -\ln\alpha(0) = \ln(1 + \frac{1}{q(0)}) = \mu_{max} \times \lambda \quad (5)$$

Where: α(0) is defined as adjustment function, related to the proportion of the specific growth rate; q(0) indicates the physiological state of the cells at inoculation point, which is determined by the pre-culturing history and the growth stage of the cells (*9*). After logarithmic transformation, the relationship between maximum growth rate (μ_{max}) and lag phase duration (λ) is shown in **Eq.5**. Given that the physiological states of the cells at inoculation point are all identical (h(0) is a constant), it is possible to calculate either μ_{max} or λ when one the other is known since they are inversely proportional.

As a means of interpreting α(t), Baranyi and Roberts (*9*) hypothesized that bacterial growth is controlled by a critical substance P(t). However, they failed to figure out what the critical substance could be, which made the definition of P(t) vague to some extent, not to mention bring up a method to directly measure it. Thus, since q(0) is defined a posteriori, it can only be determined by fitting procedure (*160*). This is a

huge disadvantage of the Baranyi model. Moreover, the results of some other experiments raised doubts about q(0) being a constant. For instance, when investigating the influence of temperature shifts on lag phase duration, Mellefont and Ross (*113*) revealed that the assumption of q(0) being a constant was only valid when cells were transferred from a lower temperature to a higher temperature. Alavi et al. (*1*) reported similar results in 1999.

The most commonly used form of Baranyi model is described as:

$$y_t = y_0 + \mu_{max} \times A(t) - \frac{1}{m} \times ln(1 + \frac{e^{m \times \mu_{max} \times A(t)} - 1}{e^{m \times (y_{max} - y_0)}}) \quad (6)$$

$$A(t) = t + \frac{1}{\nu} \times \ln(\frac{e^{\nu t} + q_0}{1 + q_0}) \quad (7)$$

$$\lambda = \frac{\ln(1 + \frac{1}{q_0})}{\nu} \quad (8)$$

where y_0 is the initial population density at inoculation point [ln (CFU/g)]; y_{max} is the maximum population density [ln (CFU/g)]; μ_{max} is the maximum growth rate [ln (CFU/g)·h^{-1}]; q_0 is the initial physiological state of the cell; ν is the curvature parameter that indicates the transition period from lag to exponential phase, here equals μ_{max}; m is the curvature parameter which describe the transition from exponential to stationary phase, usually defined as 1 if assuming the incubation environment <ENV2> is stable. λ is obtained by the value at the intersection of the tangent to the growth curve to the initial population density. Vadasz (*161*) commented it as a "arbitrary geometrical convenience without any biological significance".

Gompertz and modified Gompertz model

Gompertz model, named after Benjamin Gompertz, is a mathematical function for a time series. It has been widely used in many areas including data uptake, demography, and tumor research. Unlike Baranyi and three-phase linear model, Gompertz model is a purely empirical sigmoidal relationship.

The original function was adapted by Gibson et al. in 1988 (*59*).

$$y_t = y_0 + Ce^{-e^{-b(t-M)}} \quad (9)$$

Where: y_t is the population density at time t [ln (CFU/g)], y_0 is the initial population density [ln (CFU/g)]; C equals to the net increase of population density; b is the relative growth rate [ln (CFU/g)·h^{-1}]; and M represents the time when it reaches the maximum growth rate (h). This equation contains mathematical parameters that do not have direct biological meaning. Additional terms were proposed to make it more microbiologically relevant:

$$Maximum\ growth\ rate\ (\mu) = \frac{bC}{e} \quad (10)$$

$$Generation\ time\ (GT) = \log(2)\frac{e}{bC} \quad (11)$$

$$Lag\ phase\ duration\ (\lambda) = M - \frac{1}{b} \quad (12)$$

Zwietering et al. (*176*) further re-modified this equation into a 3-parameter function, **Eq.13**, which is the most commonly used form nowadays:

$$y_t = y_0 + Ae^{-e^{\left(\frac{\mu_m \times e}{A}\right)(\lambda - t)+1}} \quad (13)$$

Where: A is the population density at stationary phase [ln (CFU/g)]; μ_m is the maximum growth rate [ln (CFU/g)·h^{-1}]; and λ is the lag phase duration (h). Here, μ_m is defined as the tangent to the growth curve at the inflection and λ is derived from the intercept of the tangent at the inflection point with the horizontal line of y_0.

Three-phase linear model

Buchanan et al. (*28*) proposed the three-phase linear model in 1997 to describe microbial growth. According to their hypothesis, the growth curve is divided into three phases based on the exponential growth rate:

1) The lag phase: when the cells are transferred and trying to adapt to the new environment and preparing for the first division. At this period, the exponential growth rate μ equals to zero.

2) The exponential phase: when the cells initiate growth, the growth rate is assumed to be a constant, μ=k. After logarithmic transformation, the exponential phase displays as a straight line.

3) The stationary phase: the cells reach the maximum population density and the growth rate is equal to the death rate, so the net increase equals to zero. During this period, the growth rate μ=0.

This model is described by the equation below (**Eq.14**):

$$\begin{cases} t < t_{LAG}, N_t = N_o \\ t_{LAG} < t < t_{MAX}, N_t = N_o + \mu \times (t - t_{LAG}) \\ t > t_{MAX}, N_t = N_{MAX} \end{cases} \quad (14)$$

Where: N_o, N_t, N_{MAX} represent the population density at time 0, time t, and stationary phase, respectively [log (CFU/ml)]; t_{LAG} (h) is the lag phase duration; t_{MAX} (h) is the time point when the maximum population density is reached; and μ is the exponential growth rate [log (CFU/g)·h^{-1}].

Using the example of *E. coli* growth on both glucose and lactose, they further proposed that the lag phase could be separated into two distinct portions, namely adjustment time (t_a) and generation (metabolite) time (t_m) (*28*).

$$t_{LAG} = t_a + t_m \quad (15)$$

t_a is the time interval when the cells sense the need and alter their physiological status correspondingly to adapt to and take advantage of the new environment. Similar to the definition of "adjustment function", which was proposed by Baranyi and Roberts in 1994 (*12*), t_a depends on the cell's culturing history as well as its overall metabolic rate. Generally, the more intense the change is, the longer the expected adjustment period.

t_m, on the other hand, is the metabolic time. During this period, cells are generating energy and synthesizing critical cellular components, and getting ready for the first division. To re-initiate growth, cells need to overcome an activation energy barrier (*26*). Any slight changes in environment may have either positive or negative influence on t_m. For example, when temperature is above the optimum growth temperature, more energy is required to repair the cell damage, which induces a longer t_m; similarly, the addition of acid will result in a relatively longer t_m since it would cost extra energy to maintain appropriate pH gradient within the cells.

Other than the discontinuous step function in three-phase linear model, a curvilinear segment during the transition period from lag to exponential phase is always observed. This discrepancy has been interpreted by several scientists in early 90s, claiming that this was caused by the gradual increasing of the specific growth rate (*9*, *29*). The three-phase linear model alternatively hypothesized the sigmoidal shape of the lag to exponential phase transition reflected the biological variance among the population. Based on this assumption, if the variance is small, then an abrupt transition should be expected, vice versa.

In general, the three-phase linear model takes into account of the physiological behavior of bacterial cells. Moreover, it combines both the individual-based and population level concepts together in a reconciled way (*28*).

2.2.3 Secondary Models

The microbial growth is influenced by a variety of extrinsic and intrinsic factors. A number of studies have been conducted to evaluate the impacts of these factors on the characteristics of microbial growth (*54*, *55*, *90*, *99*), with emphasis on incubation temperature, water activity, and pH. Mathematical models were generated to describe the correlations between growth kinetics and these factors. These models are referred to as secondary models, which predict the changing trends of primary models under different environmental conditions.

The most famous secondary model is the "square root" model, which was proposed by Ratkowsky et al. in 1982, to model the relationship between the specific growth rate and incubation temperatures (*138*), shown as below (**Eq.16**):

$$\sqrt{\mu} = b \times (T - T_{min}) \quad (16)$$

Where: μ stands for specific growth rate; T is temperature (^{o}C); b is fitting parameter (the slope); and T_{min} is the theoretical temperature at which bacterial will not grow, obtained by extrapolating the line to zero. This model is simple in format and can be applied in various situations. The biggest limitation here is that the equation is only valid when the temperature is below the optimum value. Similar functions have also been developed considering other critical environmental factors such as water activity and pH.

All of the above examples describe the mathematical relationships between the growth rate and a single environmental factor, based on the assumption that all the other variables are identical. However, it is usually not the case. The actual situation is far more complex, requires a function that can combine all the factors and to evaluate the overall effects. Based on the relevance among the factors, the secondary models can be further divided into two sub categories: one is called Gamma function (*146*), assuming all the factors are independent of each other; the other is response surface model (also called polynomial model), applied to reconcile all the variables (*21*).

2.2.4 Tertiary Models

Tertiary models refer to those user-friendly software that can be applied to predict the microbial behavior under certain environmental conditions. Widely used software nowadays include Combase Predictor (www.combase.cc) and USDA issued Pathogen Modeling Program (PMP) (http://pmp.errc.ars.usda.gov). They both cover a variety of models, i.e., they are not only limited to growth models, but also include inactivation and survival models.

All in all, significant progress and great achievements have been made over the years in predictive microbiology. Its incorporation with food microbiology benefits the whole food system and makes the predictions much more convenient. It can be applied in diverse areas, such as shelf life determination. However, as discussed before, some of the models are empirical, i.e., without a sound physiological or biological basis, which brings into question their reliability, particularly when extrapolating beyond the limits of their data set. The current models should be further

developed and improved to include more microbial associated behaviors, in other words, to be more mechanistic.

2.2.5 Application of Predictive Microbiology in Dealing with Food Safety Issues

Mathematical models are generated by culturing cells under certain environmental conditions, following the bacterial growth for a period of time, and then fitting the collected data to appropriate mathematical equations (*34*). With large quantity of experimental data, a database can be set up to make effective predictions about the growth behavior of target microorganisms. Compared to traditional culture method, which is time-consuming, costly, and labor intensive, this relatively new discipline is a lot more convenient and accurate.

Over the past few decades, predictive microbiology benefitted the practice of food microbiology in many areas (*34*). The earliest application example can be traced back to thermal inactivation process, where the thermal death curve (TDT) was widely used. It is also vital for the implementation of hazard analysis critical control point (HACCP) procedures in food industries (*156*). Moreover, predictive models can be used to predict the bacteria levels across the farm to fork continuum of certain food products, if knowing the way they are processed and the storage conditions. Thus it can provide reliable information for exposure assessment in microbial risk assessment (*34*).

2.3 Metabolic Pathways and Regulatory Mechanism

2.3.1 Physiological Events Related With the Growth Phases

<u>The Lag Phase</u>

During lag phase, cells adapt to new environment and start to take advantage of new nutrients (*28*). Although the exact mechanism has not been clearly elucidated, it was assumed that the process includes the repair of cell damage (*47*) and the synthesis of necessary enzymes and components required for cell growth.

The Exponential Phase

It was confirmed (*116*) that the duration of exponential phase was related with several factors including the total nutrient capacity that the medium can support growth. If the cells are grown in a medium that contains a sole carbon source, the exponential phase is assumed to be a steady state, which is characterized by a constant growth rate. However, if the culturing medium consists of a mixture of carbon sources, then a phenomena called "diauxie" is observed (*116*). In this kind of growth, the exponential phase can be divided into two distinct cycles, usually with different growth rates. *Escherichia coli* has been extensively studied on the carbohydrate uptake for many years (*167*). When both glucose and lactose are present, the cells always utilize glucose first since glucose is the preferred carbon source. After glucose is exhausted, growth shows a plateau during which cells synthesize essential enzymes needed to take advantage of the second sugar, after which the cells start the second growth cycle using lactose as the primary energy source.

The Stationary Phase

Bacterial cells cannot grow infinitely since ultimately the concentration of essential nutrients is decreasing until exhausted, and the modification of the culturing environment by factors such as the accumulation of metabolic waste or depression of the pH (*116*). When the cells reach the maximum population density that the medium

can support, they enter into the stationary phase. During this period, considerable changes take place (*88, 153*), influencing both the physiology and morphology of the cells, such as membrane alteration, DNA coiling, stress-resistance, etc. Surprisingly, although overall the population growth process ceased, many cell functions still continue such as energy metabolism and biosynthetic processes (*125*). This includes some degree of individual cell replication. It was recently found that a constant protein synthesis extended a long period even during stationary phase (*57*). It is well documented that there are a variety changes in cells metabolic systems as they enter the stationary phase. These new metabolic functions are often referred to as secondary metabolism.

2.3.2 Metabolic Pathway

The term metabolism refer to all the biochemical processes taking place in the cell, including both anabolism (biosynthesis) and catabolism. During this process, microorganisms metabolize nutrients (such as sugar, amino acids, and fatty acids), release energy (usually stored in ATP) and generate waste products. Cells need energy and metabolic "building blocks" generated by its catabolic pathway to support homeostasis, active transport, motility, and its various biosynthetic and related anabolic activities.

Glycolysis

Glucose is the most common carbohydrate that can be used by most microorganisms. Glycolysis is the primary pathway for the catabolism of glucose to ATP and pyruvate. The metabolism of disaccharides is more complicated since it also includes other

pathways to first digest disaccharide into monosaccharides. One example is shown as below in **Figure 2.2**:

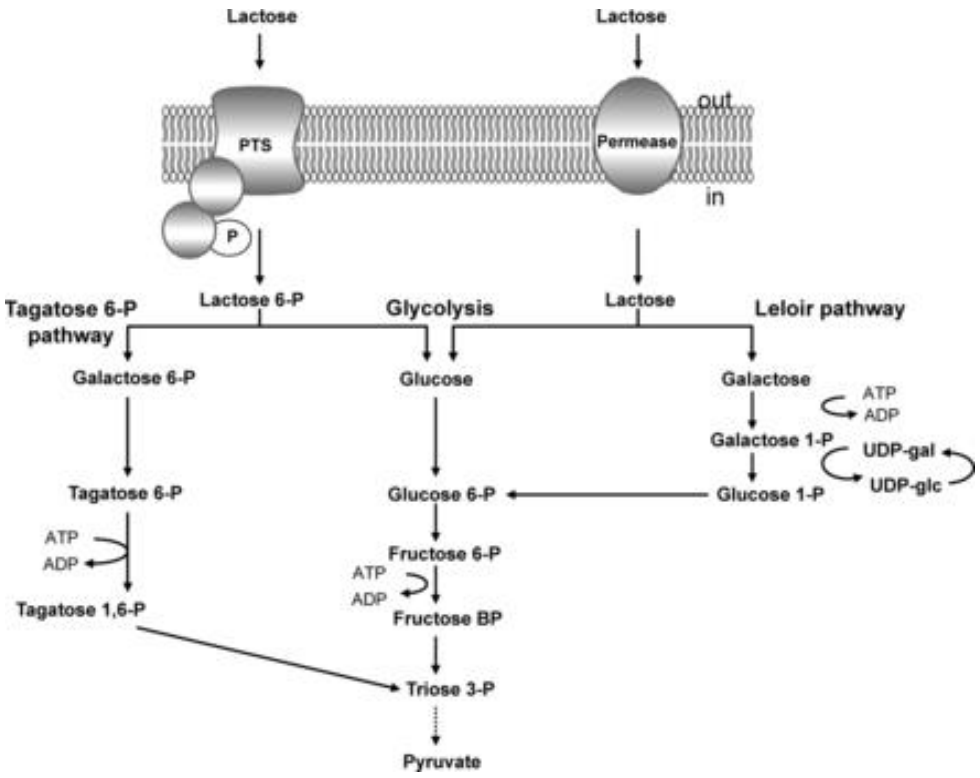

Figure 2.2 Alternative pathways for lactose transport and metabolism (*158*).

Aerobic Respiration and Anaerobic Fermentation

The post-glycolysis process can be divided into two groups depending on whether the oxygen is present or absent. The whole reaction is simplified as shown in **Figure 2.3**.

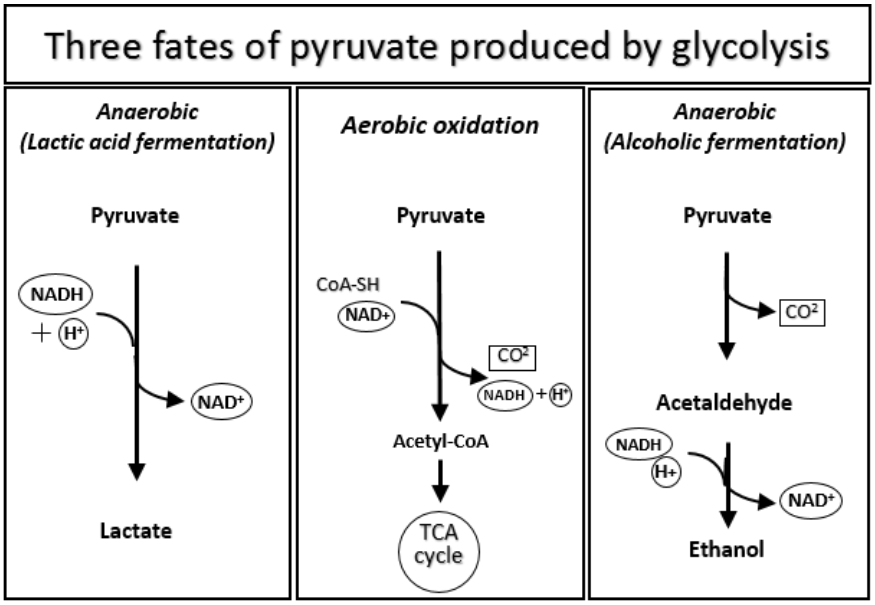

Figure 2.3 Aerobic and anaerobic (fermentative) metabolism of pyruvate

While oxygen is present, pyruvate from glycolysis is converted to acetyl-CoA and CO_2 by pyruvate dehydrogenase. The acetyl-CoA enters into the citric acid cycle (TCA), where it undergoes stepwise decarboxylation yielding CO_2, H_2O, NADH, and $FADH_2$. The energy captured in the NADH and $FADH_2$ is converted to ATP by the electron transport chain using oxygen as the acceptor (*140*, *144*).

When oxygen is absent, the pyruvate will switch to fermentative metabolism instead. Either lactic acid or ethanol is synthesized as the final products. During anaerobic metabolism, only a fraction of the ATP generated per molecule of glucose compared to that released via aerobic metabolism (*140*, *144*).

2.3.3 The lac operon

Escherichia coli has been extensively used to study metabolic mechanisms through the years. Much of our knowledge of intermediary metabolism was originally elucidated in *E. coli* and other enteric bacteria. One of the key areas studied initially in *E. coli* was the physiological and genetic basis for how metabolic pathways are

turned on or off, thereby enabling the cell to adapt to changing environments (*98*). One of the most intensely studied has been how *E. coli* regulates its ability to metabolize lactose. The ability of *E. coli* to utilize lactose is an inducible capability that is only active when lactose is present. The regulatory controls involve the inducible expression of the well-known *lac* operon model, which was first proposed by Jacob and Monod in 1961. This was considered a break-through study that set the stage for a broad understanding of cellular regulation in all microorganisms (*78*). Although half the century passed, this model remains one of the classic studies in metabolic regulations.

Structure and Function

According to Jacob and Monod (*78*), the *lac* operon functions as a coordinated unit. The system consists of three structural genes and a control region containing a promoter and an operator. The three structural genes, *lacZ, lacY*, and *lacA*, encode β-galactosidase, β-galactosidase permease and thiogalactoside transacetylase, respectively. β-galactosidase is a 500kd tetramer, serves as an intracellular enzyme that cleaves lactose into glucose and galactose. β-galactosidase permease is required for active transport of the substrate such as lactose into cells. Thiogalactoside transacetylase transfers the acetyl group from acetyl-CoA to β-galactosidase. However, this is not necessary for lactose catabolism. In addition to that, another gene (regulatory gene) called *lacI* encode the repressor protein located at the upstream of the operon (*78, 96*). The structure of *lac* operon is illustrated as below:

Figure 2.4 Structure of *lac* operon
[Image source from http://en.wikipedia.org/wiki/Image:Lac_operon1.png] (*3*)

Regulatory Mechanism

Based on the availability of carbon source, the regulatory mechanism of *lac* operon can be discussed in three conditions:

1) Glucose as the sole carbon source (glucose +; lactose -)

When no lactose is available, it would be metabolically inefficient to produce lactase, i.e., a waste of cell's energy. Thus a specific mechanism has evolved to suppress the synthesis of lactase and to completely shut down the pathway. First, the regulatory gene *lacI* produces the repressor protein, which binds tightly to the operator, so the binding of RNA polymerase to the promotor is blocked. The gene is completely turned off, no enzymes are produced under this situation (*173*).

2) When both glucose and lactose are present (glucose +; lactose +)

When both glucose and lactose are present in the medium, a phenomenon named diauxie (*116*) can be expected. Catabolite repression is taking place during the first growth phase, allowing the cells to utilize more preferable carbon source only, i.e., glucose. This is achieved by repression of synthesis of lactase, which is essential in lactose digestion (*84*). The repression is caused by two control mechanisms. The first control mechanism is related to catabolite activator protein (CAP) and cyclic adenosine monophosphate (cAMP), which have been proved to significantly increase the efficiency of binding between RNA polymerase and promotor. In the presence of

glucose, however, the concentration of cAMP is low, the production of CAP is inactivated. Although there is no obstacle on the operator, without the aid of CAP-cAMP, the RNA polymerase is still not able to bind to the promotor (*166*). Thus the production of enzyme is minimal. The second control mechanism is achieved by $EIIA^{glc}$ which shuts down the production of β-galactosidase permease resulting in the unsuccessful transportation of lactose (*30, 64, 107*). However, when glucose is depleted, the bacteria will start the second phase by metabolizing the alternative nutrients (lactose). Between the two phases, a delay or plateau can be observed, representing the time needed for adaption (*98*).

3) Lactose as the sole carbon source (glucose -; lactose +)

On the contrary, if there is an ample supply of lactose and it serves as the only carbon source, allosteric control will take in charge. On the one hand, lactose molecule (also referred to as allolactose or inducer) will bind to the repressor protein, occupying the active binding site, so the repressor protein will no longer blocking the transcription. On the other hand, the CAP-cAMP dimer will significantly facilitate the binding of RNA polymerase to the promotor. Without any obstacles on the pathway, *lac* genes are transcribed, β-galactosidase, β-galactosidase permease and thiogalactoside transacetylase are produced to hydrolyze lactose (*22, 30, 78, 85*).

2.3.4 The rpoS Gene

Sigma Factors

Sigma factors are a series of proteins that aid the binding of RNA polymerase to specific promoters thus initiate mRNA transcription (*76, 94*). They can be activated in response to harsh or stressed environmental conditions such as heat or osmotic shock,

oxidative stress, starvation, acid, etc. (*45*). The number of sigma factors may vary in different bacteria strains. *Escherichia coli* has seven recognized sigma factors, distinguished by their molecular weights (*66*). They are highly specific, each factor only corresponds to one specific environmental signal (*122*). Details are summarized in **Table 2.1**.

Table 2.1 Sigma factors and their functions

Symbol	Name	Function
σ^{70} (RpoD)	Housekeeping	Transcribe essential genes
σ^{19} (FecI)	Ferric citrate	Regulate iron transportation
σ^{24} (RpoE)	Extra cytoplasmic	Respond to extreme heat
σ^{28} (RpoF)	Flagella	Synthesize flagella
σ^{32} (RpoH)	Heat shock	Respond to heat treatment / DNA-repair related
σ^{38} (RpoS)	Stationary phase	Respond to starvation (nutrient depletion)
σ^{54} (RpoN)	Nitrogen-limitation	Nitrogen metabolism motility

The *rpoS*

The gene *rpoS*, short for RNA polymerase, sigma S, encodes for stationary phase related protein σ^{38} (RpoS) (*94*). *rpoS* was first discovered in 1984 (*102*), however, its function in stationary phase regulation has not been recognized until 1993 (*70*). Mulvey and Loewen (*121*) found that the nucleotide sequence of the product of this gene is highly homologous to the family of sigma factors, especially related to σ^{70}. Thus the protein was designated as σ^{S}, and the gene encodes it is called *rpoS*. A number of studies have confirmed that while *rpoS* is being transcribed in late exponential phase, a significant increase of RpoS occurs during the entry into

stationary phase and plays a critical role in response to multiple stimulus in environment including acid or osmotic stress, heat shock, nutrient depletion, etc.

Regulatory Mechanism

The *rpoS* gene might be transcribed since late exponential phase, however, a significant increase of the RpoS concentration can only be detected at the onset of stationary phase (*93*). The cellular level of RpoS is controlled through several regulatory mechanisms at different levels including transcription, translation, and protein stability (degradation and activity) (*101*). The whole regulatory system is very complex and many details remain to be elucidated.

1) Transcriptional control

One of the most important factors that controls the transcription is the promoter of *rpoS*, named *rpoS*p (*95*). This promoter has two cAMP-CRP (cyclic AMP-cAMP receptor protein) binding sites with undetermined controlling mechanism(s). While investigating the role of cAMP-CRP on transcription of *rpoS*, contradictory data were observed. The existence of both activating and inhibitory effects indicate the potential presence of dual function of these binding sites (*93*, *94*, *109*). The unanswered question is how the cell selects the "right" (appropriate) binding site at different stages.

Other modulators that are related to *rpoS* transcription include: ppGpp (guanosine-bispyrophosphate) which has been confirmed to play a positive role during starvation (*37*, *58*); BarA which promotes porin synthesis via OmpR activation; and inorganic polyphosphate which regulatory mechanism is still uncertain (*152*).

2) Translational control

RpoS synthesis is controlled by a series of sRNAs (small noncoding RNA) (*65*), including but not limited to: DsrA, a temperature-related sRNA that inhibits the promoter recognition at higher temperatures while increases at lower temperatures (*154*); RprA, induces RpoS synthesis via RcsC while encounter surface stress (*105*); OxyS, influences the translation level in response to oxidative shock (*2*).

Additional proteins are also involved in these processes to form a complex global network to regulate the translation of *rpoS*. One example is Hfq, a RNA-binding protein (*25*). It has been confirmed to up-regulate *rpoS* translation via the activation of both DsrA and RprA (*25*, *119*). Another assumption related to Hfq is that it may promote the disruption of secondary structure of *rpoS* mRNA, thus initiate the translation (*101*). On the contrary, HN-S, a histone-like protein, was demonstrated to be associated with a decrease of translation. However, the inhibitory mechanism remains obscure (*16*, *101*, *175*). Similarly, the LysR-like protein, LeuO, inhibits the RpoS synthesis by repressing the production of DsrA (*86*).

To conclude, the overall regulation at the translational level is fulfilled by coordination of all the modulators mentioned above. Furthermore, many of the control mechanisms are still unknown and more details must be included to get a thorough understanding.

3) RpoS stability

Another level of regulation occurs through RpoS degradation (*122*) with the help of an essential protease named ClpXP (*151*). The Clp is composed of ClpP and an ATPase, along with two regulatory subunits, namely ClpA and ClpX (*32*, *139*). A few other factors have also been discovered and confirmed to regulate RpoS degradation.

For example, the response regulator RssB can either aid the ClpXP proteolysis or increase RpoS sensitivity, which eventually results in RpoS degradation (*118*). A similar factor, RssA, was found but its mechanism is still uncertain. Another critical factor here is DnaK, which has been proved to enhance the stability of RpoS and protect it from degradation (*117*). Since RssB and DnaK play antagonistic roles in mediating RpoS degradation, a specific balance should exist (*101*).

RpoS-dependent Genes

RpoS is a central regulator that controls the expression of a large number of genes in both stress conditions and stationary phase (*101*). More than 400 genes have been identified as RpoS-dependent genes and this number has been increasing over the years (*45, 101*). These genes belong to diverse categories based on their functions including stress resistance, cell morphology, metabolism, etc.

A number of genes which are under control of RpoS are involved in resistance mechanisms to environmental stresses such as osmotic shock, oxidative stress, DNA damage, etc. For example, *otsB* and *otsA* are both associated with the production of trehalose which is involved in osmo-protection (*83*). Likewise, the resistance in response to excessive hydrogen peroxide molecules need a synergistic effect of several genes, includes: *katG* and *katE*, encode catalase HPI and HPII, respectively (*149*); *dps*, encodes a DNA-binding protein which might protect the DNA from attack (*70*). *xthA* is another critical gene that encodes the exonuclease III, participate in both DNA repair and H_2O_2 removal (*102*). The *osm* family, containing *osmB*, *osmE*, and *osmY*, are mainly involved in alteration of cell membrane permeability, with *osmB* encoding an outer lipoprotein, *osmE* affecting lipoprotein function, and *osmY*

encoding periplasmic protein (*39*, *68*). Other factors related to cell morphology include *bolA* and *fts* family (*95*). When cells enter stationary phase or are under starvation conditions, glycogen synthesis starts to take place, preparing to take advantage of alternative carbon sources (*70*). Both RpoS-dependent and independent genes are involved in this process, mainly belongs to *glg* family (*145*). *glgS* is an RpoS-dependent gene which experience a significant increase of expression level while entering into stationary phase (*67*).

To conclude, the regulatory mechanisms associated with *rpoS* is achieved at transcriptional, translational, and post-translational levels. RpoS acts as a central regulator that affects the expression of a large number of genes involved in stress-resistance and onset of stationary. Recently, researchers have also paid attention to exponential phase-expressed genes. These studies show that RpoS may also play an important role in the regulation of certain genes expressed during exponential phase (*45*).

Chapter 3: Research Objectives

The ultimate goal of this research was to develop a model that is more directly based on the physiological behavior of the microorganism by better describing the transition periods of lag to exponential and exponential to stationary phases. The specific objectives were:

1) To test the hypothesis that the curvilinear transition from lag to exponential phase represents the variability of cells in adjustment and metabolic periods.
2) To test the hypothesis that the lag phase can be subdivided into two separate periods (t_a and t_m) by measuring the activity of induced enzyme.
3) To investigate the potential influence of nutrient diffusion rate on the transition from exponential phase to stationary phase by changing agitation rates and inoculum size.
4) To study the correlation between specific gene mRNA expression levels and the onset and end point of the exponential growth phase.

Chapter 4: Transition from Lag Phase to Exponential Phase

4.1 Background

When cells are grown initially in one environment <ENV1> and then transferred to a different environment <ENV2>, the culture will experience a lag phase (*160*). For example, if the cells are shifted from a peptone-based medium to lactose-containing medium, a lag phase is induced because the utilization of the new carbon source requires induction of a catabolic enzyme (*28*). This is called "nutritional-shift" procedure. Based on this concept, Buchanan et al. (*28*) proposed that the lag phase can be divided into two separate segments, adjustment period (t_a) when cells synthesize new enzymes and metabolic period (t_m) when cells prepare for the first division. Various factors have been confirmed to affect lag phase duration include pH, temperature, age and size of the inoculum, and nutrient content in the medium (*6*, *48*, *54*, *113*). To investigate the influence of a single factor on lag phase duration, all the other undesirable interventions should be eliminated, in other words, should remain identical by strict control.

If the growth of an individual cell is followed, a discontinuous step function appears instead of the traditional sigmoidal curve. The curvilinear transition between lag and exponential phase was interpreted as the gradual increase of growth rate from zero to maximum (*9*, *29*). When Buchanan et al. (*28*) developed the three-phase linear model, an alternative explanation was proposed, i.e., the curvilinear portion represented the population variability in adjustment (t_a) and metabolic (t_m) periods (thus the variability in lag phase duration, since $t_{LAG} = t_a + t_m$). If that is the case, then the

traditional sigmoidal curve with smooth transition should be obtainable through three-phase linear model by Monte Carlo simulation using standard deviations among trials. The experiment strain we used throughout the study was *E. coli* K-12, a non-pathogenic *E. coli* which has been frequently used and well-studied in modern biotechnology and microbiology (*97*). It is also the first organism to have its DNA sequenced, with the complete genome published in 1997 (*22*).

4.2 Study Objectives

The major objective of this experiment was to test the hypothesis that the curvilinear transition from lag to exponential phase represents the variability of cells in t_a and t_m periods. The specific objectives were:

1) To estimate growth kinetics: lag phase duration (t_{LAG}) and exponential growth rate (μ);
2) To use standard deviations from the trials and Monte Carlo simulation method to describe the smooth lag/exponential transition;
3) To investigate the temperature dependency of the growth kinetics;
4) To use t_{LAG} and μ to estimate t_a and t_m.

4.3 Materials & Methods

In this experiment, *E. coli* K-12 cells were grown in brain heart infusion (BHI) broth (BD/Difco Laboratories, Sparks, MD) to early stationary phase and transferred to two liquid media: tryptic soy broth without dextrose (T-G) and tryptic soy broth without dextrose but 0.5% w/v lactose (T-G+L) (BD/Difco Laboratories, Sparks, MD). Cells were cultured on low speed orbital shaker (Corning, MA, USA) at 15^{o}C – 40^{o}C incubators until mid-exponential phase. Samples were taken at designated time

intervals and growth was measured both by optical density at 550 nm and viable count method. The flow chart of this experiment is shown in **Figure 4.1**.

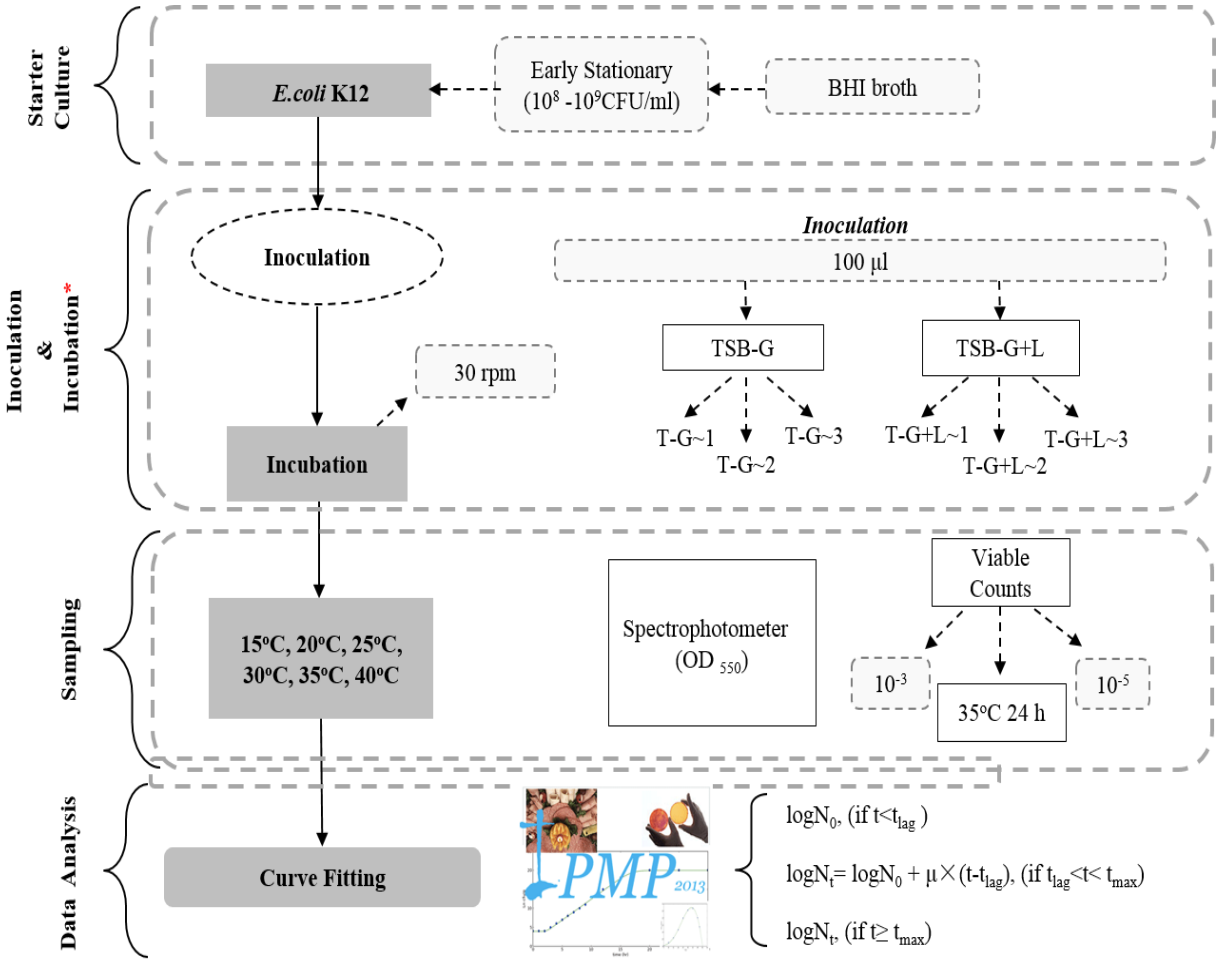

Figure 4.1 Flow diagram of sampling plan for nutritional-shift procedure

4.3.1 Preparation of Starter Culture

Bacterial Strain Used

The bacterial strain used in this study is *Escherichia coli* K-12 (ATCC 23716), obtained from the culture collection in microbiology lab at University of Maryland,

College Park. The strain was stored frozen (-80^{o}C) in BHI broth supplemented with glycerol (20% v/v) as long-term stock culture.

Preparation of Inoculum

The frozen culture was activated by streaking a loopful of thawed culture on freshly prepared brain heart infusion agar plate (BHIA, BD/Difco Laboratories, Sparks, MD) and incubating at 37^{o}C for 24 h. The working culture was kept in 4^{o}C refrigerator as a short-term preservation and renewed every other week. A single colony from the stock plate was picked and grown in 10 ml of sterile BHI broth and incubated at 37^{o}C for 24 h. A second subculture was prepared by transferring a loopful of the first culture into a new portion of 10 ml BHI broth and pre-adapting the cells 24 h at the temperature into which the cells would be transferred during the nutritional shift studies. These cell suspensions served as the starter inoculum for the growth kinetics experiments. The final population density of the early stationary cells was approximately $10^{8} – 10^{9}$ CFU/ml.

4.3.2 Inoculation & Incubation

Inoculation

Two media broth were used in this experiment: tryptic soy broth without dextrose (TSB-G, BD/Difco Laboratories, Sparks, MD) and TSB broth without dextrose supplemented with 0.5% w/v lactose (TSB-G+L, BD/Difco Laboratories, Sparks, MD). Both media were prepared and autoclaved at 121^{o}C for 15 min and then distributed to a set of three sterile 250 ml Erlenmeyer flasks each containing 100 ml broth. 100 µl of the starter culture was transferred to each flask homogeneously by gently mixing.

Incubation

The inoculated cultures were incubated on a low speed orbital shaker (Corning, MA, USA) with a speed of 30 rpm at 35^{o}C incubator for designated time periods. Same procedures were followed for a total of six temperatures: 15^{o}C, 20^{o}C, 25^{o}C, 30^{o}C. 35^{o}C, and 40^{o}C (±0.5^{o}C).

4.3.3 Sampling

Sampling

Immediately after inoculation, 5 ml of the culture from each flask was saved as the 0 h sample (2 ml for optical density measurement, 1 ml for viable counts method, and the remaining 2 ml for lactase activity assay which stored in -20^{o}C freezer until analyzed). Samples were taken at specified time intervals, with extensive sampling during the lag phase and a few points during the exponential phase. The sampling times were determined by incubation temperatures since previous studies showed that higher temperatures induced shorter lag phase (*7*, *27*).

Optical Density

2 ml sample was transferred to a disposable cuvette and the absorbance (ABS) at 550 nm was measured by GENESYS^{TM} 20 Visible Spectrophotometer (Thermo Scientific, 4001/000, USA) using uninoculated TSB-G and TSB-G+L as blanks. All absorbance measurements were recorded in Excel sheets and were logarithm transformed to calculate OD values.

Viable Count

Viable count method was used to determine cell levels in the samples. During sampling, 1 ml sample was transferred into a sterile 9.0 ml dilution blank of 0.1%

peptone water (0.1% PW, BD/Difco Laboratories, Sparks, MD) to generate a 10^{-1} dilution. 10^{-3} and 10^{-5} dilutions were further obtained by transferring 0.1 ml of the previous dilutions into new 9.9 ml 0.1% PW blanks. After serial dilution, a small volume (50 µl) of both 10^{-3} and 10^{-5} dilutions were plated onto pre-hardened tryptic soy agar plates (TSA, BD/Difco Laboratories, Sparks, MD) using Eddy Jet 2 Spiral Plater (Neutec Group. Inc, Farmingdale, NY). All the plates were cultured inverted in 35ºC incubator for 24 h. Enumeration was conducted using Flash & Go automatic plate counter (Neutec Group. Inc, Farmingdale, NY). Both dilutions (10^{-3} and 10^{-5}) were checked for reliability and appropriate data were chosen for growth study. All the results were recorded in Excel sheets and logarithmic transformation (base-10) was performed.

Repeated Trials

At least two trials of experiments were conducted for each temperature following exactly the same procedures. For each single trial, three replicates were conducted simultaneously.

4.3.4 Data Analysis

Standard curve construction

It is widely accepted that there is a proportional correlation between ABS and bacterial concentration (*7*, *15*, *41*, *43*) which can be described using a two-phase linear equation:

$$y = \begin{cases} y_o & , \ x < x_o \\ y_o + k(x + 3 - x_o), & x \geq x_o \end{cases} \quad (17)$$

In **Eq.17**, y_o is the intercept represents the initial population density [log (CFU/ml)]; x_o is absorbance readings during the lag phase when no significant increase of cell

number is observed [log (ABS)]; and *k* is the regression coefficient; also numerical value 3 (equals to log 0.001) is added in the equation to shift the entire plot to the positive side. Previous studies (*75*) showed that incubation temperature as well as culturing medium might influence the size of bacterial cells. Since spectrophotometer is to measure the light scattering on small particles (cell), different cell sizes might result in inconsistent ABS readings while the number of cells remains the same. To eliminate the potential influences of temperature and culturing medium on the relationship between ABS and concentration, data sets were fitted to Eq.17 separately under different culturing conditions. The resulting equations from fitting were used as standard curves to calculate *E. coli* K-12 counts based on ABS readings for further analyses.

Primary Model

Microbial counts from both optical density method and viable count method were logarithmic transformed (base-10) (log CFU/ml) and were used in model fitting. To take into account the variability within replicates and trials under same temperature, data from each replicate was fitted separately by primary model. Either two-phase (without stationary phase) or three-phase linear model (*28*) was used to describe growth curves and to estimate critical growth kinetics such as exponential growth rate (μ) and lag phase duration (t_{LAG}). The model is described in chapter 2 in **Eq.14**:

$$\begin{cases} t < t_{LAG}, N_t = N_o \\ t_{LAG} < t < t_{MAX}, N_t = N_o + \mu \times (t - t_{LAG}) \\ t > t_{MAX}, N_t = N_{MAX} \end{cases} \quad (14)$$

where N_o, N_t, N_{MAX} represent the population density at time 0, time t, and stationary phase, respectively [log CFU/ml]; t_{LAG} (h) is the lag phase duration; t_{MAX} (h) is the

time point when the maximum population density is reached; and μ is the exponential growth rate [log CFU/ml·h^{-1}].

Secondary Models

To evaluate the effect of temperature on the growth of *E. coli* K-12, the exponential growth rates (μ) under different temperatures were fitted using both modified Ratkowsky (contains the full temperature range) square root model and Cardinal parameter model.

Modified Ratkowsky square root model (*137*):

$$\sqrt{r} = a(T - T_o)\{1 - exp[b(T - T_{max})]\} \quad (18)$$

In **Eq.18**, r is the growth rate [ln CFU/ml·h^{-1}]; a and b are regression coefficients; T_o is the notional minimum temperature and T_{max} represents the maximum temperature (°C).

Cardinal parameter model (*148*):

$$\mu_{max} = \frac{\mu_{opt}(T-T_{max})(T-T_{min})^2}{[(T_{opt}-T_{min})(T-T_{opt})-(T_{opt}-T_{max})(T_{opt}+T_{min}-2T)](T_{opt}-T_{min})} \quad (19)$$

In **Eq.19**, μ_{opt} is the optimum growth rate [ln CFU/ml·h^{-1}]; T_{min}, T_{opt}, and T_{max} are the estimated minimum, optimum, and maximum growth temperatures (°C), respectively.

Monte Carlo Simulation

Parameter estimates were entered into an Excel (2011) spreadsheet. Initial population density N_o and maximum population density N_{MAX} were defined as fixed values, 6.0 log CFU/ml and 9.0 log CFU/ml, respectively. t_{LAG} and μ were defined using truncated normal distributions with mean and standard deviation. @Risk 6.0 Professional Edition (Palisade Corporation, Newfield, New York, USA) was used to perform Monte Carlo simulations of 30 iterations.

Estimate t_a and t_m

Metabolic periods (t_m), also referred to as the generation time (GT), was calculated through μ by **Eq.3**:

$$GT = \frac{t}{n} = \frac{t \times log2}{logN - logN_0} = \frac{0.301}{\mu} \quad (3)$$

Adjustment period (t_a) was determined by re-arranging **Eq.15** and solving for t_a:

$$t_{LAG} = t_a + t_m \quad (15)$$

Curve-fitting and Statistical Analysis

All the curve-fitting of primary and secondary models were conducted using USDA Integrated Pathogen Modeling Program 2013 (IPMP, USDA, Wyndmoor, PA) based on least-square method. Growth kinetics (μ and t_{LAG}) generated from curve-fitting of primary model for each growth condition were summarized and were used to calculate the means and standard deviations. Analysis of Variance (ANOVA) was performed for μ and t_{LAG} to determine the effect of different growth conditions (temperature and culturing media). Tukey's HSD test was used to compare the difference of t_{LAG} under different growth conditions. Student's t tests were performed to compare the results obtained from optical density method and viable count method. A P - value ≤ 0.05 was considered to be statistically significant. All the statistical analyses were performed in JMP® Pro 10 (SAS Institute, Cary, NC).

4.4 Results

4.4.1 Growth Kinetics Estimated from Absorbance Data

Figure 4.2 shows an example of standard curve for cells cultured in T-G at 20°C. Parameters of standard curves under different temperatures and media are listed in **Table 4.1**, standard errors were calculated account for different sample sizes.

Escherichia coli K-12 counts calculated from these standard curves were fitted using either two-phase (without stationary phase) or three-phase linear model. The fitting result is shown below (**Table 4.2**).

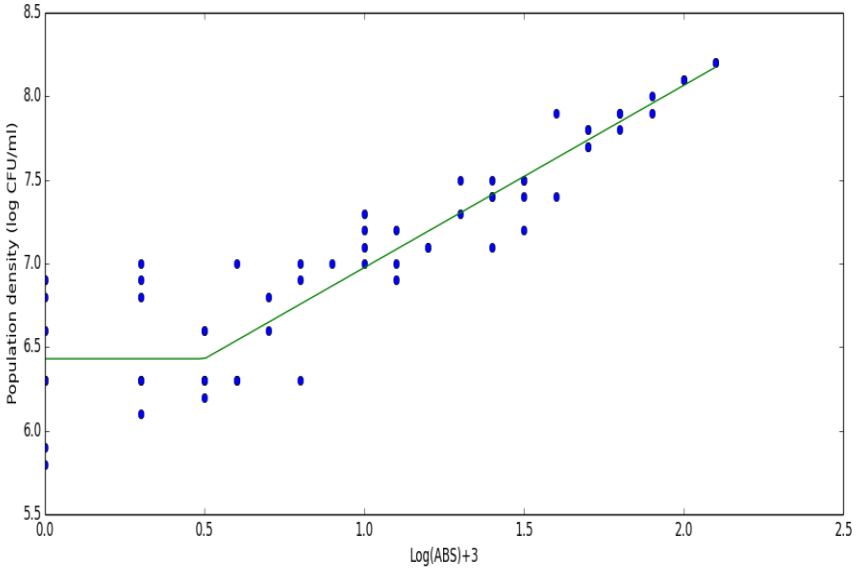

Figure 4.2 Standard curve of absorbance data conversion for cells cultured in T-G at 20°C.

Table 4.1 Parameters for standard curves of ABS and viable count conversion under different temperatures and media.

Temperature (°C)	**Parameters**					
	T-G			T-G+L		
	y_0	k	x_0	y_0	k	x_0
15	6.19[a] (0.06)[b]	1.09 (0.08)	0.35 (0.08)	6.30 (0.04)	1.10 (0.06)	0.34 (0.06)
20	6.43 (0.05)	1.09 (0.08)	0.50 (0.08)	6.30 (0.05)	1.10 (0.07)	0.37 (0.08)
25	6.38 (0.05)	0.96 (0.01)	0.55 (0.09)	6.34 (0.04)	1.02 (0.06)	0.44 (0.06)
30	6.38 (0.04)	1.31 (0.05)	0.85 (0.05)	6.30 (0.04)	1.25 (0.05)	0.69 (0.05)
35	6.38 (0.16)	1.64 (0.25)	1.29 (0.17)	6.43 (0.10)	1.46 (0.17)	1.13 (0.13)
40	6.39 (0.08)	1.79 (0.12)	1.40 (0.07)	6.45 (0.05)	1.21 (0.08)	0.82 (0.09)

[a] Estimate value
[b] Standard error

Table 4.2 Growth kinetics of *E. coli* K-12 grown in T-G and T-G+L medium at different temperatures (Absorbance data).

Temperature (ºC)	Parameters			
	T-G		T-G+L	
	$\mu(ABS)$ (log CFU/ml·h^{-1})	$t_{LAG}(ABS)$ (h)	$\mu(ABS)$ (log CFU/ml·h^{-1})	$t_{LAG}(ABS)$ (h)
15	0.09 ± 0.01[a]	6.13 ± 1.21	0.08 ± 0.01	6.81 ± 1.50
20	0.30 ± 0.07	3.75 ± 2.12	0.31 ± 0.13	4.17 ± 1.74
25	0.36 ± 0.05	1.80 ± 0.28	0.45 ± 0.10	2.05 ± 0.24
30	0.54 ± 0.02	1.76 ± 0.27	0.51 ± 0.03	1.52 ± 0.60
35	0.64 ± 0.08	1.59 ± 0.25	0.65 ± 0.06	1.80 ± 0.32
40	0.96 ± 0.15	1.49 ± 0.51	1.01 ± 0.30	1.53 ± 0.19

[a] Means and standard deviations are shown

4.4.2 Growth Kinetics Estimated from Viable Count Data

Figure 4.3 shows the growth curve of *E. coli* K-12 at 25ºC as an example. From the figure, at 25ºC, *E. coli* K-12 grown on both T-G and T-G+L medium fit the two-phase linear model well with the RMSE (root mean square error) of 0.058 and 0.032, respectively. **Table 4.3** reports all the fitting results with means and standard deviations shown.

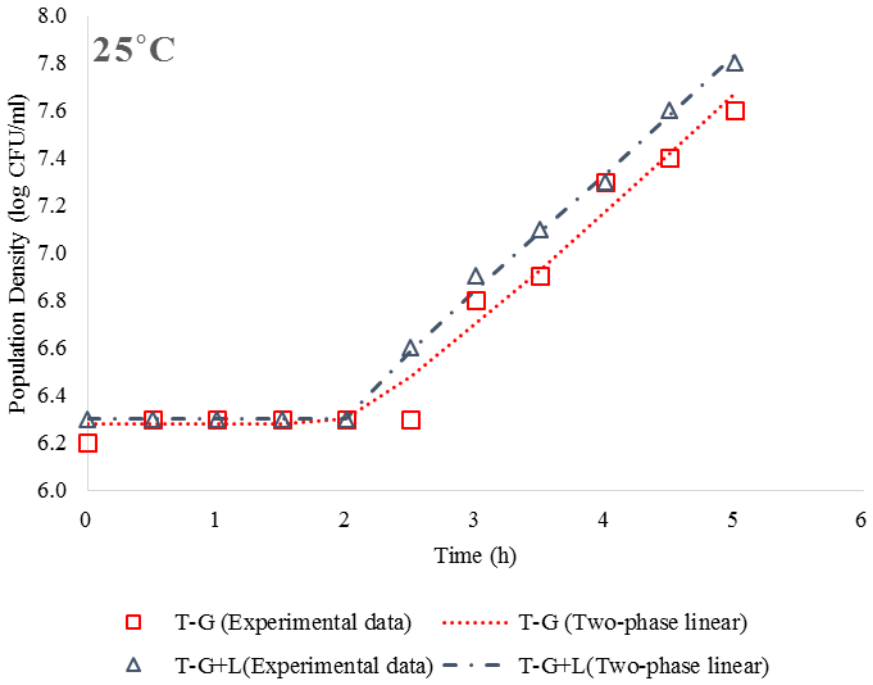

Figure 4.3 Growth of *E. coli* K-12 at 25ºC (T-G: TSB without dextrose; T-G+L: TSB without dextrose but 0.5% lactose). Symbols represent experimental data and dotted lines correspond to the fit of two-phase linear growth model.

Table 4.3 Growth kinetics of *E. coli* K-12 grown in T-G and T-G+L medium at different temperatures (Viable count data)

Temperature (ºC)	**Parameters**			
	T-G		T-G+L	
	$\mu(VC)$ (log CFU/ml·h^{-1})	$t_{LAG}(VC)$ (h)	$\mu(VC)$ (log CFU/ml·h^{-1})	$t_{LAG}(VC)$ (h)
15	0.09 ± 0.02	9.08 ± 3.42	0.10 ± 0.06	6.74 ± 2.25
20	0.23 ± 0.04	2.38 ± 1.27	0.22 ± 0.05	2.58 ± 0.68
25	0.43 ± 0.04	1.46 ± 0.40	0.41 ± 0.10	1.59 ± 0.49
30	0.58 ± 0.12	1.71 ± 0.57	0.54 ± 0.10	1.37 ± 0.50
35	0.71 ± 0.12	1.48 ± 0.65	0.70 ± 0.10	1.56 ± 0.47
40	0.75 ± 0.10	1.04 ± 0.32	0.77 ± 0.09	1.28 ± 0.31

[a] Means and standard deviations are shown

Comparison of growth kinetics obtained from absorbance and viable count data

Figure 4.4 shows the comparison of μ and t_{LAG} estimated using optical density method and viable count method. For μ, significant differences were observed between methods in T-G medium at 20, 25, and 40°C, with *P* value of 0.0415, 0.0146, and 0.0192, respectively; in T-G+L medium, only at 40°C, the difference was significant ($P = 0.0451$).

For t_{LAG}, no significant differences between these two methods in T-G medium at all temperatures; while in T-G+L medium, estimated t_{LAG} were significantly greater using ABS readings than that using viable count method at 20, 25, and 40°C (with *P* value of 0.0266, 0.0121, and 0.0362, respectively).

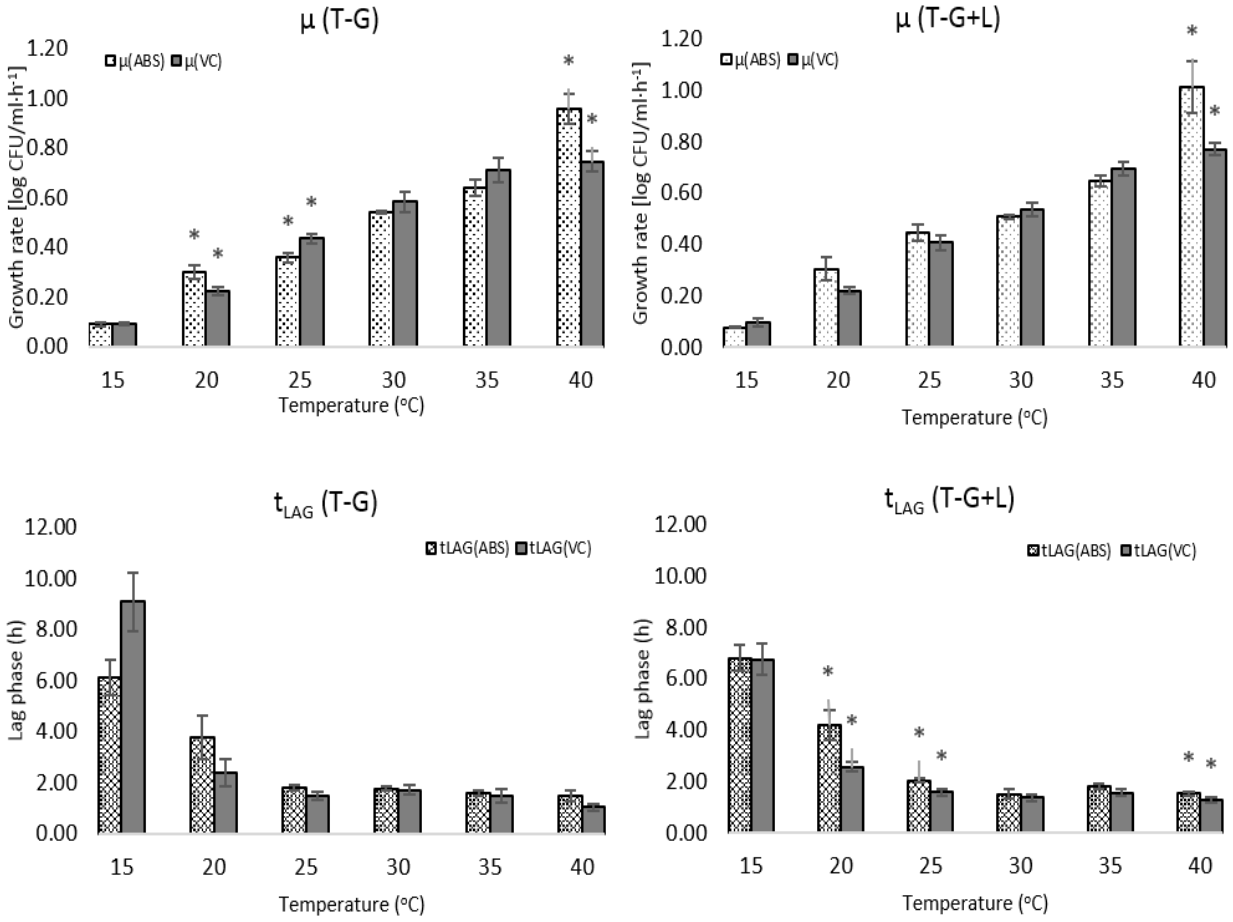

Figure 4.4 Comparison of growth kinetics of *E. coli* K-12 obtained from absorbance and viable count data (top left and right: exponential growth rates in T-G and T-G+L broth, respectively; bottom left and right: lag phase duration in T-G and T-G+L broth, respectively). Data sets with * mark were significantly different ($P \leq 0.05$).

4.4.3 Temperature Dependency of Growth Kinetics

Growth rate as a function of temperature

The results from ANOVA are shown in **Table. 4.4**: neither the medium type nor the interaction between medium and temperature had significant influence on the *E. coli* K-12 growth rates ($P = 0.5133$, $P = 0.8519$, respectively). Temperature was identified as the only significant factor that associated with *E. coli* K-12 growth rates, with a *P*

value less than 0.0001. Since the effect of different medium was negligible, the growth rates in these two media were combined during secondary model fitting.

Table 4.4 Effect of temperature and medium on the growth rate of *E. coli* K-12

Source	DF	Sum of squares	F ratio	Prob > F
Temperature	5	6.430266	176.182	<.0001
Medium	1	0.00314	0.4301	0.5133
Temperature × Medium	5	0.014384	0.3941	0.8519

Figure 4.5 and **4.6** show the results from secondary model fitting: both secondary models and linear regression can describe the effect of temperature on exponential growth rate of *E. coli* K-12 well. In general, exponential growth rate increases with temperature: the higher temperature, the larger growth rate.

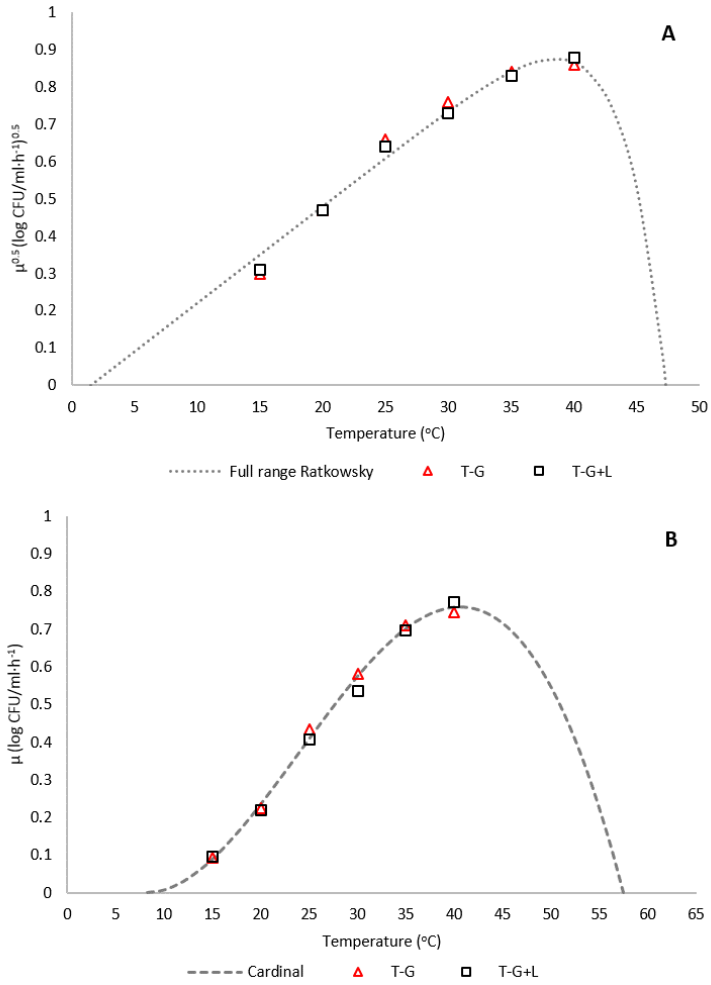

Figure 4.5 Growth rate curve-fitting to secondary models. A: fitting to full range Ratkowsky model; B: fitting to Cardinal model. Symbols represent experimental data and dotted lines correspond to the fit of secondary model.

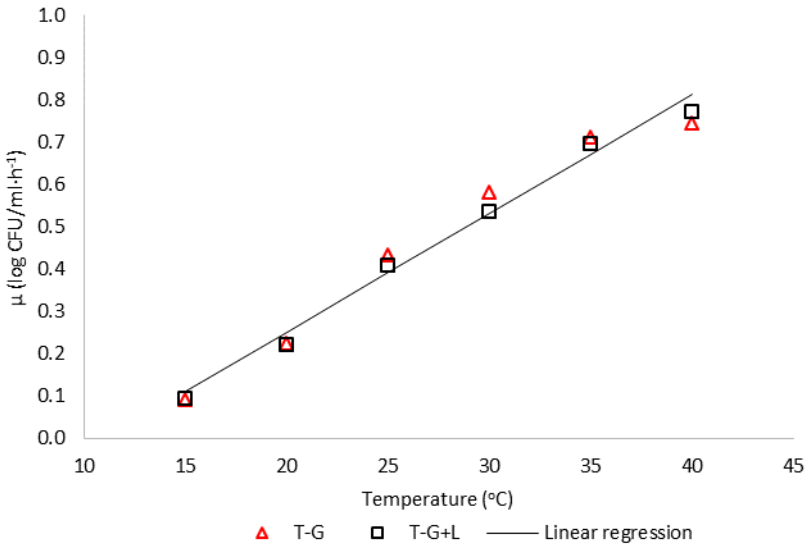

Figure 4.6 Linear regression of *E. coli* K-12 growth rate using viable count data

Table 4.5 lists the parameters of all the three fittings. As shown in **Table 4.5**, the maximum (T_{max}) and notional minimum (T_o) growth temperatures of *E. coli* K-12 estimated by modified Ratkowsky model were 47.3 and 1.5°C, respectively. The maximum, optimum, and minimum growth temperatures generated from Cardinal model were 57.5, 40.6, 8.3°C, respectively. The R^2 for linear regression was 0.9757.

Table 4.5 Parameters of secondary models for exponential growth rate of *E. coli* K-12.

Model	Parameter	Estimate	Std Error	t ratio	Prob > |t|
Ratkowsky	a	0.026	0.002	16.757	< 0.001
	T_{max}	47.270	5.794	8.159	< 0.001
	b	0.274	0.238	1.151	0.280
	T_0	1.514	1.036	1.461	0.178
Cardinal	T_{max}	57.476	7.815	7.354	< 0.001
	T_{opt}	40.58	2.198	18.46	< 0.001
	T_{min}	8.264	1.700	4.86	1.26E-03
	μ_{opt}	0.759	0.018	41.822	< 0.001
Linear	a	-0.310	0.040	-7.69	< 0.001
	b	0.028	0.001	20.03	< 0.001

Lag phase duration as a function of temperature

The results of ANOVA for lag phase duration is shown in **Table. 4.6**: both the temperature and the interaction between temperature and medium type had significant influences on the lag phase duration ($P < 0.0001$, $P = 0.0167$, respectively). However, no significant differences were observed between t_{LAG} of *E. coli* K-12 grown on T-G and T-G+L ($P = 0.20$). Since the interaction also played a role, temperature effect on the t_{LAG} of these two media were evaluated separately.

Table 4.6 Effect of temperature and medium on the lag phase duration of *E. coli* K-12.

Source	DF	Sum of squares	F ratio	Prob > F
Temperature	5	703.3486	79.5177	<.0001
Medium	1	3.00766	1.7002	0.1951
Temperature × Medium	5	25.73256	2.9092	0.0167

When t_{LAG} was plotted against temperature, it can be observed that while the temperature increases, the length of lag phase decreases (**Figure 4.7**). Specifically, a sharp decrease in t_{LAG} can be observed between 15 - 25°C, while t_{LAG} at 30, 35, and 40°C are relatively close in both media. Indeed, the results from Tukey's test shows that for *E. coli* K-12 grown in T-G broth, t_{LAG} at 15°C was significantly longer than t_{LAG} at all the other temperatures ($P < 0.0001$), while no significant differences were observed among t_{LAG} at other temperatures; for *E. coli* K-12 grown in T-G+L broth, t_{LAG} was significant longer at 15°C than t_{LAG} at all the other temperatures; t_{LAG} at 20°C was significantly longer than that from 35 and 40°C; t_{LAG} at 25, 30, 35, and 40°C were not significantly different (**Figure 4.8**).

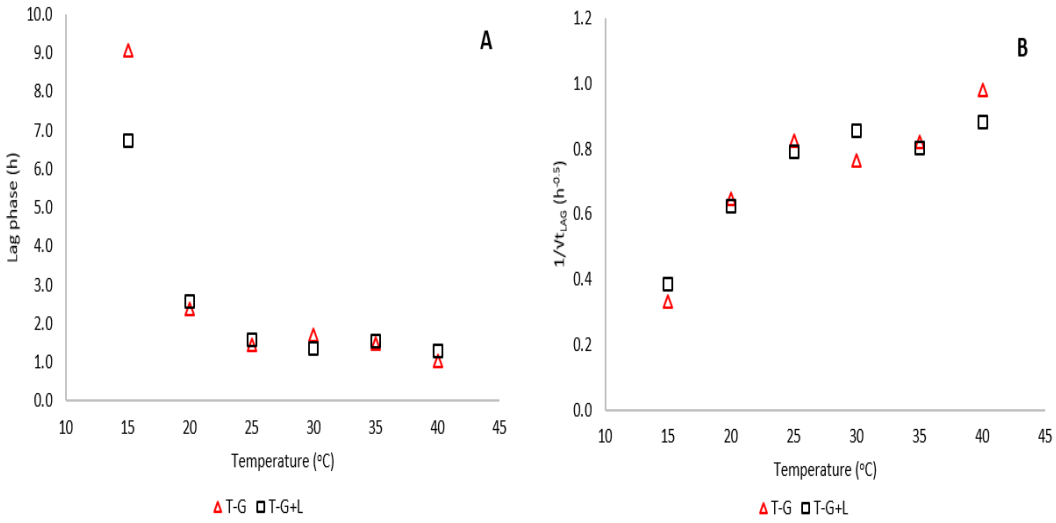

Figure 4.7 Temperature effect on lag phase duration in two media (A: relation between temperature and lag phase; B: relation between temperature and reciprocal of lag phase square root).

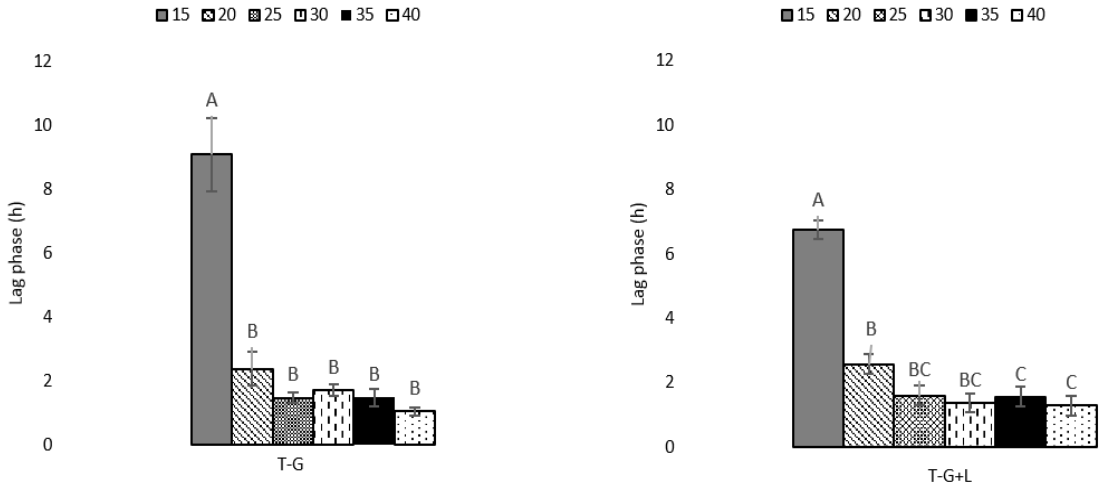

Figure 4.8 Comparison of lag phase at different temperatures. Means have different letters are significantly different. ($P \leq 0.05$)

A generally accepted equation to describe the interdependence between lag phase and temperature was illustrated in **Eq. 20** (*73*, *160*):

$$\frac{1}{\sqrt{\lambda}} = a(T - T_0)\left[1 - e^{b(T - T_{max})}\right] \quad (20)$$

Reciprocal of the square root of lag phase was used to fit the modified Ratkowsky model in IPMP (**Figure 4.9**).

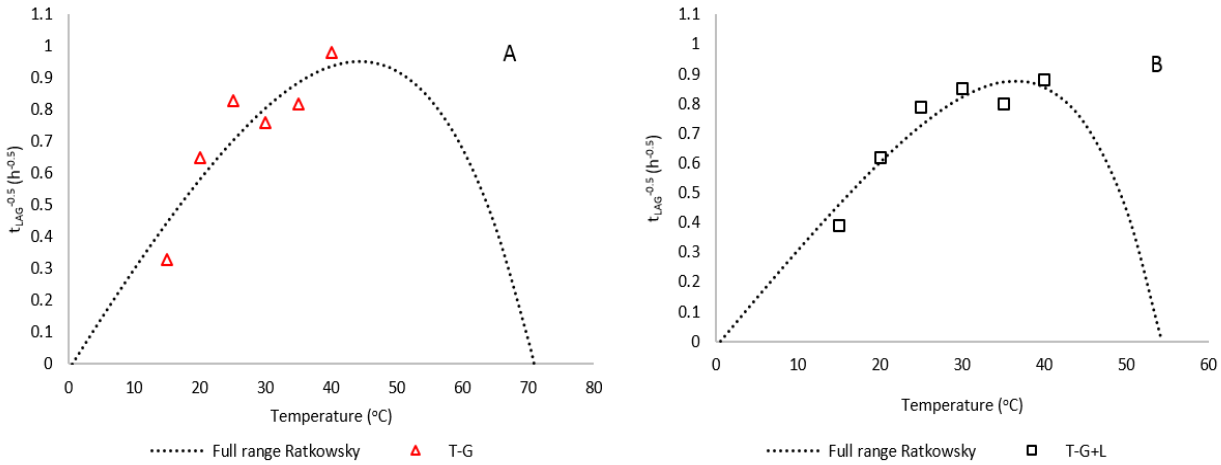

Figure 4.9 Relationship between the reciprocal of lag phase duration and temperature as described by modified Ratkowsky model. Symbols represent experimental data and dotted lines correspond to the fit of secondary model. (A: cells cultured in T-G; B: cells cultured in T-G+L)

Table 4.7 lists all the parameters derived from modified Ratkowsky model for *E. coli* K-12 grown in T-G and T-G+L broth. As shown in **Table 4.7**, the maximum (T_{max}) and notional minimum (T_o) growth temperatures of *E. coli* K-12 estimated by modified Ratkowsky model were 70.8 and 0.54°C for cells grown in T-G, and 54.3 and 0.53°C for cells grown in T-G+L.

Table 4.7 Parameters of secondary models for lag phase of *E. coli* K-12.

Model	Parameter	Estimate	Std Error	t ratio	Prob > |t|
Ratkowsky	a	0.036	0.058	0.619	0.579
(T-G)	T_{max}	70.791	114.366	0.619	0.5798
	b	0.035	0.227	0.156	0.886
	T_o	0.544	3.34	0.163	0.881
Ratkowsky	a	0.034	0.012	2.743	0.07117
(T-G+L)	T_{max}	54.292	16.068	3.379	0.04313
	b	0.071	0.114	0.627	0.575
	T_o	0.532	2.193	0.243	0.8239

4.4.4 Monte Carlo Simulation

Figure 4.10 and **Figure 4.11** show the results of Monte Carlo simulation for both T-G and T-G+L media at different temperatures. From the figures, for each temperature × medium combination, smooth transition of lag to exponential phase was obtained through three-phase linear model by Monte Carlo simulation.

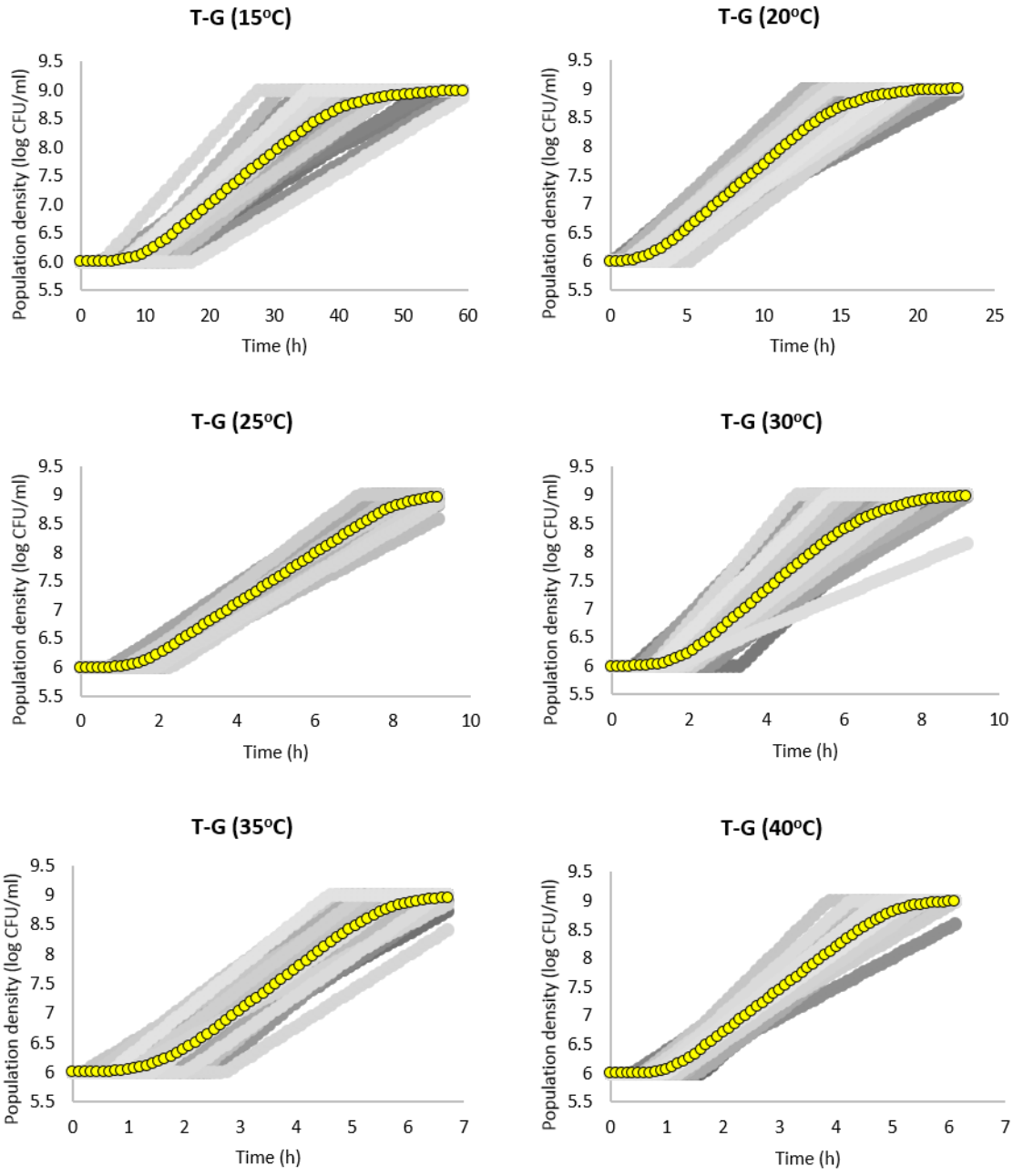

Figure 4.10 Monte Carlo simulation of *E. coli* K-12 growth curve in T-G at different temperatures (yellow lines are the average of 30 iterations).

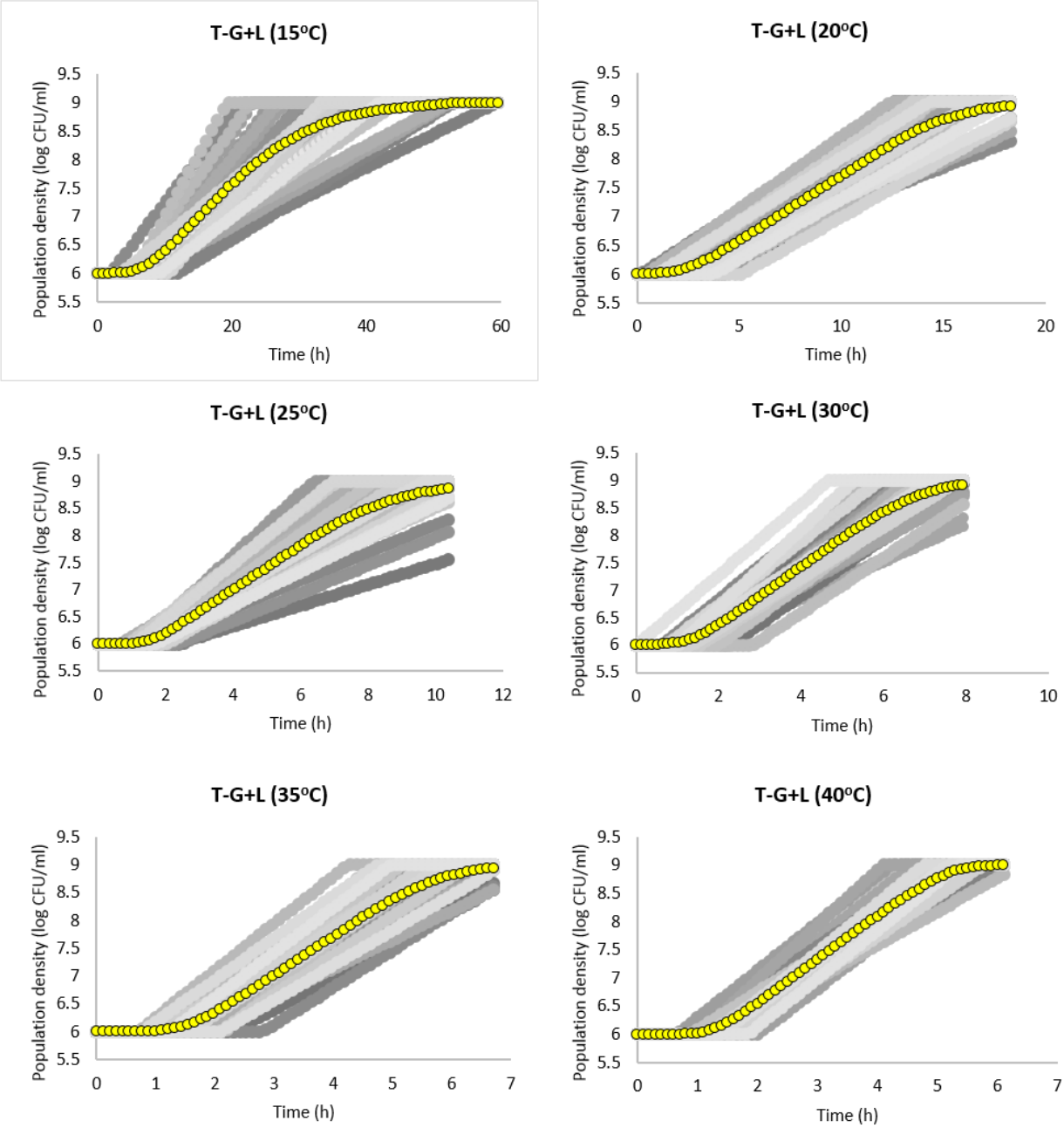

Figure 4.11 Monte Carlo simulation of *E. coli* K-12 growth curve in T-G+L at different temperatures (yellow lines are the average of 30 iterations).

4.4.5 Estimate of t_a and t_m

Estimate of t_a

Metabolic time (t_m) and adjustment time (t_a) were calculated as described in Material & Methods. **Table 4.8** lists these two parameters at different temperatures with means and standard deviations shown.

Table 4.8 t_a and t_m of *E. coli* K-12 grown in T-G and T-G+L medium at different temperatures (Viable count data)

Temperature (ºC)	**Parameters**			
	T-G		T-G+L	
	t_m (h)	t_a (h)	t_m (h)	t_a (h)
15	3.43 ± 1.07	5.65 ± 2.98	3.69 ± 1.03	3.05 ± 2.97
20	1.38 ± 0.03	1.00 ± 1.28	1.42 ± 0.29	1.16 ± 0.65
25	0.58 ± 0.26	0.88 ± 0.42	0.78 ± 0.17	0.82 ± 0.60
30	0.50 ± 0.10	1.20 ± 0.67	0.58 ± 0.09	0.79 ± 0.58
35	0.43 ± 0.07	1.05 ± 0.70	0.44 ± 0.06	1.12 ± 0.51
40	0.41 ± 0.06	0.63 ± 0.34	0.40 ± 0.05	0.89 ± 0.35

[a] Means and standard deviations are shown

Figure 4.12 shows the relationship between temperature and t_m, t_a, t_{LAG}.

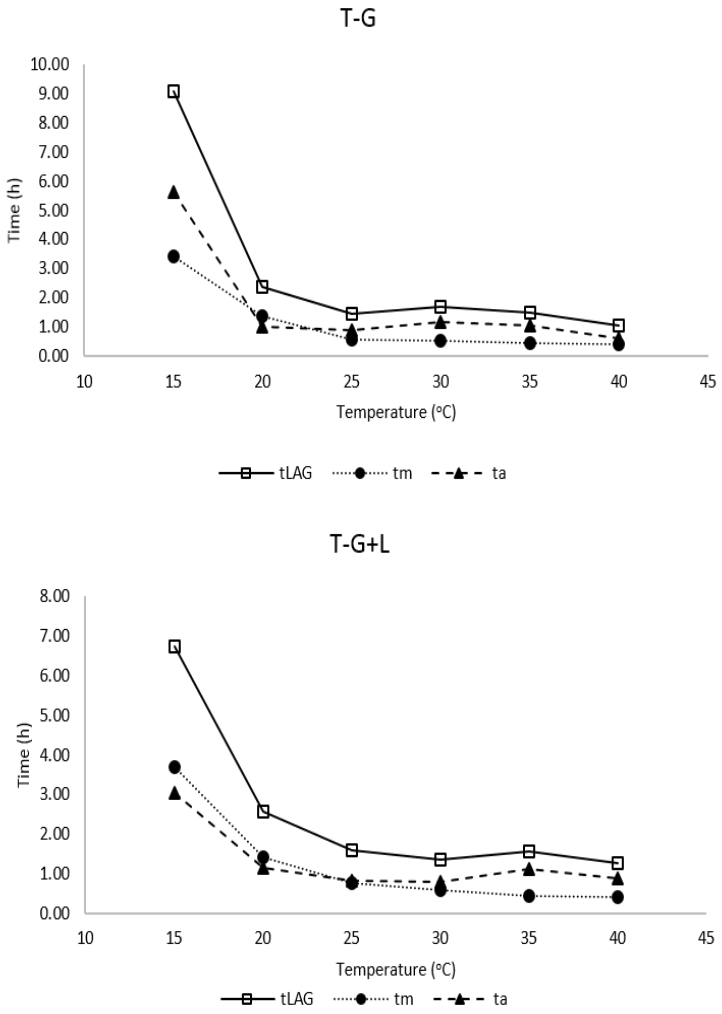

Figure 4.12 Relationship between temperature and lag, generation, and adjustment time. (Top: cells cultured in T-G; Bottom: cells cultured in T-G+L)

t_a as a function of temperature

The temperature dependency of adjustment time was also assessed (**Figure 4.13**). It displayed a similar trend as lag phase shown in **Figure 4.7** (A): a sharp decrease in t_a can only be observed between 15°C and 20°C while t_a at other temperatures are relatively close. Results from ANOVA and Tukey's test confirmed this observation: significant difference was only between t_a at 15°C and other temperatures ($P < 0.05$) (**Figure 4.14**).

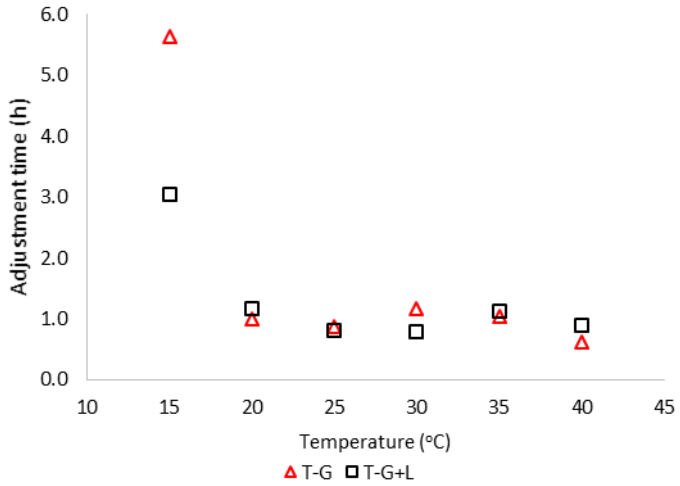

Figure 4.13 Temperature effect on adjustment time in two media.

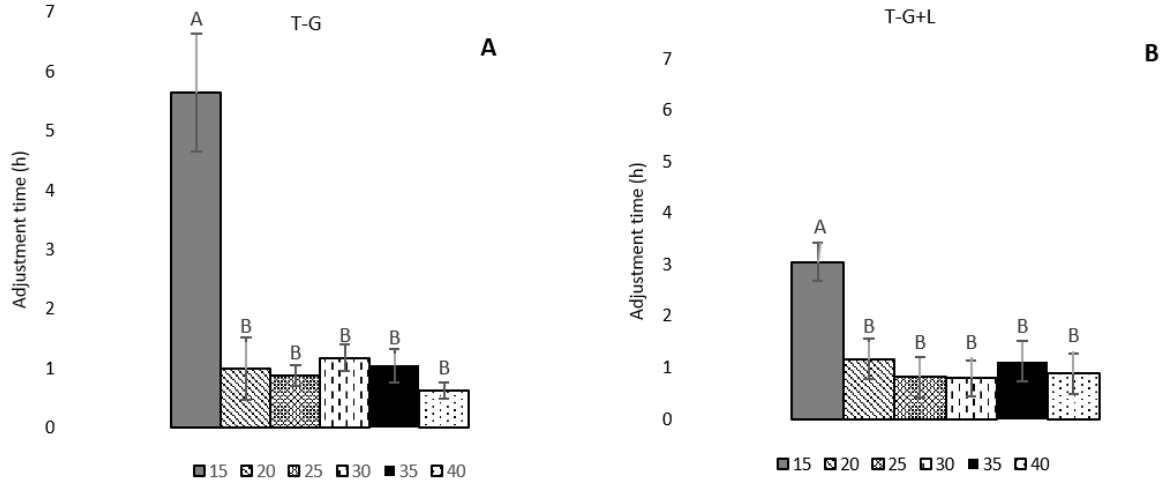

Figure 4.14 Comparison of adjustment time at different temperatures. Means have different letters are significantly different. ($P \leq 0.05$)

4.5 Discussion

As a standard method, plate counting has been widely used in predictive microbiology to describe bacterial growth (*19*). In order to get accurate estimates, a large number of observations is usually needed which is time-consuming, labor

intensive, and also expensive (*24*). More real time methods such as turbidimetry have been developed and used nowadays by many predictive microbiologists (*7*). However, this method depends largely on the apparatus and therefore has its own limitations. The absorbance data needs to be evaluated with caution before being used to get reliable estimations of growth parameters.

It is widely accepted that there is a proportional relationship between absorbance and bacterial concentration (*7*, *15*, *41*, *43*). This was confirmed in this study. Using log (ABS) as x-axis, log (CFU/ml) as y-axis, the plot showed a clear two-phase linear relation (Figure 4.2). During the first period, generally, the absorbance readings kept constant with minor fluctuations and no significant increase in the corresponding viable counts was observed. This period was referred to as "lag phase (x_o)" and displayed a horizontal line in the plot. It is when the bacterial concentration is below the detection threshold, approximately 10^6-10^7 CFU/ml (*42*). The exponential growth rates were derived from relative dense bacterial cultures when absorbance measurements started to increase (*87*). According to Friedrich (*171*), the proportionality between OD and cell concentration only exists when OD $\leq$ 0.4. In this study, growth of *E. coli* K-12 was followed until mid-exponential phase, where most absorbance data were below 0.4. Therefore, the two-phase linear model was suitable to conclude the correlation between absorbance and viable count data.

While comparing the μ and t_{LAG} estimated from absorbance and viable count data, significant discrepancies were observed at some temperatures while others were assumed to be identical. For example, for growth rate in T-G broth, at 20 and 40°C, μ(ABS) were significantly larger than μ(VC); at 25, 30, and 35°C, μ(ABS) were

smaller than μ(VC): the pattern was not clear. For lag phase duration, t_{LAG}(ABS) were constantly longer than t_{LAG}(VC), although at most temperatures, the differences were not statistically different. This result is opposite to other studies, while they all reported a relatively shorter lag phase and larger growth rate obtained from absorbance data (*43*, *75*, *130*). This discrepancy might ascribe to several reasons. Firstly, other than the transformed absorbance data, they used direct absorbance value to fit the growth curve. Since spectrophotometer measures light scattering on particles, the size of cells would affect the results. During lag phase, cell sizes increase while the total number of cells doesn't (*75*). This will result in an underestimation on lag phase duration by absorbance data. Secondly, spectrophotometer measures both live and dead cells in the culture while plate counting only detects viable cells. Another possible explanation is the different fitting methods and varies definitions of the parameters chosen in the studies (*129*). Research showed that the growth parameters were unequal while using different mathematical models (*42*). All in all, the method we were using in this study can be applied in future research to estimate critical growth kinetics from absorbance data. Calibration curve is needed when the inoculum size is below the detection threshold (*7*). This is quite common in food safety study since the spoilage and pathogenic microorganisms often start at very low levels.

Exponential growth rate is considered to be associated with post-incubation environment <ENV2> only. It is controlled by a variety of factors (*54*, *55*, *90*, *99*). In this study, we investigated the effects of medium type and incubation temperature on *E. coli* K-12 growth rates. The results of ANOVA showed that temperature was the

only factor that significantly influence growth rate. Judging from Figure 4.4 and 4.5, generally speaking, within certain range, the higher temperature, the larger growth rate. It can be explained as when the temperature increases, both the chemical and enzymatic activities in the cells proceed much faster, resulting more rapid growth. *Escherichia coli* is classified as mesophilic bacterium, with a minimum growth temperature around 8 to 10^{o}C under optimum conditions (*26*), a maximum temperature of 50^{o}C, and optimum temperature being 35^{o}C to 39^{o}C (*53*). The conceptual T_o as estimated by the modified Ratkowsky model was 1.5^{o}C, which is below the biological value; while the Cardinal model gave a more close value of 8.3^{o}C. T_{max} obtained from Ratkowsky model was similar to the theoretical value while Cardinal model seemed to overestimate the upper limit.

Unlike growth rate, the duration of lag phase is not only dependent on the incubation environment, but also on the pre-culturing conditions (*44*). In this study, the inoculum was prepared by incubating the subculture at designated temperature (same as the following incubation temperature) until stationary phase. Since the pre- and post-incubation temperatures remained stable, the influence of temperature shift on lag phase was negligible (*74*). Therefore, in this case, the lag phase was mainly affected by the medium type and post-incubation temperatures. However, differences still existed among the initial physiological states of the cells. While investigating the changing trend of t_{LAG} with temperature, inconsistent conclusions could be reached for different medium types. Cells cultured in T-G, t_{LAG} at 15^{o}C were significantly different from others, while t_{LAG} at all the other temperatures were identical. A similar conclusion was reported by Muller (*44*) who found that *Listeria monocytogenes* cells

pre-cultured at temperatures far from optimum temperature tend to have significantly longer lag phase. This can be explained by higher stress levels, cells need more time to overcome the energy barrier (e.g. repair cell damage) and to adapt to the new environment (*54*). For cells culturing in T-G+L, it is much more complicated, probably due to the addition of lactose in the medium which requires synthesis of new enzymes.

While evaluating the interdependence of lag phase and temperature, the modified Ratkowsky model was used based on the assumption that lag time is proportional to generation time (*73, 135, 177*). This relationship was confirmed by fitting the inverse of the square root of lag phase to the full range Ratkowsky model. However, T_{max} and T_o of *E. coli* K-12 estimated by modified Ratkowsky model were 70.8 and 0.54^{o}C for cells grown in T-G, and 54.3 and 0.53^{o}C for cells grown in T-G+L, which is deviated from the published results (*26, 53*). The biggest problem of this model is that it was built on the assumption that the cultures studied all have identical physiological conditions, thus lag phase is not influenced by previous history (*44*, *160*).

Adjustment period t_a had the similar temperature tendency as t_{LAG}. For both T-G and T-G+L, only at 15^{o}C, the differences were significant, partially because at temperatures far from optimum temperature, more effort is needed to reinitiate growth. Furthermore, at low temperature, the transcriptional and translational activities are slower.

Using standard deviations from the trials, it was possible to effectively describe the shape of the growth curve of *E. coli* K-12. Monte Carlo simulation allowed the generation of traditional sigmoidal growth curves by considering the biological

variance among the population. If the variance is relatively small, the transition becomes abrupt, while larger variation within the population generates a much more gradual transition.

Chapter 5 Timing of Metabolic Activities during Lag Phase

5.1 Background

When cells are transferred from one environment to another environment, a lag phase is usually observed before the actual growth is reinitiated. For example, if cells are transferred from peptone-based medium to lactose-containing medium, the cell number does not increase immediately (*28*). If lactose serves as the preferred carbon source, the expression of *lac* operon is turned on and specific enzymes are formed to metabolize lactose (*28*, *116*).

The complete enzyme system functions as a coordinated unit. Three critical enzymes, β-galactosidase, β-galactosidase permease, and thiogalactoside transacetylase (encoded by *lacZ*, *lacY*, and *lacA*, respectively) are involved (*78*). **Figure 5.1** illustrates the critical chemical reaction involved in lactose hydrolysis.

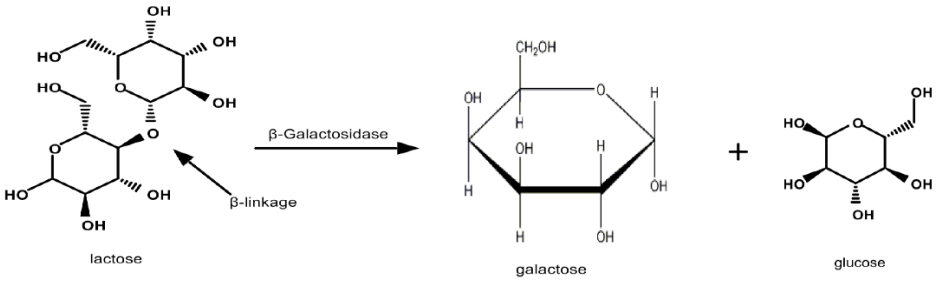

Figure 5.1 Chemical reaction of lactose hydrolysis

Ortho-Nitrophenyl-β-galactoside (ONPG) has structure similar to that of lactose and has been extensively used as substrate in β-galactosidase activity analysis (*103*). Colorless ONPG can be hydrolyzed by β-galactosidase and the production orthonitrophenol (ONP) appears bright yellow which can be used as the reaction

indicator. The β-galactosidase activity is determined by measuring color intensity at 420 nm (*115*).

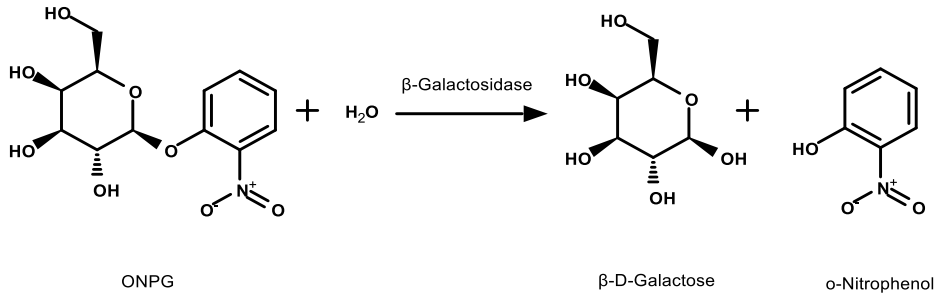

Figure 5.2 Chemical reaction of ONPG hydrolysis

In order to thoroughly investigate the time course of metabolic events taking place, it is of great importance to not only investigating post-translation level, but also at gene expression level. Currently, the most sensitive and widely used technique to detect mRNA expression is quantitative reverse transcription polymerase chain reaction (RT-qPCR) (*81*). Briefly summarizing, RNA template is converted to complementary DNA (cDNA) by reverse transcriptase then followed by regular PCR amplification. Real time detection is enabled by the use of DNA-binding dyes or sequence-specific primers labeled with fluorescence. While the amplification occurs, the amount of product DNA increases, thus the fluorescence emission increases as well. Eventually, the signal accumulates to a certain threshold that can be detected by the apparatus. The cycle number at which the signal becomes detectable is called the quantification cycle or Ct value. It is proportional to the initial input target quantity: Ct value decreases linearly with increasing template (*61*). Therefore, mRNA expression level can be estimated by Ct value and standard curve afterwards (*31*, *60*). Compared to conventional end-point PCR, the amplicons are detected in real time manner, no post-amplification handling such as agarose gel electrophoresis is needed. Furthermore, potential contamination is prevented since the reaction is performed in a closed tube

chamber environment. More importantly, it is much more sensitive and allows the detection of target in limited amounts (*61*).

5.2 Study Objectives

It was hypothesized that the lactase related activities should occur at some point during the lag phase, approximately at the end of adjustment period and the beginning of metabolic period. Therefore, the lag phase could be separated into two distinct components. The objective of this experiment was to use β-galactosidase and its encoded gene *lacZ* to determine the timing of the series physiological events taking place.

5.3 Materials & Methods

5.3.1 Lactase Activity

Colorless ONPG was cleaved into galactose and yellowish ONP by lactase at 30^{o}C and pH 6.5. The reaction was terminated by the addition of Na_2CO_3 which inactivated β-galactosidase by modifying the pH to 11.0. The absorbance of product was measured by spectrophotometry at 420 nm (*4*).

Preparation of Reagents

1) Phosphate Buffer Solution

The phosphate buffer solution contained KH_2PO_4, K_2HPO_4, $MgSO_4 \cdot 7H_2O$, and EDTA solution. The pH of the mixture was adjusted to 6.5. Buffer solution was prepared freshly before use.

2) ONPG Substrate

ONPG (Thermo Scientific Pierce Technology, IL) was stored at -20^{o}C upon receipt and protected from moisture and light. Before use, 250.0 mg ONPG was dissolved in small volume with phosphate buffer solution and diluted to 100 ml. The final concentration was 2.5 mg/ml. The mixed solution was equilibrated for 10 min at 30^{o}C.

3) Sodium Carbonate Solution

Na_2CO_3 and Na_2EDTA were dissolved in small volume of H_2O and then diluted to volume. The final concentration of the solution was 1 M.

Enzyme activity measurement

2 ml sample and 2 ml phosphate buffer solution were mixed and equilibrated in 30^{o}C water bath for exactly 5 min. 5 ml ONPG substrate was added in the tube and mixed thoroughly by vigorously shaking. After shaking, the mixture was incubated at 30^{o}C water bath for 10 min. 2 ml Na_2CO_3 solution was then added to stop the reaction. The addition of ONPG and Na_2CO_3 solution was staggered at 1 min intervals to account for the time difference. The final products were measured for absorbance at 420 nm by GENESYS^{TM} 20 Visible Spectrophotometer (Thermo Scientific, 4001/000, USA). To eliminate potential interference of free ONP in ONPG substrate, reactant mixture which the enzyme activity has been inactivated beforehand was used as a blank. Two trials of experiments were conducted for each temperature following exactly the same procedures. For each single trial, three replicates were conducted simultaneously.

5.3.2 The lacZ mRNA Expression

RNA isolation & purification

1) RNA isolation

Sample collection was performed as described in Chapter 4 section 4.3. Two trials of experiments were conducted for each temperature following exactly the same procedures. For each single trial, three replicates were conducted simultaneously. Briefly, BHI-grown *E. coli* K-12 cells were cultured to early stationary phase and then transferred to T-G+L broth. The cultures were incubated on orbital shaker (Corning, MA, USA) at 30 rpm under six different temperatures (15-40^{o}C). At designated time point, 3 ml sample was taken and stored in two 1.5 ml centrifuge tubes. Cells were harvested and centrifuged at 4^{o}C at 2,000×g for 5 min. 1 ml TRIzol® (Life technologies, Carlsbad, CA) was added to lyse *E.coli* K-12 cells. RNA extraction was conducted through homogenizing, phase separation (0.2 ml chloroform), RNA precipitation (0.5 ml isopropanol) and RNA wash (75% ethanol), as per manufacturer's instructions. The RNA pellet was resuspended in RNase-free water and incubated in a heat block set at 55°C for 10 min.

2) RNA purification

Remaining DNA that might influence downstream applications was removed by adding 2 µl RNase-free DNase I (Life technologies, Carlsbad, CA) into 2 µg RNA and incubating with 2 µl 10× reaction buffer with $MgCl_2$ and appropriate amount of DEPC-treated water in a total volume of 20 µl at 37^{o}C for 30 min. DNase I activity was stopped by addition of 2 µl 50mM EDTA and incubated at 65^{o}C for 10 min (*49*). RNA yield and quality was determined using NanoDrop 1000 spectrophotometer (Thermo Fisher Scientific, Wilmington, DE) based on A_{260}/A_{280} ratio (1.8 ~ 2.0).

cDNA synthesis

The cDNA synthesis was carried out using iScript™ cDNA kit (Bio-Rad, Hercules, CA) following the manufacturer's instructions. A total volume of 20 µl reaction mixture was used containing 4 µl of 5× iScript™ reaction mix (using random primers), 1 µl iScript™ reverse transcriptase, and 500-1000 ng RNA template. Appropriate amounts of ultrapure N-free water was added to adjust the volume. The synthesis was performed in Bio-Rad T100™ thermal cycler (Bio-Rad, Hercules, CA). Complete thermal cycle consists of incubating at 25°C for 5 min, synthesis at 42°C for 30 min followed by 85°C for 5 min to inactivate reverse transcriptase. Synthesized cDNA was stored at -20°C freezer until used.

RT-qPCR

The *lacZ* gene which encoding β-galactosidase was the target gene in this study. The housekeeping gene 16S rRNA was used as an endogenous reference to normalize the variance in total RNA quantity. The primer pairs used for amplification were synthesized by Integrated DNA Technologies with T_m (melting temperature) set to 60°C (IDT, San Diego, CA). The primers are described in **Table 5.1**.

Table 5.1 RT-qPCR primer pairs for 16S rRNA and *lacZ* of *E. coli* K-12

Gene name	Product size	Primer (5'-3')	Reference
16S rRNA	330 bp	F: GTTAATACCTTTGCTCATTGA	(*56*)
		R: ACCAGGGTATCTAATCCTGTT	
lacZ	264 bp	F: ATGAAAGCTGGCTACAGGAAGGCC	(*20*)
		R: GGTTTATGCAGCAACGAGACGTCA	

Universal SYBR Green super mix kit (Bio-Rad, Hercules, CA) was used in qPCR according to manufacturer's protocol. Briefly, the reaction was carried out in 10 µl of

total volume containing 5 µl of SYBR Green super mix, 1 µl of each primer (4 µM), 2 µl 1:10 diluted cDNA, and 1 µl DEPC-treated water. To minimize the inter-assay variability, one PCR master mix (including all the essentials except cDNA template) was prepared, mixed thoroughly and distributed to each individual well. The reaction was performed in triplicates under following conditions by CFX96 Bio-Rad system (Bio-Rad, Hercules, CA): 95^{o}C for 10 min followed by 40 cycles of denaturing at 95^{o}C for 5 sec, annealing and extension at 60^{o}C for 30 sec. Fluorescence readings were taken after each cycle following the extension step. Melting curve analysis was also performed to determine the specificity of the reaction using default program: 65-95^{o}C, 0.5^{o}C increments at 5 sec/step. Additional NTC (no template) and NRT (no reverse transcriptase) controls were run at the same time to eliminate contamination of reagents and remaining DNA fragments.

5.3.3 Data Analysis

Lactase activity

Absorbance readings at 420 nm were recorded in Excel sheets and logarithmic transformation (base-10) was performed before data analyses. In addition to the traditional method (*4*, *115*) which calculated lactase enzyme activity from standard curve, we also used a "break point" to represent time point when lactase activity was first detected. Reduced two-phase linear model (*28*) was used to fit experiment data and the end of "lag phase" was considered as the break point. To take into account the variances within replicates and trials under same temperature, data from each replicate was fitted separately. All the curve-fitting were conducted using USDA Integrated Pathogen Modeling Program 2013 (IPMP, USDA, Wyndmoor, PA) based

on least-square method. Estimated first time lactase production point ($t_{\beta\text{-GAL}}$) for each growth condition were summarized and were used to calculate the means and standard deviations. Results were compared to t_{LAG} and t_a from Chapter 4.

The *lacZ* mRNA expression

In this study, reactions with Ct values higher than 35 or N/A were defined as negative (no detectable) according to manufacturer's instructions. SYBR Green is used as the fluorescent dye in this study for convenience and financial consideration. The biggest disadvantage is the non-specific binding. To confirm the specificity of amplification, each target gene was double checked with melting-curve analysis. A positive amplification should have a reasonable Ct value smaller than 35 and a single peak in melting curve with the right Tm. The threshold time of induction of *lacZ* gene was determined as the first time point of positive amplification result.

5.4 Results

5.4.1 Lactase activity

Figure 5.3 shows an example of the curve-fitting of *E. coli* K-12 lactase detection at 30^{o}C. In the example, lactase absorbance at 420 nm of *E. coli* K-12 fit the two-phase linear model well with the RMSE (root mean square error) of 0.097. Two-phase linear model was suitable to estimate break point ($t_{\beta\text{-GAL}}$).

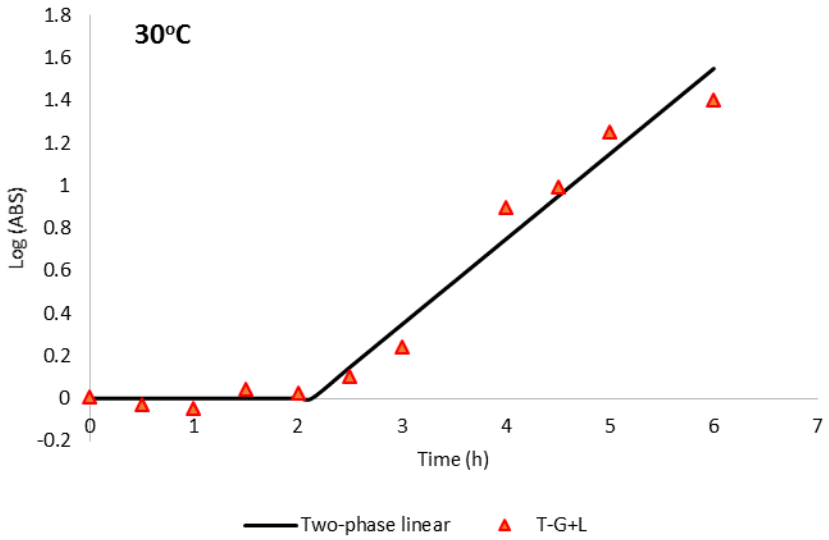

Figure 5.3 Curve-fitting of *Escherichia coli K-12* lactase data after shift from BHI to T-G+L medium at 30°C

Table 5.2 lists the growth kinetics values of *E. coli* K-12 grown in both T-G and T-G+L media. Adjustment time, lag time, and estimated time to first lactase production were reported with means and standard deviations shown. Detectable lactase activity was limited to T-G+L cultures, with initial detection occurring slightly after the lag phase.

Table 5.2 Comparison of critical time points during lag to exponential phases after nutritional shift from BHI to T-G and T-G+L media (means and standard deviations).

Temperature (°C)	15	20	25	30	35	40
T-G						
t_a (h)[a]	5.7 ± 3.0	1.0 ± 1.3	0.9 ± 0.4	1.2 ± 0.7	1.1 ± 0.7	0.6 ± 0.3
t_{LAG} (h)	9.1 ± 3.4	2.4 ± 1.3	1.5 ± 0.4	1.7 ± 0.6	1.5 ± 0.7	1.0 ± 0.3
$t_{\beta\text{-GAL}}$ (h)[b]	ND[c]	ND	ND	ND	ND	ND
T-G+L						
t_a (h)	3.1 ± 3.0	1.2 ± 0.7	0.8 ± 0.6	0.8 ± 0.6	1.1 ± 0.5	0.9 ± 0.4
t_{LAG} (h)	6.7 ± 2.3	2.6 ± 0.7	1.6 ± 0.5	1.4 ± 0.5	1.6 ± 0.5	1.3 ± 0.3
$t_{\beta\text{-GAL}}$ (h)	7.6 ± 3.7	3.4 ± 1.5	1.8 ± 1.3	2.6 ± 0.3	2.5 ± 0.2	2.1 ± 0.3

[a] t_a: calculated adjustment time;
[b] $t_{\beta\text{-GAL}}$: Estimated time to first lactase production;
[c] ND: no lactase detected over course of trial.

Figure 5.4 shows the order of events taking place at different temperatures. At all incubation temperatures, the estimated occurrence of lactase activity was first detected slightly after the completion of lag phase. At 25°C, the lag time and the estimated first time lactase production overlapped. The occurrence also followed the temperature dependency as expected: the higher incubation temperature was, the earlier lactase activity was detected.

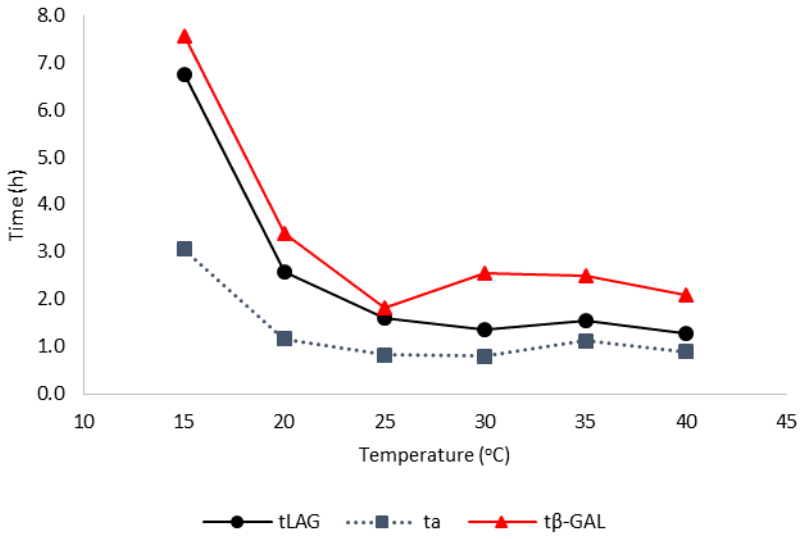

Figure 5.4 Comparison of t_{LAG}, t_a, and $t_{\beta\text{-}GAL}$ of *Escherichia coli K-12* after a nutritional shift from BHI to T-G+L medium at different temperatures

5.4.2 The lacZ mRNA expression

An example of amplification plot is shown in **Figure 5.5**. The amplification plot was constructed by plotting fluorescence emission data versus corresponding cycle number. The horizontal line represents the arbitrary threshold cycle (limit of detection). No amplification was detected in neither NTC nor NRT controls.

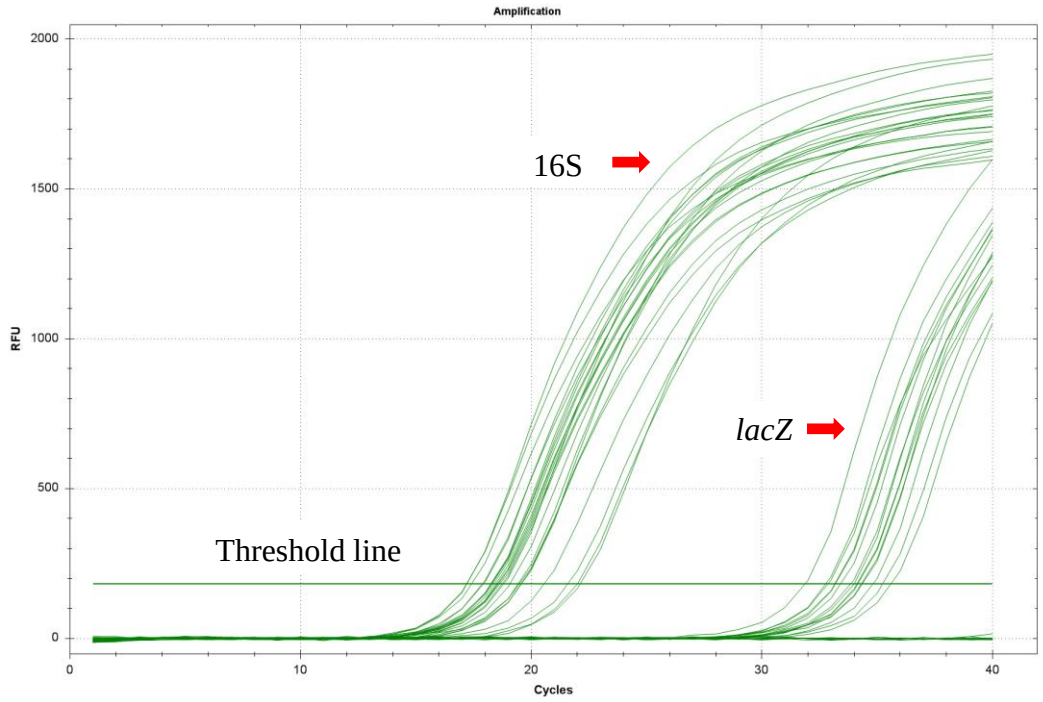

Figure 5.5 Amplification plot of 16S rRNA and *lacZ* gene of *E. coli* K-12 at 15ºC

Table 5.3 and **Figure 5.6** show the induction time point of *lacZ* gene of *E. coli* K-12 culturing in T-G+L compared to other critical time points. For cells cultured at 15, 20, 25, 30, and 35ºC, the time course of events taking place is: $t_a \rightarrow t_{lacZ} \rightarrow t_{LAG} \rightarrow t_{\beta\text{-}GAL}$. For cells cultured at 30ºC, the first time *lacZ* mRNA detection was slightly after the completion of lag phase, but the difference was small.

Table 5.3 Comparison of *lacZ* induction and other growth kinetics values after nutritional shift in T-G+L.

Temperature (°C)	15	20	25	30	35	40
T-G+L						
t_a (h)[a]	3.1 ± 3.0	1.2 ± 0.7	0.8 ± 0.6	0.8 ± 0.6	1.1 ± 0.5	0.9 ± 0.4
t_{LAG} (h)	6.7 ± 2.3	2.6 ± 0.7	1.6 ± 0.5	1.4 ± 0.5	1.6 ± 0.5	1.3 ± 0.3
$t_{\beta\text{-GAL}}$ (h)[b]	7.6 ± 3.7	3.4 ± 1.5	1.8 ± 1.3	2.6 ± 0.3	2.5 ± 0.2	2.1 ± 0.3
t_{lacZ} (h)[c]	4.4 ± 1.0	2.5 ± 1.3	1.3 ± 0.3	1.7 ± 1.2	1.5 ± 0.7	1.3 ± 0.8

[a] t_a: calculated adjustment time;
[b] $t_{\beta\text{-GAL}}$: estimated time to first lactase production;
[c] t_{lacZ}: first time *lacZ* mRNA detection.

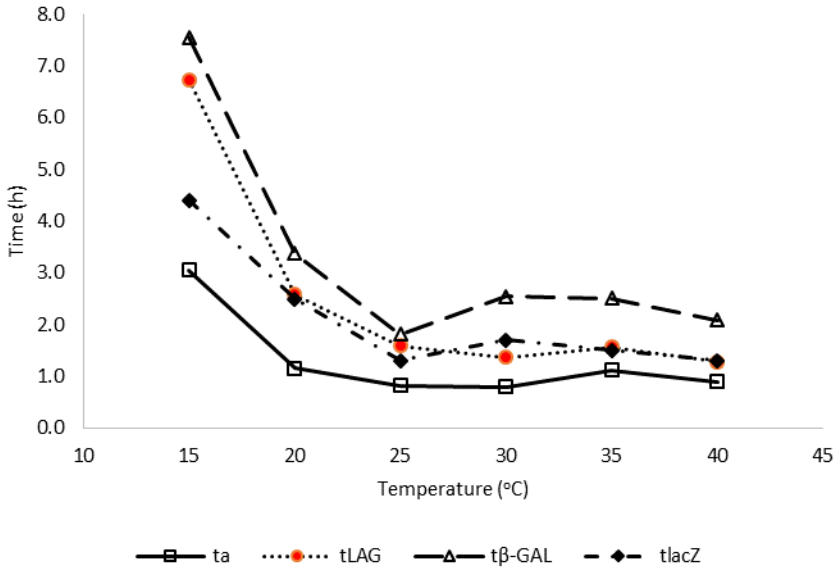

Figure 5.6 Comparison of t_{LAG}, t_a, $t_{\beta\text{-GAL}}$, and t_{lacZ} of *Escherichia coli K-12* after a nutritional shift from BHI to T-G+L medium at different temperatures

5.5 Discussion

While cells are initially cultured in one environment and then being transferred to a different environment, a lag phase is induced. Although a number of studies have been published, most of them focused on estimating the duration of lag phase and on evaluating environmental factors that may influence the length of lag phase.

Surprisingly few works have been done to investigate possible metabolic events including gene expression and enzyme activity during this adaption process (*104*). This knowledge gap is partly due to the relative low concentration and metabolic activity of cells during this period (*150*). These technical difficulties were overcome by using high-sensitivity instrumentation and modified data analyses strategies.

Regular analysis of lactase activity usually includes the construction of standard curve using ONP standard solution with known concentrations. The absorbance data is further calculated for corresponding enzyme activity through standard curve and converting equation (*4, 115*). Considering the extremely low enzyme activity during lag phase, the conventional analysis was not appropriate in this study. However, the main purpose of this experiment was to identify the time course of a series metabolic events. Therefore, it is more important to estimate the critical times when key events taking place rather than to quantify the effects. The same situation occurred in gene expression study. As indicated in **Table 5.2**, no lactase activity was detected in cells cultured in T-G broth as expected since lactase is only induced with presence of lactose or other allolactoses. On the contrary, for all the cells cultured in T-G+L broth, the existence of break points were confirmed under all six temperatures. A comparison was made among the adjustment time, lag time and the estimated time to first lactase production. At all temperatures (**Figure 5.4**), the estimated time to first lactase production consistently occurred slightly after the completion of lag phase. The exact mechanism has not been clearly elucidated, so it is difficult to give a confirmed explanation. One possible reason lies in the insensitivity of ONPG method and its high detection threshold. Combined with the results obtained from *lacZ*

mRNA study, a more likely explanation is proposed based on regulatory mechanism of *lac* operon. While cells cultured to stationary phase, the overall metabolite activity and physiological state are relatively low. After it being transferred to a new medium containing different carbon source, it seems to first live on the limited initial resources to synthesize transporter and other critical catabolic genes. After that, substrate influx increases, resulting in increased expression. When the expression level crosses the bottleneck, cells start to grow afterwards (*150*). For example, if lactose is added as alternative carbon source, half of the molecules are transformed into inducer allolactose that further binds to the *lac* repressor thereby initiate expression of *lac* operon and produce *lacZYA* mRNA (*82*, *173*). During the first part of lag period (t_a), it seems that the promotor of *lac* operon was not activated or was activated in an extremely low level, instead, cells repaired previous cell damage (*47*) and generated enough activation energy for catalytic hydrolysis (*92*). Similar result was reported by Madar et al. (*104*) that only a few promoters was measurably active during adjustment period and *lacZ* was not one of them. After the transcription to messenger RNA, translation of corresponding protein follows (*85*). However, we observed a considerable time span between these two events. This result is controversial with previously published study which demonstrated an almost immediate induction of *lacZ* expression and lactase activity (*8*). Considering that they were using *Salmonella* instead of *E. coli*, it is not appropriate to make analogous conclusion in our study, not to say they use exponentially-grown cells with high metabolic activity.

RT-qPCR was performed to detect the *lacZ* mRNA expression of *E. coli* K-12 during lag and early exponential phase. Normally, the results of qPCR is further analyzed and mRNA level is quantified through either absolute or relative method (*127*). Briefly, for absolute quantification, a standard curve is constructed beforehand using a template with known concentration; for relative quantification, the target gene is normalized to a reference gene first and then described as an increase or decrease relative to the calibrator (*100, 131*). In this study, an attempt was made to quantify the *lacZ* mRNA expression levels and to compare the fold change at different sampling points. However, we failed to provide accurate estimates due to several reasons:

1) Unequal efficiency of the PCR reaction.

While performing relative quantification, the most widely used method is the delta-delta Ct method proposed by Livak in 2001 (*100*). The prerequisite of using this method is that the amplification efficiency for both target and reference genes should be close to 100% and within 5% to each other (*63*). However, this assumption cannot be fulfilled in this study due to the extremely low abundance of *lacZ* mRNA expression during lag phase.

2) Too many undetermined or absent Ct values.

Missing data include undetermined value that expressed under the limit of detection or absent value when no reaction takes place (*63*). The handling of N/A values is of great importance since it may arise statistical bias. Currently, three methods are commonly used to deal with the N/A data. First and also the simplest way is, if enough replicates are available, the missing data can be excluded as an outlier. However, this is not applicable in our situation since too many values were marked as

non-detectable. The second method is to assign the maximum cycle number (40 in Bio-Rad) to substitute the missing data. Recent study showed that it might produce a deviation in the sample mean due to outlier creation (*127*). And also this is only valid on the assumption that the target gene can be detected if more cycles are performed. Thirdly, the missing value can be imputed according to other existing data, which, again, may lead to inflated results (*108*).

3) Inappropriate reference gene.

Reference gene is often used as an internal control to compensate for variability in the amount of input template, as well as the difference in efficiency of RNA extraction and reverse transcription (*49*). The reference gene should remain a constant level under most conditions and is not influenced by different treatments. One of the most commonly used reference gene is 16S rRNA (*20*, *71*, *72*). In this study, 16S rRNA was chosen as the reference gene and its quantity was relatively steady during both lag and stationary phases. However, the *lacZ* mRNA level was extremely low during the lag phase, the corresponding Ct value was around 28-35, which is much larger compared to 16S rRNA. This results in large delta Ct value and therefore meaningless $2^{-\text{delta-delta Ct}}$ in data analysis. Therefore, 16S rRNA might not be a perfect reference gene while investigating a target gene with relative low expression level.

Because of all the reasons mentioned above, a qualitative result showing whether the *lacZ* mRNA was present or absent at specific time point is presented. Rather than quantifying and comparing the expression level, the focus was addressed on the first time point when the signal was detectable. The amplification of reference gene was used to ensure the extracted RNA quantity and quality.

To improve the reliability and accuracy of this experiment, we recommend the use of probe-based method such as TaqMan probes instead of SYBR Green to achieve increased specificity and sensitivity (*127*). Moreover, new primers need to be designed with product size shorter than 200 bp for the sake of higher efficiency. There is a potential that alternative gene other than 16S rRNA might be more suitable as the reference gene while the expression level of target gene is relatively low.

Chapter 6: Transition from Exponential Phase to Stationary Phase

6.1 Background

Bacterial growth is influenced by an array of environmental conditions. One of the chief factors is oxygen concentration. *Escherichia coli* K-12 is classified as facultative anaerobe that can survive with or without the presence of oxygen, with appropriate amounts of oxygen being preferable. Bacterial growth rate depends largely on the amount of dissolved oxygen available (*35*). Usually a typical growth study is carried out in liquid broth with limiting soluble oxygen. Agitation during culturing can substantially enhance aeration and nutrient diffusion, and has been confirmed to have a significant impact on bacterial growth kinetics (*38*). One hypothesis is with accelerated agitation rates, the transition period of exponential to stationary phase is more abrupt compared to mild or non-agitation.

When studying the transition period from exponential to stationary phase, another critical factor to be considered is the inoculum size. A number of studies have reported that as the inoculum size decreases, both the mean lag phase duration and the corresponding variation increase (*11*, *14*, *90*, *164*). However, this finding was based on liquid culture and the difference was only significant when the inoculum size was relatively small. The effect of inoculum size on late exponential and early stationary phase in solid matrices has not been finely investigated. By adding appropriate amount of agar into the culturing broth, the newly-formed solid matrices restricts the movement of microorganisms, thus the cells will develop into micro-colonies (*106*).

Since the nutrient diffusion distance varies, it is assumed that the transition period will be more abrupt while the inoculum size is higher compared to the one with lower inoculum size.

During stationary phase, considerable changes take place in cells metabolic systems (*88, 153*). One critical protein involved in this process is RpoS. RpoS is a central regulator that affects the expression of a large number of genes in response to multiple stimulus in environment such as nutrient depletion, heat shock, acid stress, etc. (*101*). It is assumed that the gene encoding RpoS, which called *rpoS*, is being transcribed in late exponential and early stationary phase. Thus, it can be used as a specific indicator that independently verifies the transition from exponential to stationary phase.

6.2 Study Objectives

The major objective of this experiment was to test the hypothesis that the transition from exponential to stationary phase is primarily associated with spatial nutrient depletion where growth rates are increasingly dependent upon nutrient diffusion rates. The specific objectives were:

1) To investigate the influence of agitation rate on the shape of growth curve;
2) To study the influence of inoculum size on the transition period of exponential/stationary phase in solid matrices;
3) To test if *rpoS* gene could be used as an indicator of the onset of stationary phase.

6.3 Materials & Methods

6.3.1 Agitation Rate

In this experiment, *E. coli* K-12 cells were grown in BHI broth to early stationary phase and transferred to two liquid media: tryptic soy broth without dextrose (T-G) and tryptic soy broth without dextrose supplemented with 0.5% w/v lactose (T-G+L). Cells were cultured with different agitation rates (0 rpm, 10 rpm, and 30 rpm) at 15, 25, and 35ºC until early stationary phase. Samples were taken at designated time intervals and growth was measured by viable count method. The flow chart of this experiment is shown in **Figure 6.1**.

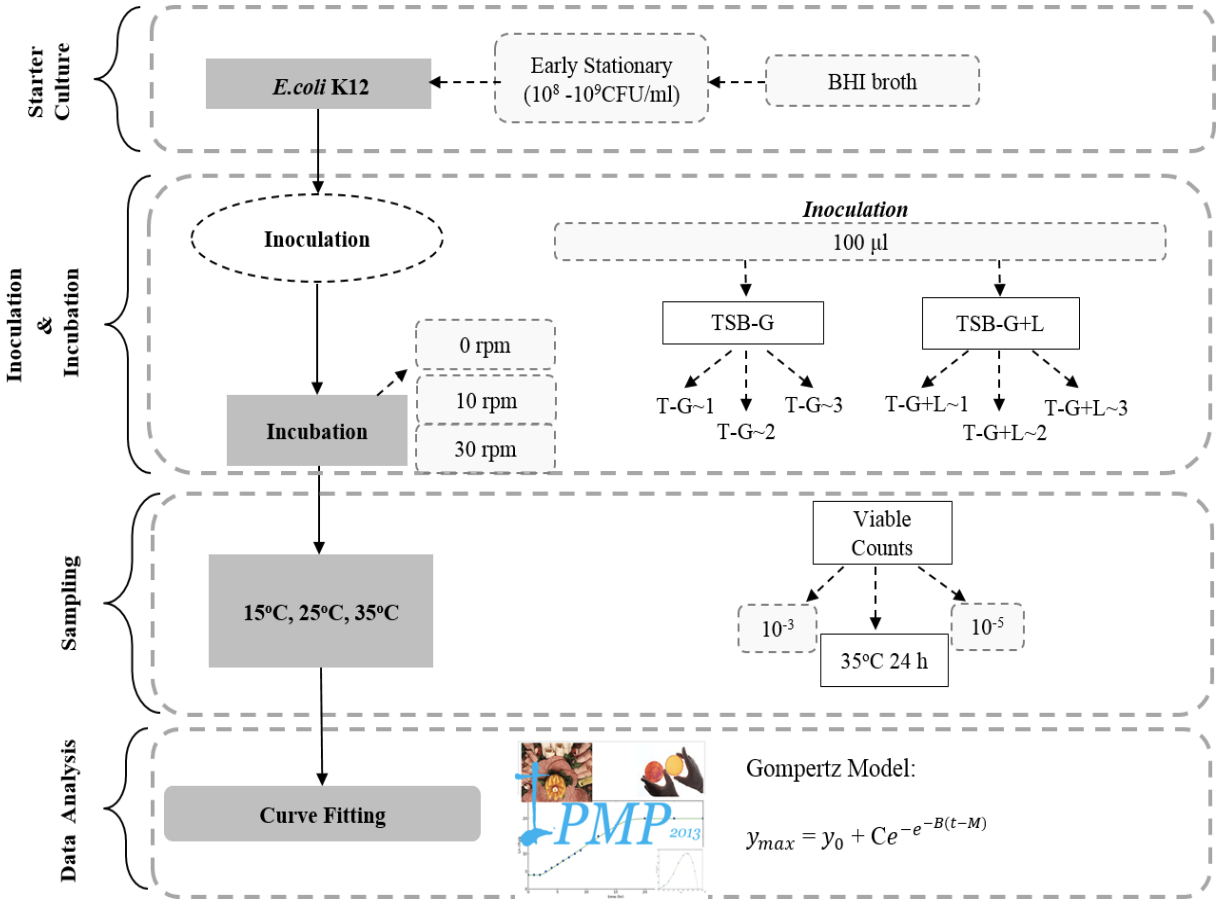

Figure 6.1 Flow diagram of sampling plan of *E. coli* K-12 cultured at different agitation rates

Preparation of Inoculum

Preparation of inoculum was performed as described in Chapter 4 section 4.3.1. Briefly, a single colony was picked from the stock plate and revived in BHI broth. After 24 h incubation at 37^{o}C, *E. coli* K-12 cells were sub-cultured again in a second BHI broth and pre-adapted at the temperature into which the cells would be transferred.

Inoculation

Two media broths were used in this experiment: tryptic soy broth without dextrose (TSB-G) and TSB broth without dextrose supplemented with 0.5% w/v lactose (TSB-G+L). Both media were prepared and autoclaved at 121^{o}C for 15 min and then distributed to a set of three sterile 250 ml Erlenmeyer flasks each containing 100 ml broth. 100 µl of the starter culture was transferred to each flask, and randomly distributed by gently mixing.

Incubation

The inoculated cultures were incubated at 15^{o}C, 25^{o}C, and 35^{o}C (±0.5^{o}C) at different agitation rates, 0 rpm, 10 rpm, and 30 rpm, on a low speed orbital shaker (Corning, MA, USA) for designated time periods.

Sampling

Immediately after inoculation, 1 ml of the culture from each flask was saved as the 0 h sample. Samples were taken at specified time intervals, with extensive sampling during the transition of exponential/stationary phase and a few points during the lag and exponential phases. The sampling times were determined by incubation temperatures and agitation rates.

Viable Count

Viable count method was used to determine cell levels in the samples. Serial dilutions were obtained using 0.1% peptone water as described in Chapter 4 section 4.3.3. After serial dilution, a small volume (50 µl) of both 10^{-3} and 10^{-5} dilutions were plated onto pre-hardened tryptic soy agar plates (TSA) using Eddy Jet 2 Spiral Plater (Neutec Group. Inc, Farmingdale, NY). All the plates were cultured inverted in 35ºC incubator for 24 h. Enumeration was conducted using Flash & Go automatic plate counter (Neutec Group. Inc, Farmingdale, NY). Both dilutions (10^{-3} and 10^{-5}) were checked for reliability and appropriate data were chosen for growth study. All the results were recorded in Excel sheets and logarithmic transformation (in natural base) was performed.

Repeated Trials

At least two trials of the experiments were conducted for each temperature × agitation rate condition following exactly the same procedures. For each single trial, three replicates were conducted simultaneously.

Curve-fitting and Data Analysis

Microbial counts from viable count method were transformed in natural logarithm (ln CFU/ml) and were used in model fitting. To take into account the variability within replicates and trials under same culturing condition, data from each replicate was fitted separately by primary model.

Re-parameterized Gompertz model (*176*) was used to describe growth curves and to estimate critical growth kinetics. The model is described in **Eq.13**:

$$y_t = y_0 + Ce^{-e^{\left(\frac{\mu_m \times e}{C}\right)(\lambda - t)+1}} \quad (13)$$

Where: y_o is the initial population density (ln CFU/ml); C is the total increase of population density when cells achieve stationary phase (ln CFU/ml); μ_m is the maximum growth rate [ln (CFU/ml)·h^{-1}]; and λ is the lag phase duration (h).

All the curve-fitting of primary models were conducted using USDA Integrated Pathogen Modeling Program 2013 (IPMP, USDA, Wyndmoor, PA) based on least-square method. Growth kinetics generated from curve-fitting of primary model for each growth condition were summarized and were used to determine other parameters (B and M) by re-arranging **Eq.10** and **Eq.12**:

$$\mu = \frac{BC}{e} \quad (10)$$

$$\lambda = M - \frac{1}{B} \quad (12)$$

Where: C equals to the net increase of population density (y_{max} - y_o); B is the relative growth rate [ln (CFU/ml)·h^{-1}]; and M represents the time when it reaches the maximum growth rate (h).

The abruptness of transition from exponential to stationary phase was estimated by the time interval (Δt) between the end of exponential phase (t_{EXP}) and the beginning of stationary phase (t_{STAT}). The time points were obtained by calculating the first and second derivatives of the Gompertz function (*29*).

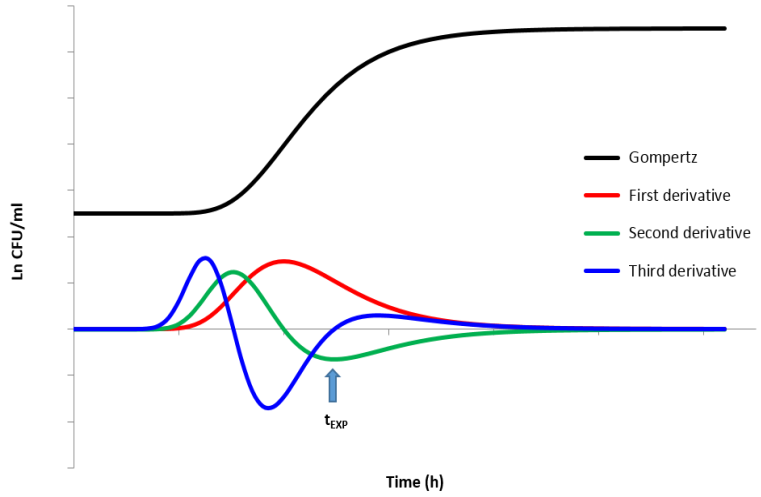

Figure 6.2 First, second, and third derivatives of Gompertz function. (Black: original Gompertz function; red: first derivative; green: second derivative; blue: third derivative)

In the second derivative plot (green), the minimum point represents the end of exponential phase (t_{EXP}). The value of t_{EXP} was further calculated by setting the third derivative equals to zero. As time elapse, the second derivative curve infinitely approaches zero. In this study, for calculation convenience, the beginning of stationary phase (t_{STAT}) was defined as the time point when the third derivative reached 0.00001. The first, second, and third derivatives are described in **Eq.21**:

$$\frac{dy(t)}{dt} = BCe^{-e^{-B(t-M)}-B(t-M)}$$

$$\frac{dy^2(t)}{dt^2} = CB^2(e^{-B(t-M)} - 1)e^{-e^{-B(t-M)}-B(t-M)}$$

$$\frac{dy^3(t)}{dt^3} = CB^3(e^{2B(t-M)} - 3e^{B(t-M)} + 1)e^{-e^{-B(t-M)}-3B(t-M)}$$

$$Minimum\ point: t_{EXP} = \frac{BM+\ln(\frac{\sqrt{5}}{2}+\frac{3}{2})}{B} \quad (21)$$

Where: C equals to the net increase of population density (y_{max} - y_o); B is the relative growth rate [ln (CFU/ml)·h^{-1}]; and M represents the time when it reaches the maximum growth rate (h).

Analysis of Variance (ANOVA) was performed for Δt to determine the effect of different growth conditions (agitation rate and culturing media). Tukey's HSD test and student's t test were used to compare the difference of abruptness (Δt) under different growth conditions. A *P* - value ≤ 0.05 was considered to be statistically significant. All the statistical analyses were performed in JMP® Pro 10 (SAS Institute, Cary, NC).

6.3.2 Inoculum Size

Starter Culture Preparation

Escherichia coli K-12 (ATCC 23716) was kept as described in Chapter 4 section 4.3.1. A single colony from the plate was then picked and sub-cultured twice in sterile BHI broth at 37°C for 24 h. Early stationary phase cells at level of 10^8 - 10^9 CFU/ml were yielded. Serial dilutions were then made to obtain the desired initial inoculum density. A total of five inoculum sizes were prepared and examined: 10^2, 10^3, 10^4, 10^5, and 10^6 CFU/ml.

Inoculation and Incubation

A 2% (w/v) agar was added to both media broth T-G and T-G+L to create the solid system. After being autoclaved at 121°C for 15 min, the broth was kept liquid under 50°C. Appropriate amount of the prepared inoculum were transferred and mixed thoroughly. A total of 60 petri dishes were used and filled with the modified media broth (30 plates for each medium). After the gel solidified, a pipette was used to add

another 5 ml gel on top of the solidified plates to prevent surface growth. All the plates were incubated at 35ºC incubator.

Sampling

After inoculation, one set of plates (6 plates each sampling time) was immediately sampled to provide the 0-h sample. After the first sampling, at specified time intervals, a set of plates was taken out of the incubator and processed until early stationary phase. The whole content in each plate was transferred into a Whirl-Pak® filter bag (NASCO, Fort Atkinson, WI). 180 ml 0.1% peptone water was added in each bag and stomached in stomacher (Seward, Stomacher 400 circulator, U.K.) for 2 minutes at 250 pulses per min at room temperature. This served as 10^{-1} dilution. 10^{-3} and 10^{-5} dilutions were further obtained by transferring 0.1 ml of the previous dilutions into new 9.9 ml 0.1% PW blanks. After serial dilution, 50 µl of the 10^{-3} and 10^{-5} dilutions were plated onto pre-hardened TSA plates using Eddy Jet 2 Spiral Plater (Neutec Group. Inc, Farmingdale, NY). All TSA plates were cultured inverted in 35ºC incubator for 24 h. Enumeration was conducted using Flash & Go automatic plate counter (Neutec Group. Inc, Farmingdale, NY). Both dilutions (10^{-3} and 10^{-5}) were checked for reliability and appropriate data were chosen for growth study. All the results were recorded in Excel sheets and logarithmic transformation (in natural base) was performed.

Repeated Trials

At least two trials of experiments were conducted for each inoculum size following exactly the same procedures. For each single trial, three replicates were conducted simultaneously.

Curve-fitting and Data Analysis

Microbial counts from viable count method were transformed in natural logarithm (ln CFU/ml) and were used in model fitting. To take into account the variability within replicates and trials under same culturing condition, data from each replicate was fitted separately by primary model.

Modified logistic model without lag phase (*52*) was used to describe growth curves and to estimate critical growth kinetics. The model is described in **Eq.22**:

$$y_t = y_o + y_{max} - \ln[e^{y_o} + (e^{y_{max}} - e^{y_o}) \times e^{-\mu_{max} t}] \quad (22)$$

Where: y_o and y_{max} are the initial and maximum population density, respectively (ln CFU/ml); μ_{max} is the maximum growth rate [ln (CFU/ml)·h^{-1}]; and t is time (h).

All the curve-fitting of primary models were conducted using USDA Integrated Pathogen Modeling Program 2013 (IPMP, USDA, Wyndmoor, PA) based on least-square method. Growth kinetics generated from curve-fitting of primary model for each growth condition were summarized and were used to determine the transition abruptness.

The abruptness of transition from exponential to stationary phase was estimated by the time interval (Δt) between the end of exponential phase (t_{EXP}) and the beginning of stationary phase (t_{STAT}). The time points were obtained by calculating the first, second, and third derivatives of the modified logistic function (*29*).

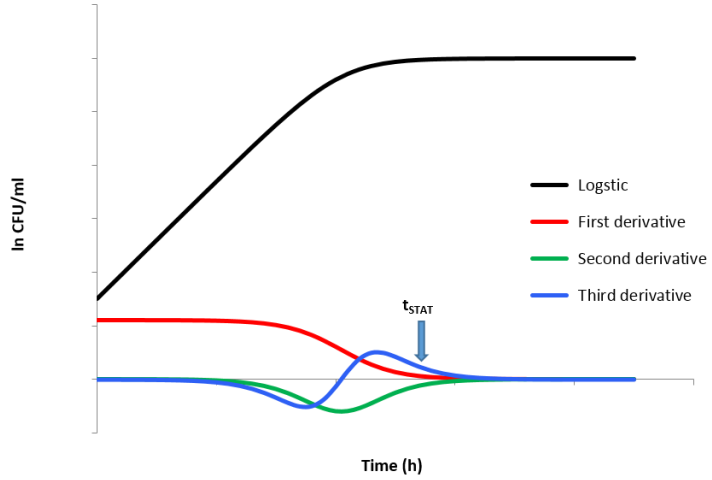

Figure 6.3 First, second, and third derivatives of modified logistic function. (Black: reduced logistic function; red: first derivative; green: second derivative; blue: third derivative)

In the first derivative plot (red), during the transition, the curve infinitely approaches zero. In this study, for calculation convenience, the beginning of stationary phase (t_{STAT}) was defined as the time point when the first derivative reached 0.01. In the second derivative plot (green), the minimum point (t_{INF}) represents the inflection point of the first derivative curve and it sits in the middle of the whole transition. The difference between t_{STAT} and t_{INF} equals to ½ Δt. The value of t_{INF} was further calculated by setting the third derivative equals to zero. The first, second, and third derivatives are described in **Eq.23**:

$$\frac{dy(t)}{dt} = \frac{(e^{y_{max}} - e^{y_o}) \times \mu_{max}}{e^{\mu_{max}t+y_o} + e^{y_{max}} - e^{y_o}}$$

$$\frac{dy^2(t)}{dt^2} = -\frac{(e^{y_{max}-e^{y_o}}) \times {\mu_{max}}^2 \times e^{\mu_{max}t+y_o}}{(e^{\mu_{max}t+y_o+e^{y_{max}-e^{y_o}}})^2}$$

$$\frac{dy^3(t)}{dt^3} = \frac{(e^{y_{max}} - e^{y_o}) \times {\mu_{max}}^3 \times e^{\mu_{max}t+y_o} \times (e^{\mu_{max}t+y_o} - e^{y_{max}} + e^{y_o})}{(e^{\mu_{max}t+y_o} + e^{y_{max}} - e^{y_o})^3}$$

$$Minimum\ point: t_{INF} = \frac{\ln(e^{y_{max}} - e^{y_o}) - y_o}{\mu_{max}} \quad (23)$$

The end of exponential phase (t_{EXP}) was then determined by re-arranging **Eq.24** and solving for t_{EXP}:

$$t_{STAT} - t_{INF} = \frac{1}{2}\Delta t = \frac{1}{2}(t_{STAT} - t_{EXP}) \quad (24)$$

Analysis of Variance (ANOVA) was performed for Δt to determine the effect of different inoculum sizes. Tukey's HSD test and student's t test were used to compare the difference of abruptness (Δt) under different inoculum sizes. A *P* - value ≤ 0.05 was considered to be statistically significant. All the statistical analyses were performed in JMP® Pro 10 (SAS Institute, Cary, NC).

6.3.3 The rpoS mRNA Expression

RNA isolation & purification

1) RNA isolation

Sample collecting was performed as described in section 6.3.2. Two trials of experiments were conducted for each inoculum size following exactly the same procedures. For each single trial, three replicates were conducted simultaneously. Briefly, BHI-grown *E. coli* K-12 cells were cultured to early stationary phase and then diluted to obtain the desired inoculum sizes (10^2, 10^4, and 10^6 CFU/ml). The prepared inoculum were transferred to 2% (w/v) agar system (T-G+L), solidified, and then overlaid with additional top agar to prevent surface growth. The cultures were incubated at 35ºC incubator and sampled for designated time period until early stationary phase. A 3-ml aliquot of the 10^{-1} dilution was divided between two 1.5 ml centrifuge tubes. Cells were harvested and centrifuged at 4ºC at 2,000×g for 5 min. 1

ml TRIzol® (Life technologies, Carlsbad, CA) was added to lyse *E.coli* K-12 cells. RNA extraction was conducted through homogenizing, phase separation (0.2 ml chloroform), RNA precipitation (0.5 ml isopropanol) and RNA wash (75% ethanol), as per manufacturer's instructions. RNA pellet was resuspended in RNase-free water and incubated in a heat block set at 55°C for 10 min.

2) RNA purification

Remaining DNA that might influence downstream applications was removed by adding 2 µl RNase-free DNase I (Life technologies, Carlsbad, CA) into 2 µg RNA and incubating with 2 µl 10× reaction buffer with $MgCl_2$ and appropriate amount of DEPC-treated water in a total volume of 20 µl at 37°C for 30 min. DNase I activity was stopped by addition of 2 µl 50mM EDTA and incubated at 65°C for 10 min (*49*). RNA yield and quality was determined using NanoDrop 1000 spectrophotometer (Thermo Fisher Scientific, Wilmington, DE) based on A_{260}/A_{280} ratio (1.8 ~ 2.0).

cDNA synthesis

The cDNA synthesis was carried out using iScript™ cDNA kit (Bio-Rad, Hercules, CA) following the manufacturer's instructions. A total volume of 20 µl reaction mixture was used containing 4 µl of 5× iScript™ reaction mix (using random primers), 1 µl iScript™ reverse transcriptase, and 500-1000 ng RNA template. Appropriate amount of ultrapure N-free water was added to adjust the volume. The synthesis was performed in Bio-Rad T100™ thermal cycler (Bio-Rad, Hercules, CA). Complete thermal cycle consists of incubating at 25°C for 5 min, synthesis at 42°C for 30 min followed by 85°C for 5 min to inactivate reverse transcriptase. Synthesized cDNA was stored at -20°C freezer until used.

RT-qPCR

The *rpoS* gene which encoding RpoS was the target gene in this study. The "housekeeping gene" 16S rRNA was used as endogenous reference to normalize the variance in total RNA quantity. The primer pairs used for amplification were synthesized by Integrated DNA Technologies with T_m (melting temperature) set to 60°C (IDT, San Diego, CA). The primers are described in **Table 6.1**.

Table 6.1 RT-qPCR primer pairs for 16S rRNA and *rpoS* of *E. coli* K-12

Gene name	Primer (5'-3')	Reference
16S rRNA	F: GTTAATACCTTTGCTCATTGA	(*56*)
	R: ACCAGGGTATCTAATCCTGTT	
rpoS	F: GCAGAGCATCGTCAAATGGCTGTT	(*77*)
	R: ATCTTCCAGTGTTGCCGCTTCGTA	

Universal SYBR Green super mix kit (Bio-Rad, Hercules, CA) was used in qPCR according to manufacturer's protocol. Briefly, the reaction was carried out in 10 µl of total volume containing 5 µl of SYBR Green super mix, 1 µl of each primer (4 µM), 2 µl 1:10 diluted cDNA, and 1 µl DEPC-treated water. To minimize the inter-assay variability, one PCR master mix (including all the essentials except cDNA template) was prepared, mixed thoroughly and distributed to each individual well. The reaction was performed in triplicates under following conditions by CFX96 Bio-Rad system (Bio-Rad, Hercules, CA): 95°C for 10 min followed by 40 cycles of denaturing at 95°C for 5 sec, annealing and extension at 60°C for 30 sec. Fluorescence readings were taken after each cycle following the extension step. Melting curve analysis was also performed to determine the specificity of the reaction using default program: 65-

95°C, 0.5°C increments at 5 sec/step. Additional NTC (no template) and NRT (no reverse transcriptase) controls were run at the same time to eliminate contamination of reagents and remaining DNA fragments.

Data Analysis

In this study, reactions with Ct values higher than 35 or N/A were defined as negative (no detectable) according to manufacturer's instructions. SYBR Green is used as the fluorescent dye in this study for convenience and financial considerations. The biggest disadvantage of this decision was non-specificity binding. To confirm the specificity of amplification, each target gene was double checked with melting-curve analysis. A positive amplification should have a reasonable Ct value smaller than 35 and a single peak in melting curve with the right Tm. The threshold time of induction of *rpoS* gene was determined as the first time point of positive amplification result.

6.4 Results

6.4.1 Agitation Rate

Curve-fitting

Figure 6.4 shows the growth curve of *E. coli* K-12 cultured at 25°C, 10 rpm as an example. *Escherichia coli* K-12 grown on T-G medium fit the Gompertz model well with a RMSE (root mean square error) of 0.254.

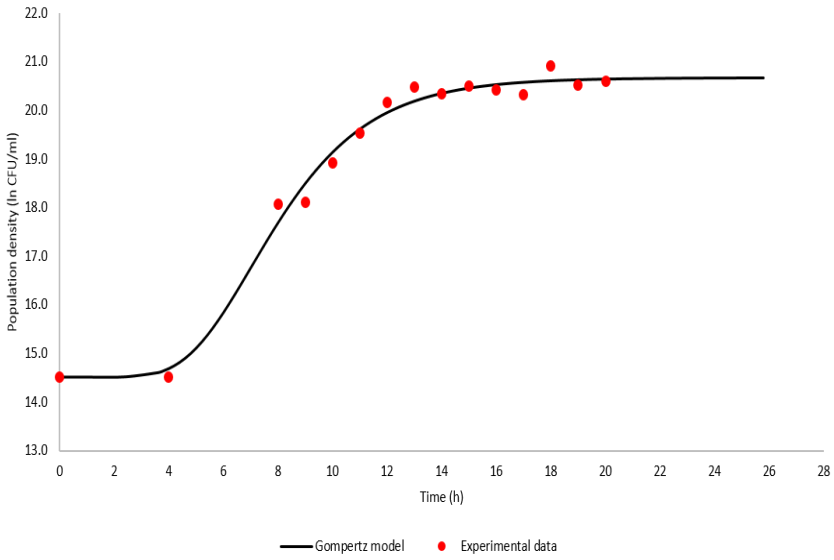

Figure 6.4 Growth of *Escherichia coli* K-12 at 25°C, 10 rpm in T-G medium. Points represent experimental data and the line corresponds to the fit of Gompertz growth model using IPMP.

Abruptness estimation

Table 6.2 summarizes the means and standard deviations of the end of exponential phase (t_{EXP}), the beginning of stationary phase (t_{STAT}), and the transition abruptness (Δt) values.

Table 6.2 Parameters of growth curve transitions of *Escherichia coli* K-12 grown in T-G and T-G+L under different temperatures and agitation rates.

Temperature (°C) - Agitation rate (rpm)	Parameters					
	T-G			T-G+L		
	t_{EXP}	t_{STAT}	Δt	t_{EXP}	t_{STAT}	Δt
15-0 rpm	32.8 ± 4.6[a]	85.4 ± 12.0	52.6 ± 7.6	38.1 ± 4.7	99.7 ± 11.9	61.5 ± 7.4
15-10 rpm	24.7 ± 0.9	64.1 ± 2.5	39.4 ± 2.9	28.3 ± 1.2	83.1 ± 5.5	54.8 ± 4.3
15-30 rpm	26.9 ± 1.3	74.0 ± 8.7	47.1 ± 8.0	30.9 ± 1.8	86.5 ± 5.4	55.6 ± 3.8
25-0 rpm	10.1 ±0.7	44.9 ± 8.0	34.9 ± 7.3	12.0 ± 1.7	50.8 ± 9.4	38.8 ± 7.6
25-10 rpm	9.4 ± 0.1	35.1 ± 3.7	25.7 ± 3.6	10.2 ± 0.2	41.7 ± 3.4	31.5 ± 3.5
25-30 rpm	9.4 ± 0.1	22.5 ± 1.2	13.1 ± 1.2	10.2 ± 0.2	33.0 ± 2.9	22.8 ± 3.0
35-0 rpm	3.5 ± 0.3	14.9 ± 2.0	11.3 ± 1.8	4.0 ± 0.1	18.1 ± 3.4	14.0 ± 3.3
35-10 rpm	4.4 ± 0.4	20.1 ± 2.3	15.7 ± 2.1	4.6 ± 0.2	19.7 ± 3.2	15.1 ± 3.1
35-30 rpm	3.9 ± 0.2	15.5 ± 3.0	11.5 ± 2.9	4.4 ± 0.3	21.3 ± 1.7	16.9 ± 1.4

[a] Mean ± standard deviation

Comparison of transition abruptness under different conditions

The results of the ANOVA indicated that agitation rate, temperature, and medium type all had significant influences on transition abruptness, with *P* value less than 0.0001 (**Table. 6.3)**. The interactions between agitation rate and temperature, and between medium type and temperature both affected the transition abruptness with a *P* value less than 0.0001 and 0.0037, respectively. However, neither the interactions between agitation rate and medium type nor the interactions among all the three variables had significant effects on the transition abruptness. ($P = 0.5828$, $P = 0.2774$, respectively). Since the interactions also played a role, the transition abruptness under different conditions were evaluated separately.

Table 6.3 Effects of agitation rate, temperature and medium type on the transition of *Escherichia coli* K-12 growth curve.

Source	DF	Sum of squares	F ratio	Prob > F
Agitation Rate (R)	2	829.771	18.3073	<.0001
Medium (M)	1	822.023	36.2728	<.0001
Temperature (T)	2	22080.15	487.1571	<.0001
R × M	2	24.675	0.5444	0.5828
R × T	4	1100.123	12.1361	<.0001
M × T	2	276.581	6.1022	0.0037
R × M × T	4	118.275	1.3048	0.2774

Transition abruptness as a function of agitation rate

The results from Tukey's test showed that for *E. coli* K-12 grown in T-G broth at 15°C, no significant differences in Δt were observed among three agitation rates. For cells cultured at 25°C, the transition was significantly more abrupt at 30 rpm, while with cells cultured at 35°C, the transition was significantly more gradual at 10 rpm. For *E. coli* K-12 grown in T-G+L broth, significant differences in Δt only existed at 25°C (**Figure 6.5**).

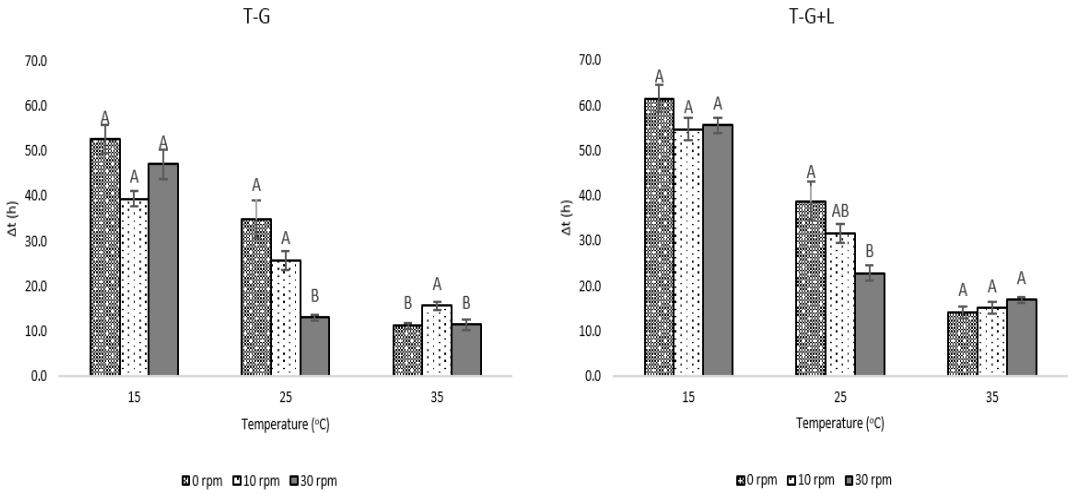

Figure 6.5 Comparison of transition abruptness (Δt) at different agitation rates. Means with different letters are significantly different. ($P \leq 0.05$)

Transition abruptness as a function of medium type

The results from Student's t test shows that for *E. coli* K-12 grown at 15ºC, the transitions for cells cultured in T-G were more abrupt than that in T-G+L, but only at 10 rpm, was the difference statistically significant. Similar conclusions were derived for cells cultured at 25ºC and 35ºC: significant differences were only observed at 30 rpm while at both 0 and 10 rpm, transitions in T-G were slightly more abrupt than that for T-G+L (**Figure 6.6**).

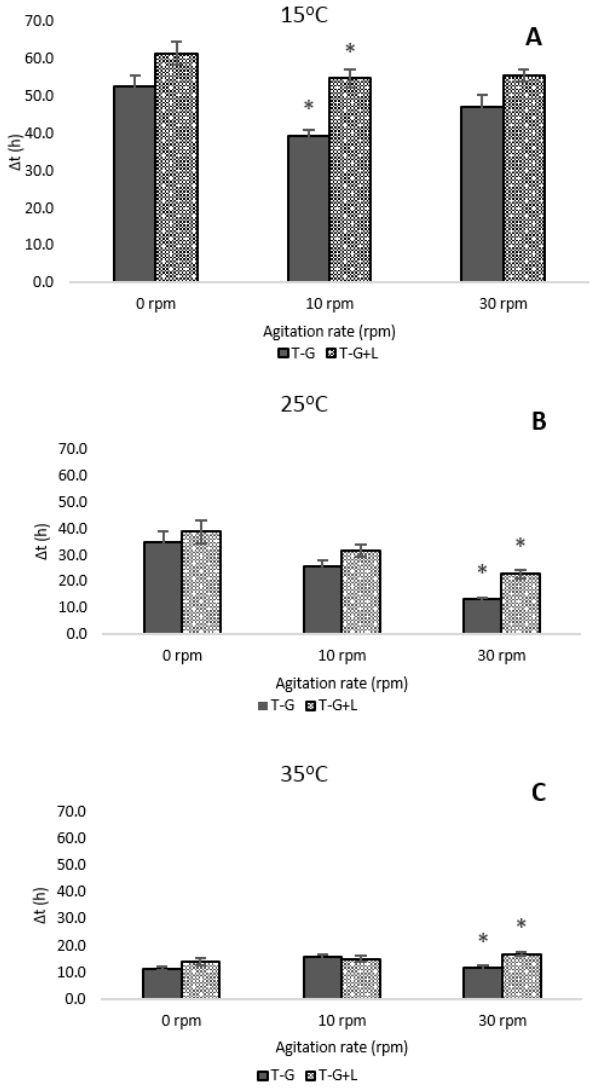

Figure 6.6 Comparison of transition abruptness (Δt) at different medium type. Data sets with * mark were significantly different ($P \leq 0.05$). (A: cells cultured at 15ºC; B: cells cultured at 25ºC; C: cells cultured at 35ºC)

Transition abruptness as a function of temperature

Results from Tukey's test shows that for *E. coli* K-12 grown in both T-G and T-G+L medium, at same agitation rate, the transition was significantly more abrupt at higher temperatures (**Figure 6.7**).

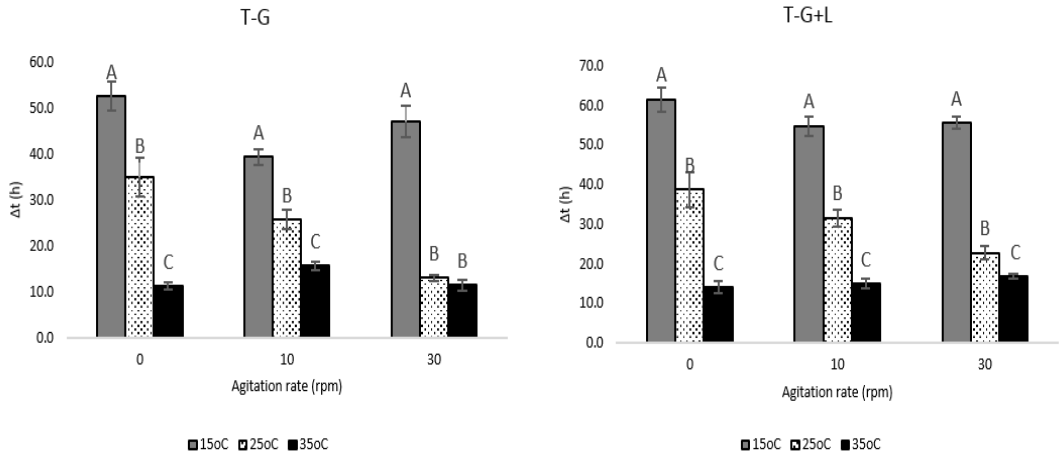

Figure 6.7 Comparison of transition abruptness (Δt) at different temperatures. Means have different letters are significantly different. ($P \leq 0.05$)

6.4.2 Inoculum Size

Curve-fitting

Figure 6.8 shows the growth curve of *E. coli* K-12 cultured in T-G+L agar with an inoculum size of 10^2 CFU/ml as an example. From the figure, *E. coli* K-12 grown on T-G+L agar fit the modified logistic model (without lag phase) well with the RMSE (root mean square error) of 0.475.

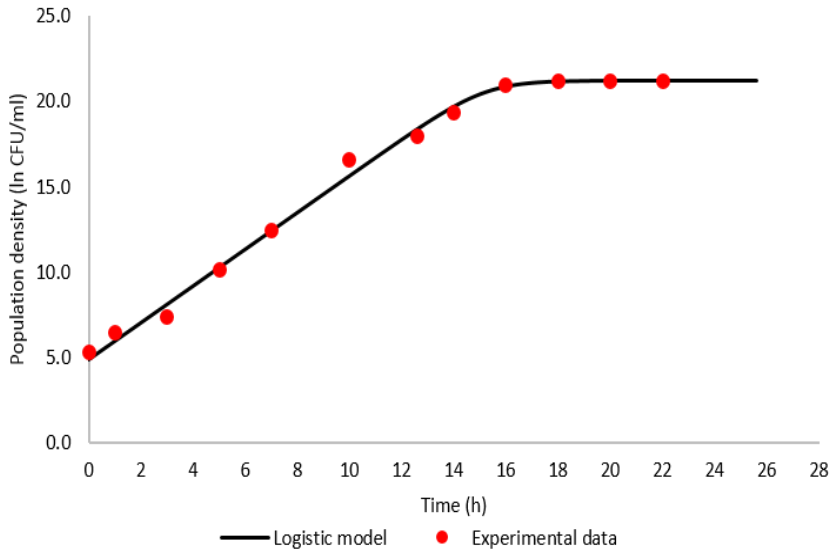

Figure 6.8 Growth of *Escherichia coli* K-12 in T-G+L agar with inoculum size of 10^2 CFU/ml. Points represent experimental data and the line corresponds to the fit of modified logistic growth model using IPMP.

Abruptness estimation

Table 6.4 summarizes the results of the end of exponential phase (t_{EXP}), the beginning of stationary phase (t_{STAT}), and transition abruptness (Δt).

Table 6.4 Parameters of growth curve transitions of *Escherichia coli* K-12 grown in T-G and T-G+L agar with different inoculum sizes.

Inoculum Size (CFU/ml)	**Parameters**					
	T-G			T-G+L		
	t_{EXP}	t_{STAT}	Δt	t_{EXP}	t_{STAT}	Δt
10^2	9.6 ± 2.1[a]	18.0 ± 3.3	8.4 ± 1.2	9.8 ± 2.0	18.2 ± 3.2	8.4 ± 1.3
10^3	8.7 ± 0.8	16.9 ± 1.5	8.2 ± 0.8	5.6 ± 2.9	11.7 ± 4.7	6.1 ± 1.8
10^4	4.6 ± 1.3	12.4 ± 1.7	7.8 ± 0.5	4.7 ± 1.2	11.7 ± 1.8	7.0 ± 0.9
10^5	3.0 ±0.7	10.4 ± 1.6	7.4 ± 0.9	3.5 ± 0.5	11.2 ± 0.8	7.7 ± 0.5
10^6	1.2 ± 0.4	8.1 ± 1.1	6.9 ± 0.9	1.8 ± 1.1	9.6 ± 2.0	7.8 ± 1.2

[a] Mean ± standard deviation

Comparison of transition abruptness at different inoculum sizes

The results of the ANOVA indicated that inoculum size and the interaction between inoculum size and medium type both significantly influenced the abruptness of the exponential to stationary phase transition (P = 0.0075, P = 0.0162, respectively) (**Table 6.5)**. No significant differences in transition abruptness were observed when medium type was evaluated as the sole factor (P = 0.1801). Since the interactions also played a role, the transition abruptness under different conditions were evaluated separately.

Table 6.5 Effects of inoculum size and medium type on the exponential/stationary transition of *Escherichia coli* K-12 growth curve.

Source	DF	Sum of squares	F ratio	Prob > F
Inoculum size	4	16.72131	3.7408	0.0075
Medium	1	2.041405	1.8268	0.1801
Inoculum size × Medium	4	14.43424	3.2291	0.0162

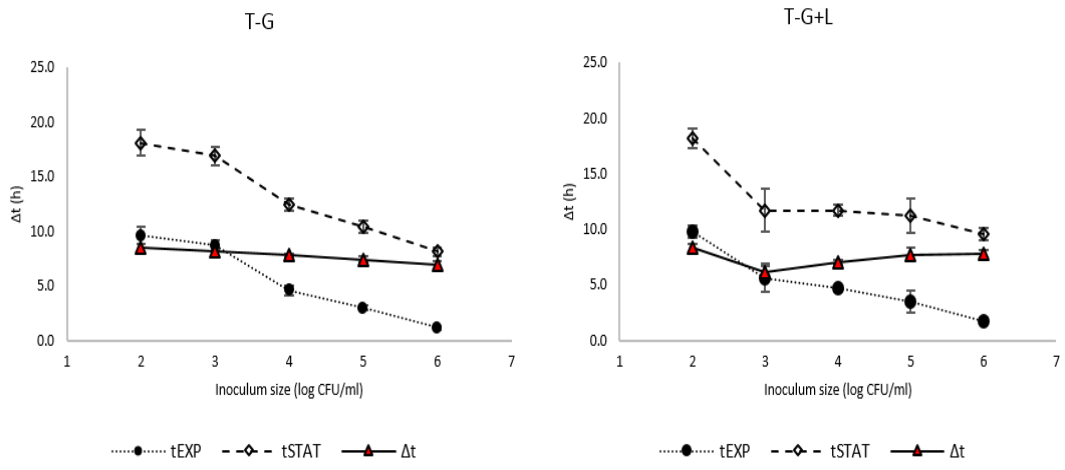

Figure 6.9 The effect of inoculum size on the transition of exponential/stationary phase for *Escherichia coli* K-12 cells cultured in both T-G and T-G+L agar (each point represents the mean of replicates with standard error shown).

When t_{EXP}, t_{STAT}, and transition abruptness (Δt) were plotted against inoculum size, it can be observed that for cells cultured in T-G agar, while the inoculum size increases, all the three parameters decrease; for cells cultured in T-G+L agar, both t_{EXP} and t_{STAT} decrease with inoculum size increase, only slight differences were observed among Δt at 10^3, 10^4, 10^5, and 10^6 CFU/ml (**Figure 6.9**).

The results from Tukey's test shows that for *E. coli* K-12 grown in T-G agar, Δt with the inoculum size of 10^2 CFU/ml was significantly longer than Δt at 10^6 CFU/ml (P = 0.0371), while no significant differences were observed among Δt at other inoculum sizes; for *E. coli* K-12 grown in T-G+L agar, Δt was significant longer at 10^2 CFU/ml than at 10^3 and 10^4 CFU/ml; Δt at 10^3 CFU/ml was significantly shorter than that at 10^6 CFU/ml, and was same as 10^4 and 10^5 CFU/ml; Δt at 10^4, 10^5, and 10^6 CFU/ml were not significantly different (**Figure 6.10**).

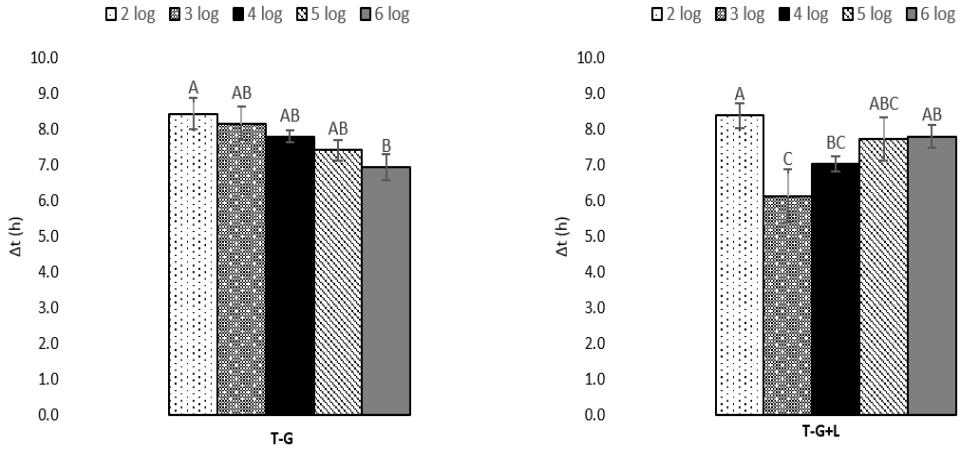

Figure 6.10 Comparison of transition abruptness from exponential to stationary phase of *Escherichia coli* K-12 cells cultured in both T-G and T-G+L agar at different inoculum sizes. Means have different letters are significantly different. ($P \leq 0.05$)

The results from student's t test indicated that no significant differences existed between the transition abruptness in T-G and T-G+L medium at all inoculum sizes

except for 10^4 CFU/ml. For 10^4 CFU/ml, cells cultured in T-G+L displayed a more abrupt transition during exponential to stationary phase (P = 0.0114) (**Figure 6.11**).

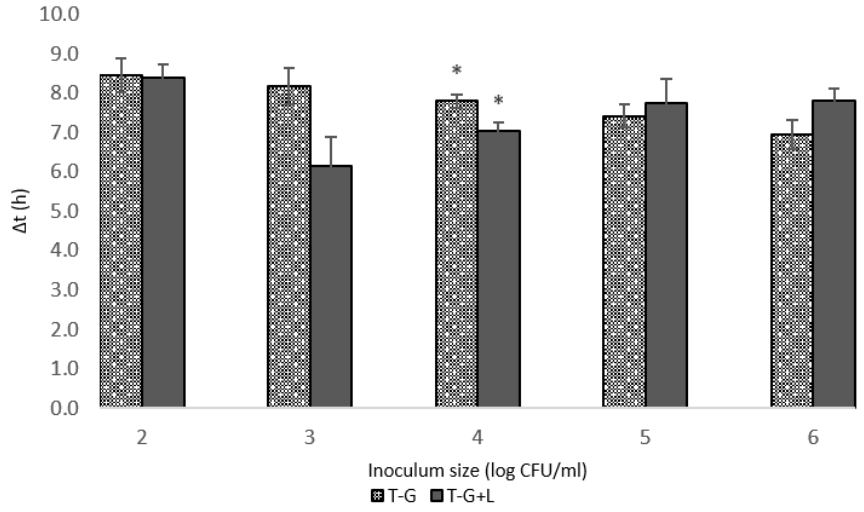

Figure 6.11 Comparison of transition abruptness of *Escherichia coli* K-12 cultured in both T-G and T-G+L medium. Data sets with * mark were significantly different ($P \leq 0.05$).

6.4.3 The rpoS mRNA expression

Table 6.6 and **Figure 6.12** show the induction time point of *rpoS* gene of *E. coli* K-12 cultured in T-G+L agar compared to other critical time points. For all the inoculum sizes, the time course of events taking place is: $t_{EXP} \rightarrow t_{rpoS} \rightarrow t_{STAT}$. The first time *rpoS* mRNA detection was slightly after the completion of exponential phase.

Table 6.6 Comparison of *rpoS* induction and critical transition points of *E. coli* K-12 cultured in T-G+L.

Inoculum size (log CFU/ml)	2	4	6
T-G+L			
t_{EXP} (h)[a]	9.8 ± 2.0[d]	4.7 ± 1.2	1.8 ± 1.1
t_{STAT} (h)[b]	18.2 ± 3.2	11.7 ± 1.8	9.6 ± 2.0
t_{rpoS} (h)[c]	11.0 ± 4.6	5.0 ± 1.0	4.5 ± 0.6

[a] t_{EXP}: estimate of the end of exponential phase;
[b] t_{STAT}: estimate of the beginning of stationary phase;
[c] t_{rpoS}: first time *rpoS* mRNA detection;
[d] mean and standard deviation.

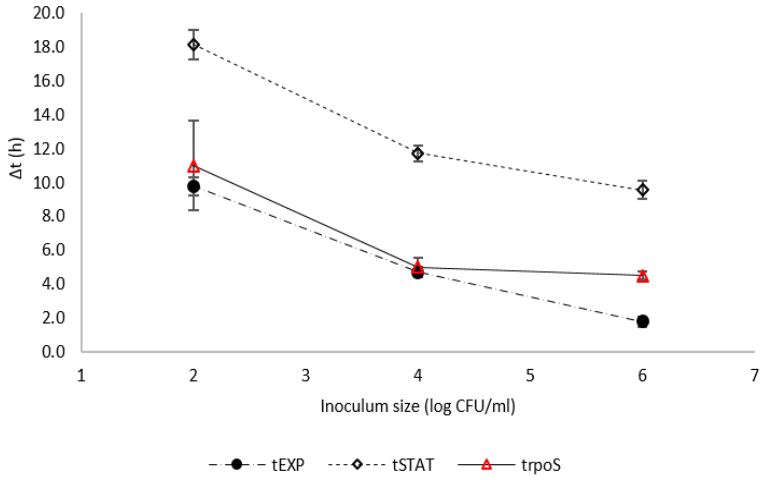

Figure 6.12 Comparison of t_{EXP}, t_{STAT}, and t_{rpoS} of *Escherichia coli K-12* cultured in T-G+L agar at different inoculum sizes (each point represents the mean of replicates with standard error shown).

6.5 Discussion

While calculating the abruptness (Δt) of exponential/stationary transition, it is important to bear in mind that the time will differ depending on what criterion is used to define the end of exponential phase (t_{EXP}) and the onset of stationary phase (t_{STAT})

(*89*). In the study of agitation rate, modified Gompertz function was chosen to fit all the growth data since it is more convenient to use Gompertz model to calculate the first, second and third derivatives than using other models such as Baranyi model. t_{EXP} was defined as the minimum point of the second derivative. The definition of t_{STAT} was relatively more implicit since the function is continuous and is approaching the maximum value infinitely. For calculation convenience, we defined t_{STAT} as the time point when third derivative reached 0.00001. This is reasonable considering that many cell functions still continue during stationary phase such as energy metabolism and biosynthetic process (*125*).

While comparing the transition abruptness at different agitation rates, it didn't follow a consistent pattern under different culturing conditions. For example, in Figure 6.5, cells cultured in T-G broth at 15^{o}C, agitation rate didn't significantly influence the transition abruptness. At 25^{o}C, with higher agitation rate, the transition was more abrupt. However, the difference was only statistically significant between the highest rate (30 rpm) and the lowest rate (0 rpm). Further, at 35^{o}C, the middle agitation rate (10 rpm), the transition to stationary phase was slightly more gradual than others. For cells cultured in T-G+L broth, impact of agitation rate only occurred at 25^{o}C. Similar to cells cultured in T-G, the difference was only statistically significant between the highest rate (30 rpm) and the lowest rate (0 rpm). It was therefore concluded that the effect of agitation rate on exponential/stationary transition abruptness in broth culture was not evident. One of the possible reasons is due to the motility characteristic of *E. coli* K-12 cells which might attenuate the impact of nutrient diffusion. An alternative explanation is that the agitation rate gradient in this study was set too small to

effectively show the actual difference. This is highly possible since another study reported that no significant differences of cell growth were found between hypoxic and anoxic conditions (*123*).

Another critical factor that may influence the transition abruptness is the composition of medium. Two media broth: T-G and T-G+L were used in this study. While investigating the possible impact of medium type, it was found that at all temperature and agitation rate combinations, the transition was consistently more abrupt in T-G broth than in T-G+L broth, although under most circumstances, the differences were not statistically different (Figure 6.6). The underlying mechanism can be ascribed to the dropping pH during growth with the addition of lactose. When oxygen is limited, the cells switched to fermentative metabolism and produced lactic acid which lowered the pH. Both the critical enzyme activities and transportation of essential nutrients slowed down because of the lower pH, therefore results in a more gradual transition to stationary phase.

A third factor that was investigated is incubation temperature. From **Figure 6.7**, it was concluded that at same agitation rate, the transition of exponential/stationary phase was significantly more abrupt at higher temperatures. This can be explained by the fact that with increasing temperature, both chemical and enzymatic activities of cells precede much faster, resulting more rapid growth.

A number of studies have reported the effect of inoculum size on bacterial growth kinetics (*11*, *14*, *90*, *164*). However, they all focused on the lag and exponential phases. To our knowledge, the effect of inoculum size on late exponential and early stationary phase is still an open field with many questions. Besides, most available

predictive models were constructed based on liquid broth. These models are routinely employed to describe the bacterial behavior in structured and solid food systems (*124*). Since the structure also played an important role in microbial growth (*23*), growth model taking account of diffusion and interaction within solid matrices is clearly desirable.

While designing this experiment, the first problem encountered was the type and concentration of solidifying reagent. Technical agar was selected as the most suitable hardening agent with a compromise between gelling and melting point and the maximum temperature that *E. coli* cells can survive (*124*). 2% (w/v) agar was added in the broth to create appropriate rigidity that allows diffusion taking place. Studies also reported considerable discrepancies of growth between surface-grown and submerged-grown cells (*124*), possibly due to oxygen concentration gradients. However, it was also suggested that among submerged-grown cells, the growth was independent of location or depth (*123*). Therefore, additional 5 ml of agar was added to solidified media in order to prevent surface growth and to eliminate undesirable interventions.

In structured system, solid matrix restricts the movement of *E. coli* K-12 cells, and forced them to form micro-colonies instead (*106*). Moreover, within and between these micro-colonies, gradient is caused by the diffusion of nutrient toward and diffusion of metabolites out of the colonies (*23*). Thus the transport distance might play a critical role in microbial growth in solid system. It was hypothesized that the higher inoculum size would display a more abrupt transition of exponential to stationary phase compared to lower inoculum size.

Reduced logistic model (no lag) was used to fit all the experimental data generated in the study of inoculum size. This model was selected to avoid false negative lag when using other full growth models. Since our research focused on the transition from late exponential to early stationary phase, this reduced model is suitable to describe *E. coli* K-12 growth.

Plotting critical time points (t_{EXP}, t_{STAT}, and Δt) against inoculum size (Figure 6.9), a general trend was observed that with higher inoculum sizes, the exponential phase ended earlier and it also entered stationary phase earlier. While comparing the effect of inoculum size on transition abruptness (Δt), different conclusions were derived for T-G and T-G+L media agar (Figure 6.10). For cells cultured in T-G agar, the transition was consistently more abrupt in higher inoculum size, although most of the differences were not statistically significant. For cells cultured in T-G+L agar, it was much more complicated: the pattern was not clear. One assumption was that while additional lactose was added in the agar, the metabolism produces lactic acid. The depression of pH and accumulation of other metabolic waste modified culturing environment together (*116*). Hence, nutrient diffusion was not the sole factor that may influence the transition abruptness.

It was also noticed that while plating the diluted *E. coli* K-12 cells on TSA plate, the size of colonies differed. A number of studies have confirmed that considerable changes occurred during stationary phase including morphological adaptions (*122*). Cells become smaller due to reductive division and dwarfing (*89*). For example, it is possible that cell division continues when most macromolecular syntheses already stopped (*126*).

The results of *rpoS* mRNA expression study show a clear time course of the critical points during exponential to stationary phase transition: first was the completion of exponential phase, slightly after that *rpoS* mRNA started to be transcribed, and finally it entered into stationary phase. This result was consistent with other studies (*77, 93*). When cells are exposed to starvation or other stresses, a reduction or cessation of growth takes place (*14*). This process is regulated by a combination of mechanism, and one of the central regulon is RpoS. It was reported that during exponential phase, the cellular RpoS level is extremely low due to basal rate of *rpoS* transcription and rapid degradation of synthesized RpoS (*69, 70*). While nutrient becomes limited, specific inducing signals such as ppGpp greatly promote *rpoS* transcription and translation, inhibits RpoS degradation, and also improves RpoS activity (*17*). Thus a dramatic increase of RpoS level can be detected at the onset of stationary phase (*80, 163*) which can be further used as the indicator stationary phase entry.

Chapter 7: Summary, Conclusions, and Recommendations for Future Research

7.1 General Findings of Study

A continuing goal in predictive microbiology is the development of more mechanistically-based models. This study tested two major hypotheses: (1) the curvilinear lag/exponential transition represents the population variability in adjustment (t_a) and metabolic (t_m) time, and (2) the exponential/stationary transition is determined by limiting nutrient diffusion rates. Findings from this research demonstrated that the traditional smooth sigmoidal curve is obtainable through three-phase linear model by simulation using standard deviations among trials. Agitation rate has very limited influence on growth kinetics in liquid broth while the transition from exponential to stationary phase is affected by inoculum size in solid system.

7.2 Conclusions

7.2.1 Transition from Lag Phase to Exponential Phase

- Both the spectrophotometric and viable count value fit the two-phase linear model (without stationary phase) well. The growth kinetics (t_{LAG} and μ) generated from these two methods were similar and convertible through standard curves.
- The exponential growth rates (μ) and their standard deviations were similar in both cultures (T-G and T-G+L), indicating that it was not influenced by medium type. The Ratkowsky model was suitable to describe the temperature

dependency of μ. It is concluded that within certain range, μ increases with higher temperature.

- The lag phase duration (t_{LAG}) and their standard deviations were similar in both cultures (T-G and T-G+L), indicating that the impact of medium type was negligible. It is concluded that higher temperatures tend to induce shorter lag phase duration. Significant differences were only observed between the lowest temperature (15^{o}C) and the other temperatures.
- Adjustment time (t_a) can be estimated by t_{LAG} and μ, and it follows the same temperature dependency as t_{LAG}, i.e., the higher temperature, the shorter t_a. However, under most circumstances, the differences were not significant.
- Using standard deviations from the trials it is possible to effectively describe the smooth sigmoidal shape of a traditional growth curve using Monte Carlo simulation method.

7.2.2 Transition from Lag Phase to Exponential Phase

- Detectable lactase activity was limited to T-G+L cultures. The estimated time for first lactose production consistently occurred slightly after the completion of lag phase.
- The estimated time for first *lacZ* mRNA transcription occurred slightly after the completion of adjustment period. The time course of the series physiological events taking place is:

  $t_a \rightarrow t_{lacZ} \rightarrow t_{LAG} \rightarrow t_{\beta\text{-GAL}}$.

7.2.3 Transition from Exponential Phase to Stationary Phase

- Modified Gompertz model was suitable for fitting the experimental data in the study of agitation rate. Agitation rate, medium type, temperature, and their interactions all influence the transition of exponential/stationary phase. The effect of agitation rate on transition abruptness is not evident. For T-G broth, the transition was more abrupt compared to T-G+L broth, but under most circumstances, the differences were not significant. For both cultures, higher temperature induced a more abrupt transition under same agitation rate.
- Reduced logistic model (without lag) was suitable for fitting the experimental data in the study of inoculum size in a solid matrix. For cells cultured in T-G medium agar, transition at higher inoculum size was consistently more abrupt than lower inoculum size, but the differences were not statistically significant. For cells cultured in T-G+L medium agar, no clear pattern was observed.
- The estimated time for first *rpoS* mRNA transcription occurred slightly after the completion of exponential phase. The time course of the series physiological events taking place is: $t_{EXP} \rightarrow t_{rpoS} \rightarrow t_{STAT}$.

7.3 Recommendations for Future Research

The results from this study support the two major hypotheses mentioned at the beginning of this chapter. These results show the possibility of developing more mechanistically-based growth models. This study is an important step in developing models that can better depict the transition periods of lag/exponential and exponential/stationary phases that take into account both the population variability

and phase-dependent physiological events. Some pitfalls still exist and a few recommendations for future research are proposed below.

- In the study of lag/exponential phase transition, a wider temperature range is required to develop the secondary model that can better describe the relationship between lag phase duration and temperature.
- In nutritional-shift experiment, the influence of medium type on both t_{LAG} and μ were not significant with current experiment design. Other modified media are potentially more powerful to maximize the differences in microbial grow kinetics.
- A specific parameter that can describe and quantify the transition abruptness of lag/exponential phase is needed. In that regard the use of second and third derivatives of different primary and secondary models appear to have potential for more quantitative metric.
- A different method that can directly quantify bacterial population density by cell size (such as flow cytometry) is necessary to get better estimate of adjustment period.
- In the study of effect of agitation rate on exponential/stationary phase transition, wider gradient and more agitation rate experiments are needed to enlarge the potential effects. Other critical factors such as pH also need to be considered, as well as quantitative data on limiting nutrients that trigger expression of RpoS synthesis.

- Specific enzyme activities such as cellular RpoS level need to be measured and tested for its reliability of being used as an indicator for the onset of stationary phase.
- Both nutrient diffusion and metabolites diffusion rate functions are required to better map the microenvironments surrounding the colonies.
- Finally, a more sophisticated growth model that includes appropriate terms for these physiological events mentioned above is needed to better describe bacterial growth.

References

1. Alavi, S. H., V. M. Puri, S. J. Knabel, R. H. Mohtar, and R. C. Whiting. 1999. Development and validation of a dynamic growth model for *Listeria monocytogenes* in fluid whole milk. *J. Food Prot.* 62:170–6.

2. Altuvia, S., D. Weinstein-Fischer, A. Zhang, L. Postow, and G. Storz. 1997. A small, stable RNA induced by oxidative stress: Role as a pleiotropic regulator and antimutator. *Cell.* 90:43–53.

3. Anonymous. 2006. lac Operons. Available at: https://en.wikipedia.org/wiki/File:Lac_operon1.png. Accessed June 10, 2016.

4. AOAC. 1995. Official method 998.04 neutral lactase (β-galactosidase) activity in industry-Dairy products, p. 10–14. *In* AOAC official methods of analysis, 17th ed. Association of Official Analytical Chemists, Washington, DC.

5. Asprey, S. P., and S. Macchietto. 2000. Statistical tools for optimal dynamic model building. *Comput. Chem. Eng.* 24:1261–1267.

6. Augustin, J. C., A. Brouillaud-Delattre, L. Rosso, and V. Carlier. 2000. Significance of inoculum size in the lag time of *Listeria monocytogenes*. *Appl. Environ. Microbiol.* 66:1706–1710.

7. Augustin, J. C., L. Rosso, and V. Carlier. 1999. Estimation of temperature dependent growth rate and lag time of *Listeria monocytogenes* by optical density measurements. *J. Microbiol. Methods* 38:137–146.

8. Balaji, B., K. O. Connor, J. R. Lucas, J. M. Anderson, and L. N. Csonka. 2005. Timing of induction of osmotically controlled genes in *Salmonella enterica* serovar typhimurium, determined with quantitative real-time reverse transcription-PCR. *Appl. Environ. Microbiol.* 71:8273–8283.

9. Baranyi, J., and T. A. Roberts. 1994. A dynamic approach to predicting bacterial growth in food. *Int. J. Food Microbiol.* 23:277–294.

10. Baranyi, J., T. A. Roberts, and P. McClure. 1993. A non-autonomous differential equation to modelbacterial growth. *Food Microbiol.* 10:43–59.

11. Baranyi, J., C. Pin, and T. Ross. 1999. Validating and comparing predictive models. *Int. J. Food Microbiol.* 48:159–166.

12. Baranyi, J., and T. A. Roberts. 1994. A dynamic approach to predicting bacterial growth in food. *Int. J. Food Microbiol.* 23:277–294.

13. Baranyi, J., and T. A. Roberts. 1995. Mathematics of predictive food microbiology. *Int. J. Food Microbiol.* 26:199–218.

14. Baranyi, J., S. M. George, and Z. Kutalik. 2009. Parameter estimation for the distribution of single cell lag times. *J. Theor. Biol.* 259:24–30.

15. Barbosa, W. B., L. Cabedo, H. J. Wederquist, J. N. Sofos, and G. R. Schmidt. 1994. Growth variation among species and strains of *Listeria* in culture broth. *J. Food Prot.* 57:5.

16. Barth, M., C. Marschall, A. Muffler, D. Fischer, and R. Hengge-Aronis. 1995. Role for the histone-like protein H-NS in growth phase-dependent and osmotic regulation of σ(S) and many σ(S)-dependent genes in *Escherichia coli*. *J. Bacteriol.* 177:3455–3464.

17. Battesti, A., N. Majdalani, and S. Gottesman. 2011. The RpoS-Mediated General Stress Response in *Escherichia coli* *. *Annu. Rev. Microbiol.* 65:189–213.

18. Baty, F., and M. L. Delignette-Muller. 2004. Estimating the bacterial lag time: Which model, which precision? *Int. J. Food Microbiol.* 91:261–277.

19. Begot, C., I. Desnier, J. D. Daudin, J. C. Labadie, and A. Lebert. 1996. Recommendations for calculating growth parameters by optical density measurements. *J. Microbiol. Methods* 25:225–232.

20. Bej, A. K., M. H. Mahbubani, J. L. Dicesare, and R. M. Atlas. 1991. Polymerase chain reaction-gene probe detection of microorganisms by using filter-concentrated samples. *Appl. Environ. Microbiol.* 57:3529–3534.

21. Bhaduri, S., C. O. Turner-Jones, R. L. Buchanan, and J. G. Phillips. 1994. Response surface model of the effect of pH, sodium chloride and sodium nitrite on growth of *Yersinia enterocolitica* at low temperatures. *Int. J. Food Microbiol.* 23:333–43.

22. Blattner, F. R., G. Plunkett, C. A. Bloch, N. T. Perna, V. Burland, M. Riley, J. Collado-vides, J. D. Glasner, C. K. Rode, G. F. Mayhew, J. Gregor, N. W. Davis, H. A. Kirkpatrick, M. A. Goeden, D. J. Rose, B. Mau, and Y. Shao. 1997. The Complete Genome Sequence of *Escherichia coli* K-12. *Sci. Mag* 277:1453–1462.

23. Boons, K., E. Noriega, R. Van den Broeck, C. C. David, J. Hofkens, and J. F. Van Impe. 2014. Effect of microstructure on population growth parameters of *Escherichia coli* in gelatin-dextran systems. *Appl. Environ. Microbiol.* 80:5330–5339.

24. Bratchell, N., A. M. Gibson, M. Truman, T. M. Kelly, and T. A. Robets. 1989. Predicting microbial growth: The consequences of quantity of data. *Int. J. Food Microbiol.* 8:47–58.

25. Brown, L., and T. Elliott. 1996. Efficient translation of the RpoS sigma factor in *Salmonella* Typhimurium requires host factor I, an RNA-binding protein encoded by the hfq gene. *J. Bacteriol.* 178:3763–3770.

26. Buchanan, R. L., and L. K. Bagi. 1994. Expansion of response surface models for the growth of *Escherichia coli* O157:H7 to include sodium nitrite as a variable. *Int. J. Food Microbiol.* 23:317–32.

27. Buchanan, R. L., and L. A. Klawitter. 1992. The effect of incubation temperature, initial pH, and sodium chloride on the growth kinetics of *Escherichia coli* O157:H7. *Food Microbiol.* 9:185–196.

28. Buchanan, R. L., R. C. Whiting, and W. C. Damert. 1997. When is simple good enough: a comparison of the Gompertz, Baranyi, and three-phase linear models for fitting bacterial growth curves. *Food Microbiol.* 14:313–326.

29. Buchanan, R. L., and M. L. Cygnarowicz. 1990. A mathematical approach toward defining and calculating the duration of the lag phase. *Food Microbiol.* 7:237–240.

30. Busby, S., and R. H. Ebright. 1999. Transcription activation by catabolite activator protein (CAP). *J. Mol. Biol.* 293:199–213.

31. Bustin, S. A. 2002. Quantification of mRNA using real-time reverse transcription PCR (RT-PCR): Trends and problems. *J. Mol. Endocrinol.* 29:23–39.

32. Butler, S. M., R. A. Festa, M. J. Pearce, and K. H. Darwin. 2006. Self-compartmentalized bacterial proteases and pathogenesis. *Mol. Microbiol.* 60:553–562.

33. Carlson, B. M. 2007. Principles of Regenerative Biology. p259-278.

34. Cassin, M. H., A. M. Lammerding, E. C. D. Todd, W. Ross, and R. S. McColl. 1998. Quantitative risk assessment for *Escherichia coli* O157:H7 in ground beef hamburgers. *Int. J. Food Microbiol.* 41:21–44.

35. Castilow, R. N. 1981. Biophysical factors in growth. *In* Gerhardt P. et al. (ed.), Manual of methods for general bacteriology. American Society for Microbiology, Washington, DC. p179-207.

36. Chang, R. 2005. Enzyme Kinetics. *Phys. Chem. Biosci.* 363–400.

37. Chesbro, W. 1988. The domains of slow bacterial growth. *Can. J. Microbiol.* 34:427–35.

38. Coleman, M. E., M. L. Tamplin, J. G. Phillips, and B. S. Marmer. 2003. Influence of agitation, inoculum density, pH, and strain on the growth parameters of *Escherichia coli* O157:H7 - Relevance to risk assessment. *Int. J. Food Microbiol.* 83:147–160.

39. Conter, A, C. Menchon, and C. Gutierrez. 1997. Role of DNA supercoiling and rpoS sigma factor in the osmotic and growth phase-dependent induction of the gene osmE of *Escherichia coli* K12. *J. Mol. Biol.* 273:75–83.

40. Contois, D. E. 1959. Kinetics of bacterial growth: relationship between population density and specific growth rate of continuous cultures. *J. Gen. Microbiol.* 21:40–50.

41. Corman, A., G. Carret, A. Pave, J. P. Flandrois, and C. Couix. 1986. Bacterial growth measurement using an automated system: mathematical modelling and analysis of growth kinetics. *Ann. l'Institut Pasteur Microbiol.* 137B:133–143.

42. Dalgaard, P., and K. Koutsoumanis. 2001. Comparison of maximum specific growth rates and lag times estimated from absorbance and viable count data by different mathematical models. *J. Microbiol. Methods* 43:183–196.

43. Dalgaard, P., T. Ross, L. Kamperman, K. Neumeyer, and T. A. McMeekin. 1994. Estimation of bacterial growth rates from turbidimetric and viable count data. *Int. J. Food Microbiol.* 23:391–404.

44. Delignette-Muller, M. L. 1998. Relation between the generation time and the lag time of bacterial growth kinetics. *Int. J. Food Microbiol.* 43:97–104.

45. Dong, T., M. G. Kirchhof, and H. E. Schellhorn. 2008. RpoS regulation of gene expression during exponential growth of *Escherichia coli* K12. *Mol. Genet. Genomics* 279:267–277.

46. Duh, Y. H., and D. W. Schaffner. 1993. Modeling the effect of temperaure on the growth rate and lag time of *Listeria innocua* and *Listeria monocytogenes*. *J. Food Prot.* 56:205–210.

47. Dukan, S., and T. Nyström. 1998. Bacterial senescence: Stasis results in increased and differential oxidation of cytoplasmic proteins leading to developmental induction of the heat shock regulon. *Genes Dev.* 12:3431–3441.

48. Dykes, G. A. 2003. Behaviour of *Listeria monocytogenes* on two processed meat products as influenced by temperature or attached growth during preincubation. *Food Microbiol.* 20:91–96.

49. Edwards, K. J., and N. A. Saunders. 2001. Real-time PCR used to measure stress-induced changes in the expression of the genes of the alginate pathway of *Pseudomonas aeruginosa*. *J. Appl. Microbiol.* 91:29–37.

50. Elliott, P. H. 1996. Predictive microbiology and HACCP. *J. Food Prot.* 48–53.

51. Esty, J. R., and K. F. Meyer. 1922. The heat resistance of the spores of *B. botulinus* and allied anaerobes. XI Comparative resistance of sporulating anaerobes to moist heat. *Source J. Infect. Dis.* 31:650–664.

52. Fang, T., J. B. Gurtler, and L. Huang. 2012. Growth kinetics and model comparison of *Cronobacter sakazakii* in reconstituted powdered infant formula. *J. Food Sci.* 77(9):247-255.

53. Fotadar, U., P. Zaveloff, and L. Terracio. 2005. Growth of *Escherichia coli* at elevated temperatures. *J. Basic Microbiol.* 45:403–404.

54. Francois, K., F. Devlieghere, K. Smet, A. R. Standaert, A. H. Geeraerd, J. F. Van Impe, and J. Debevere. 2005. Modelling the individual cell lag phase: Effect of temperature and pH on the individual cell lag distribution of *Listeria monocytogenes. Int. J. Food Microbiol.* 100:41–53.

55. Francois, K., A. Valero, A. H. Geeraerd, J. F. Van Impe, J. Debevere, R. M. Garca-Gimeno, G. Zurera, and F. Devlieghere. 2007. Effect of preincubation temperature and pH on the individual cell lag phase of *Listeria monocytogenes*, cultured at refrigeration temperatures. *Food Microbiol.* 24:32–43.

56. Gao, W., W. Zhang, and D. R. Meldrum. 2011. RT-qPCR based quantitative analysis of gene expression in single bacterial cells. *J. Microbiol. Methods* 85:221–227.

57. Gefen, O., O. Fridman, I. Ronin, and N. Q. Balaban. 2014. Direct observation of single stationary-phase bacteria reveals a surprisingly long period of constant protein production activity. *Proc. Natl. Acad. Sci. U. S. A.* 111:556–61.

58. Gentry, D. R., V. J. Hernandez, L. H. Nguyen, D. B. Jensen, and M. Cashel. 1993. Synthesis of the stationary-phase sigma factor (s) is positively regulated by ppGpp. *J. Bacteriol.* 175:7982–7989.

59. Gibson, A. M., N. Bratchell, and T. A. Roberts. 1988. Predicting microbial growth: growth responses of *salmonellae* in a laboratory medium as affected by pH, sodium chloride and storage temperature. *Int. J. Food Microbiol.* 6:155–178.

60. Gibson, U. E., C. A. Heid, and P. M. Williams. 1996. A novel method for real time quantitative RT-PCR. *Genome Res.* 6:995–1001.

61. Giulietti, a, L. Overbergh, D. Valckx, B. Decallonne, R. Bouillon, and C. Mathieu. 2001. An overview of real-time quantitative PCR: applications to quantify cytokine gene expression. *Methods* 25:386–401.

62. Gnanou Besse, N., N. Audinet, L. Barre, A. Cauquil, M. Cornu, and P. Colin. 2006. Effect of the inoculum size on *Listeria monocytogenes* growth in structured media. *Int. J. Food Microbiol.* 110:43–51.

63. Goni, R., P. García, and S. Foissac. 2009. The qPCR data statistical analysis. *Integromics White Pap.* 1:1–9.

64. Görke, B., and J. Stülke. 2008. Carbon catabolite repression in bacteria: many ways to make the most out of nutrients. *Nat. Rev. Microbiol.* 6:613–24.

65. Gottesman, S. 2005. Micros for microbes: Non-coding regulatory RNAs in bacteria. *Trends Genet.*21(7):399-404.

66. Gruber, T. M., and C. A. Gross. 2003. Multiple sigma subunits and the partitioning of bacterial transcription space. *Annu. Rev. Microbiol.* 57:441–466.

67. Hengge-Aronis, R., and D. Fischer. 1992. Identification and molecular analysis of *glgS*, a novel growth-phase-regulated and *rpoS*-dependent gene involved in glycogen synthesis in *Escherichia coli*. *Mol. Microbiol.* 6:1877–86.

68. Hengge-Aronis, R., W. Klein, R. Lange, M. Rimmele, and W. Boos. 1991. Trehalose synthesis genes are controlled by the putative sigma factor encoded by rpoS and are involved in stationary-phase thermotolerance in *Escherichia coli*. *J. Bacteriol.* 173:7918–7924.

69. Hengge-Aronis, R. 2002. Stationary phase gene regulation: What makes an *Escherichia coli* promoter σS-selective. *Curr. Opin. Microbiol.* 5:591–595.

70. Hengge-Aronis, R. 1993. Survival of hunger and stress: The role of rpoS in early stationary phase gene regulation in *E. coli*. *Cell* 72:165–168.

71. Higgins, J. A, M. C. Jenkins, D. R. Shelton, R. O. N. Fayer, and J. S. Karns. 2001. Rapid extraction of DNA from *Escherichia coli* and *Cryptosporidium parvum* for use in PCR. *AEM*. 67:5321–5324.

72. Higgins, J. A., S. Nasarabadi, J. S. Karns, D. R. Shelton, M. Cooper, A. Gbakima, and R. P. Koopman. 2003. A handheld real time thermal cycler for bacterial pathogen detection. *Biosens. Bioelectron.* 18:1115–1123.

73. Huang, L. 2011. A new mechanistic growth model for simultaneous determination of lag phase duration and exponential growth rate and a new Belehdradek-type model for evaluating the effect of temperature on growth rate. *Food Microbiol.* 28:770–776.

74. Hudson, J. A. 1993. Effect of pre-incubation temperature on the lag time of *Aeromonas hydrophila*. *Lett. Appl. Microbiol.* 16:274–276.

75. Hudson, J. A., and S. J. Mott. 1994. Comparison of lag times obtained from optical density anda viable count data for a strain of *Pseudomonas fragi*. *J. Food Saf.* 14:329–339.

76. Ishihama, A. 2000. Functional modulation of *Escherichia coli* RNA polymerase. *Annu. Rev. Microbiol.* 54:499–518.

77. Ito, A., T. May, K. Kawata, and S. Okabe. 2008. Significance of *rpoS* during maturation of *Escherichia coli* biofilms. *Biotechnol. Bioeng.* 99:1462–1471.

78. Jacob, F., and J. Monod. 1961. Genetic regulatory mechanisms in the synthesis of proteins. *J. Mol. Biol.* 3:318–356.

79. Jay, J. M., M. J. Loessner, and D. A. Golden. 2005. Intrinsic and extrinsic parameters of foods that affect microbial growth, p. 49–51. *In* Mordern food microbiologySeventh. Springer, New York.

80. Jishage, M., A. Iwata, S. Ueda, and A. Ishihama. 1996. Regulation of RNA polymerase sigma subunit synthesis in *Escherichia coli*: Intracellular levels of four species of sigma subunit under various growth conditions. *J. Bacteriol.* 178:5447–5451.

81. Joyce, C. 2002. Quantitative RT-PCR. A review of current methodologies. *Methods Mol. Biol.* 193:83–92.

82. Juers, D. H., B. W. Matthews, and R. E. Huber. 2012. LacZ β-galactosidase: Structure and function of an enzyme of historical and molecular biological importance. *Protein Sci.* 21:1792–1807.

83. Kaasen, I., P. Falkenberg, O. B. Styrvold, and A. R. Strom. 1992. Molecular cloning and physical mapping of the otsBA genes, which encode the osmoregulatory trehalose pathway of *Escherichia coli*: Evidence that transcription is activated by KatF (AppR). *J. Bacteriol.* 174:889–898.

84. Kalnins, A., K. Otto, U. Rüther, and B. Müller-Hill. 1983. Sequence of the *lacZ* gene of *Escherichia coli*. *EMBO J.* 2:593–7.

85. Kennell, D., and H. Riezman. 1977. Transcription and translation initiation frequencies of the *Escherichia coli lac* operon. *J. Mol. Biol.* 114:1–21.

86. Klauck, E., J. Böhringer, and R. Hengge-Aronis. 1997. The LysR-like regulator LeuO in *Escherichia coli* is involved in the translational regulation of rpoS by affecting the expression of the small regulatory DsrA-RNA. *Mol. Microbiol.* 25:559–569.

87. Koch, A. L. 1994. Growth measurement, p. 249–277. *In* Methods for General and Molecular Bacteriology. American Society for Microbiology, Washington. DC.

88. Kolter, R., D. A. Siegele, and A. Tormo. 1993. The stationary-phase of the bacterial life-cycle. *Annu. Rev. Microbiol.* 47:855–874.

89. Kolter, R., D. a. Siegele, and a Tormo. 1993. The stationary phase of the bacterial life cycle. *Annu. Rev. Microbiol.* 47:855–874.

90. Koutsoumanis, K. 2008. A study on the variability in the growth limits of individual cells and its effect on the behavior of microbial populations. *Int. J. Food Microbiol.* Elsevier B.V. 128:116–121.

91. Koutsoumanis, K. P., and J. N. Sofos. 2005. Effect of inoculum size on the combined temperature, pH and aw limits for growth of *Listeria monocytogenes*. *Int. J. Food Microbiol.* 104:83–91.

92. Ladero, M., A. Santos, J. L. Garca, and F. Garca-Ochoa. 2001. Activity over lactose and ONPG of a genetically engineered β-galactosidase from *Escherichia coli* in solution and immobilized: Kinetic modelling. *Enzyme Microb. Technol.* 29:181–193.

93. Lange, R., and R. Hengge-Aronis. 1994. The cellular concentration of the sigma S subunit of RNA polymerase in *Escherichia coli* is controlled at the levels of transcription, translation, and protein stability. *Genes Dev* 8:1600–1612.

94. Lange, R., and R. Hengge-Aronis. 1991. Identification of a central regulator of stationary-phase gene expression in *Escherichia coli*. *Mol. Microbiol.* 5:49–59.

95. Lange, R., D. Fischer, and R. Hengge-Aronis. 1995. Identification of transcriptional start sites and the role of ppGpp in the expression of rpoS, the structural gene for the σ(s) subunit of RNA polymerase in *Escherichia coli*. *J. Bacteriol.* 177:4676–4680.

96. Lederberg, J. 1950. The beta-D-galactosidase of *Escherichia coli*, strain K-12. *J. Bacteriol.* 60:381–392.

97. Lee, S. Y. 1996. High cell-density culture of *Escherichia coli*. *Trends Biotechnol.*14(3):98-105.

98. Lewis, M. 2013. Allostery and the lac operon. *J. Mol. Biol.* Elsevier B.V. 425:2309–2316.

99. Li, Y., J. A. Odumeru, M. Griffiths, and R. C. McKellar. 2006. Effect of environmental stresses on the mean and distribution of individual cell lag times of *Escherichia coli* O157:H7. *Int. J. Food Microbiol.* 110:278–285.

100. Livak, K. J., and T. D. Schmittgen. 2001. Analysis of relative gene expression data using real-time quantitative PCR and the 2(-Delta Delta C(T)) Method. *Methods* 25:402–8.

101. Loewen, P. C., B. Hu, J. Strutinsky, and R. Sparling. 1998. Regulation in the rpoS regulon of *Escherichia coli*. *Can. J. Microbiol.* 44:707–717.

102. Loewen, P. C., and B. L. Triggs. 1984. Genetic mapping of katF, a locus that with katE affects the synthesis of a second catalase species in *Escherichia coli*. *J. Bacteriol.* 160:668–675.

103. Macgregor, G. R., G. P. Nolan, S. Fiering, M. Roederer, and L. a Herzenberg. 1991. Use of *Escherichiu coli (E. coli) lacZ* (β-Galactosidase) as a Reporter Gene. *Methods Mol. Biol.*7:217-235.

104. Madar, D., E. Dekel, A. Bren, A. Zimmer, Z. Porat, and U. Alon. 2013. Promoter activity dynamics in the lag phase of *Escherichia coli*. *BMC Syst. Biol.* 7:136.

105. Majdalani, N., S. Chen, J. Murrow, K. St. John, and S. Gottesman. 2001. Regulation of RpoS by a novel small RNA: The characterization of RprA. *Mol. Microbiol.* 39:1382–1394.

106. Malakar, P. K., D. E. Martens, W. Van Breukelen, R. M. Boom, M. H. Zwietering, and K. Van ’t Riet. 2002. Modeling the interactions of *Lactobacillus curvatus* colonies in solid medium: Consequences for food quality and safety. *Appl. Environ. Microbiol.* 68:3432–3441.

107. Malan, T. P., A. Kolb, H. Buc, and W. R. McClure. 1984. Mechanism of CRP-cAMP activation of *lac* operon transcription initiation activation of the P1 promoter. *J. Mol. Biol.* 180:881–909.

108. McCall, M. N., H. R. McMurray, H. Land, and A. Almudevar. 2014. On non-detects in qPCR data. *Bioinformatics*. Oxford University Press 30:2310–6.

109. McCann, M. P., C. D. Fraley, and A. Matin. 1993. The putative σ factor KatF is regulated posttranscriptionally during carbon starvation. *J. Bacteriol.* 175:2143–2149.

110. McKellar, R. C., and K. Knight. 2000. A combined discrete-continuous model describing the lag phase of *Listeria monocytogenes*. *Int. J. Food Microbiol.* 54:171–180.

111. McMeekin, T. A., J. Olley, D. A. Ratkowsky, and T. Ross. 2002. Predictive microbiology: Towards the interface and beyond. *Int. J. Food Microbiol.* 73:395–407.

112. McMeekin, T. A., and T. Ross. 2002. Predictive microbiology: Providing a knowledge-based framework for change management. *Int. J. Food Microbiol.*78(1-2):133-153.

113. Mellefont, L. A., and T. Ross. 2003. The effect of abrupt shifts in temperature on the lag phase duration of *Escherichia coli* and *Klebsiella oxytoca*. *Int. J. Food Microbiol.* 83:295–305.

114. Métris, A., Y. Le Marc, A. Elfwing, A. Ballagi, and J. Baranyi. 2005. Modelling the variability of lag times and the first generation times of single cells of *E. coli*. *Int. J. Food Microbiol.*100(1-3):13-19.

115. Miller, J. H. 1972. Assay of β-galactosidase, p. 352–355. *In* Experiments in Molecular Genetics. Cold Spring Harbor Laboratory, Cold Spring Harbor, NY.

116. Monod, J. 1949. The Growth of Bacterial Cultures. *Annu. Rev. Microbiol.* 3:371–394.

117. Muffler, A, M. Barth, C. Marschall, and R. Hengge-Aronis. 1997. Heat shock regulation of sigmaS turnover: a role for DnaK and relationship between stress responses mediated by sigmaS and sigma32 in *Escherichia coli*. *J. Bacteriol.* 179:445–452.

118. Muffler, A., D. Fischer, S. Altuvia, G. Storz, and R. Hengge-Aronis. 1996. The response regulator RssB controls stability of the sigma(S) subunit of RNA polymerase in *Escherichia coli*. *EMBO J.* 15:1333–9.

119. Muffler, A., D. Fischer, and R. Hengge-Aronis. 1996. The RNA-binding protein HF-I, known as a host factor for phage Q RNA replication, is essential for rpoS translation in *Escherichia coli*. *Genes Dev.* 10:1143–1151.

120. Müller, M. 1895. Ueber den Einfluss von Fiebertemperaturen auf die Wachsthumsgeschwindigkeit und die Virulenz des Typhusbacillus. *Zeitschrift für Hyg. und Infect.* Springer-Verlag 20:245–280.

121. Mulvey, M. R., and P. C. Loewen. 1989. Nucleotide sequence of kat F of *Escherichia coli* suggests Kat F protein is a novel σ transcription factor. *Nucleic Acids Res.* 17:9979–9991.

122. Navarro Llorens, J. M., A. Tormo, and E. Martenez-Garcua. 2010. Stationary phase in gram-negative bacteria. *FEMS Microbiol. Rev.*34(4):476-495.

123. Noriega, E., A. Laca, and M. Diaz. 2009. *Listeria* growth under diffusional limitations in synthetic meats. *Int. J. Food Sci. Technol.* 44:725–734.

124. Noriega, E., A. Laca, and M. Diaz. 2008. Modelling of diffusion-limited growth to predict *Listeria* distribution in structured model foods. *J. Food Eng.* 87:247–256.

125. NOVICK, A. 1955. Growth of bacteria. *Annu. Rev. Microbiol.* 9:97–110.

126. Nyström, T. 2004. Stationary-Phase Physiology. *Annu. Rev. Microbiol.* 58:161–181.

127. Pabinger, S., S. Rödiger, A. Kriegner, K. Vierlinger, and A. Weinhäusel. 2014. A survey of tools for the analysis of quantitative PCR (qPCR) data. *Biomol. Detect. Quantif.* 1:23–33.

128. Panikov, N. S. 2010. Kinetics, Microbial Growth. *Encycl. Ind. Biotechnol.* 1513–1543.

129. Perni, S., P. W. Andrew, and G. Shama. 2005. Estimating the maximum growth rate from microbial growth curves: Definition is everything. *Food Microbiol.* 22:491–495.

130. Peter J Mcclure,Martin Barry Cole, K W Davies, W. A. A. 1993. The use of automated tubidimetric data for the construction of kinetic models. *J. Ind. Microbiol. Biotechnol.* 12:277–285.

131. Pfaffl, M. 2004. Quantification strategies in real-time PCR Michael W . Pfaffl. *A-Z Quant. PCR* 87–112.

132. Poschet, F., K. Bernaerts, A. H. Geeraerd, N. Scheerlinck, B. M. Nicolai, and J. F. Van Impe. 2004. Sensitivity analysis of microbial growth parameter distributions with respect to data quality and quantity by using Monte Carlo analysis. *Math. Comput. Simul.* 65:231–243.

133. Prats, C., D. Lopez, A. Giro, J. Ferrer, and J. Valls. 2006. Individual-based modelling of bacterial cultures to study the microscopic causes of the lag phase. *J. Theor. Biol.*241(4):939-953.

134. Presser, K. A., T. Ross, and D. A. Ratkowsky. 1998. Modelling the growth limits (growth/no growth interface) of *Escherichia coli* as a function of temperature, pH, lactic acid concentration, and water activity. *Appl. Environ. Microbiol.* 64:1773–1779.

135. Ratkowsky,D. A., Ross,T., McMeekin,T. A., and Olley,J. 1991. Comparison of Arrhenius-type and Belehradek-type models for prediction of bacterial growth in foods. *J. Appl. Microbiol.* 71:452–459.

136. Ratkowsky, D. A., J. Olley, T. A. Mcmeekin, and A. A. Ball3. 1982. Relationship between temperature and growth rate of bacterial cultures. *J. Bacteriol.* 149:1–5.

137. Ratkowsky, D. A., R. K. Lowry, T. A. McMeekin, A. N. Stokes, and R. E. Chandler. 1983. Model for bacterial culture growth rate throughout the entire biokinetic temperature range. *J. Bacteriol.* 154:1222–1226.

138. Ratkowsky, D. A., J. Olley, T. A. McMeekin, and A. Ball. 1982. Relationship between temperature and growth rate of bacterial cultures. *J. Bacteriol.* 149:1–5.

139. Repoila, F., N. Majdalani, and S. Gottesman. 2003. Small non-coding RNAs, co-ordinators of adaptation processes in *Escherichia coli*: The RpoS paradigm. *Mol. Microbiol.*48(4):855-861.

140. Rich, P. R. 2003. The molecular machinery of Keilin's respiratory chain. *Biochem. Soc. Trans.* 31:1095–1105.

141. Robinson, T. P., O. O. Aboaba, A. Kaloti, M. J. Ocio, J. Baranyi, and B. M. Mackey. 2001. The effect of inoculum size on the lag phase of *Listeria monocytogenes*. *Int. J. Food Microbiol.* 70:163–173.

142. Robinson, T. P., M. J. Ocio, A. Kaloti, and B. M. MacKey. 1998. The effect of the growth environment on the lag phase of *Listeria monocytogenes*. *Int. J. Food Microbiol.* 44:83–92.

143. Rolfe, M. D., C. J. Rice, S. Lucchini, C. Pin, A. Thompson, A. D. S. Cameron, M. Alston, M. F. Stringer, R. P. Betts, J. Baranyi, M. W. Peck, and J. C. D. Hinton. 2012. Lag phase is a distinct growth phase that prepares bacteria for exponential growth and involves transient metal accumulation. *J. Bacteriol.* 194:686–701.

144. Romano, A. H., and T. Conway. 1996. Evolution of carbohydrate metabolic pathways. *Res Microbiol.* 147(6-7):448-455.

145. Romeo, T., and J. Preiss. 1989. Genetic regulation of glycogen biosynthesis in *Escherichia coli*: in vitro effects of cyclic AMP and guanosine 5'-diphosphate 3'-diphosphate and analysis of in vivo transcripts. *J. Bacteriol.* 171:2773–2782.

146. Ross, T., D. A Ratkowsky, L. A Mellefont, and T. A McMeekin. 2003. Modelling the effects of temperature, water activity, pH and lactic acid concentration on the growth rate of *Escherichia coli*. *Int. J. Food Microbiol.* 82:33–43.

147. Ross, T., and T. A. McMeekin. 1994. Predictive microbiology. *Int. J. Food Microbiol.* 23:241–264.

148. Rosso, L., J. R. Lobry, and S. Bajard. 1995. Convenient model to describe the combined effects of temperature and pH on microbial growth. *Appl. Environ. Microbiol.* 61:610–616.

149. Schellhorn, H. E., and V. L. Stones. 1992. Regulation of katF and katE in *Escherichia coli* K-12 by weak acids. *J. Bacteriol.* 174:4769–4776.

150. Schultz, D., and R. Kishony. 2013. Optimization and control in bacterial Lag phase. *BMC Biol.* 11:120.

151. Schweder, T., K. H. O. Lee, O. Lomovskaya, and A. Matin. 1996. Regulation of *Escherichia coli* starvation sigma factor (σs) by ClpXP protease. *J. Bacteriol.* 178:470–476.

152. Shiba, T., K. Tsutsumi, H. Yano, Y. Ihara, a Kameda, K. Tanaka, H. Takahashi, M. Munekata, N. N. Rao, and a Kornberg. 1997. Inorganic polyphosphate and the induction of rpoS expression. *Proc. Natl. Acad. Sci. U. S. A.* 94:11210–11215.

153. Siegele, D. A., and R. Kolter. 1992. Life after log. *J. Bacteriol.*174(2):345-348.

154. Sledjeski, D. D., A Gupta, and S. Gottesman. 1996. The small RNA, DsrA, is essential for the low temperature expression of RpoS during exponential growth in *Escherichia coli*. *EMBO J.* 15:3993–4000.

155. Smelt, J. P. P. M., G. D. Otten, and A. P. Bos. 2002. Modelling the effect of sublethal injury on the distribution of the lag times of individual cells of *Lactobacillus plantarum*. *Int. J. Food Microbiol.* 73:207–212.

156. Soboleva, T. K., A. B. Pleasants, and G. Le Roux. 2000. Predictive microbiology and food safety. *Int. J. Food Microbiol.* 57:183–192.

157. Solberg, M., and J. T. R. Nickerson. 1963. A biological after-effect in radiation-processed chicken muscle. *J. Food Sci.* 28(3):243–244.

158. Solopova, A., H. Bachmann, B. Teusink, J. Kok, A. R. Neves, and O. P. Kuipers. 2012. A specific mutation in the promoter region of the silent cel cluster accounts for the appearance of lactose-utilizing *Lactococcus lactis* MG1363. *Appl. Environ. Microbiol.* 78:5612–5621.

159. Standaert, A. R., K. Francois, F. Devlieghere, J. Debevere, J. F. Van Impe, and A. H. Geeraerd. 2007. Modeling individual cell lag time distributions for *Listeria monocytogenes*. *Risk Anal.* 27:241–254.

160. Swinnen, I. A. M., K. Bernaerts, E. J. J. Dens, A. H. Geeraerd, and J. F. Van Impe. 2004. Predictive modelling of the microbial lag phase: A review. *Int. J. Food Microbiol.* 94:137–159.

161. Vadasz, P., and A. S. Vadasz. 2007. Biological implications from an autonomous version of Baranyi and Roberts growth model. *Int. J. Food Microbiol.* 114:357–365.

162. van Derlinden, E., L. Mertens, and J. F. van Impe. 2013. The impact of experiment design on the parameter estimation of cardinal parameter models in predictive microbiology. *Food Control*. Elsevier Ltd 29:300–308.

163. Venturi, V. 2003. Control of rpoS transcription in *Escherichia coli* and *Pseudomonas*: Why so different? *Mol. Microbiol.* 49:1–9.

164. Verhulst, A. J., A. M. Cappuyns, E. Van Derlinden ., K. Bernaerts, and J. F. Van Impe. 2011. Analysis of the lag phase to exponential growth transition by incorporating inoculum characteristics. *Food Microbiol.* Elsevier Ltd 28:656–666.

165. Vijayakumar, S. R. V, M. G. Kirchhof, C. L. Patten, and H. E. Schellhorn. 2004. RpoS-regulated genes of *Escherichia coli* identified by random lacZ fusion mutagenesis. *J. Bacteriol.* 186:8499–8507.

166. Vinuselvi, P., M. K. Kim, S. K. Lee, and C. M. Ghim. 2012. Rewiring carbon catabolite repression for microbial cell factory. *BMB Rep.* 45:59–70.

167. Vollmer, M., E. Nagele, and P. Horth. 2003. Differential proteome analysis: two-dimensional nano-lc/ms of *E. coli* proteome grown on different carbon sources. *J Biomol Tech* 14:128–135.

168. Whiting, R.C., Buchanan, R. L. 1993. A classification of models for predictive microbiology. *Food Microbiol.* 10:175–177.

169. Whiting, R. C. 1995. Microbial modeling in foods. *Crit. Rev. Food Sci. Nutr*.35(6):464-494.

170. Whiting, R. C., and L. K. Bagi. 2002. Modeling the lag phase of *Listeria monocytogenes*. *Int. J. Food Microbiol.*73(2-3):291-295.

171. Widdel, F. 2007. Theory and measurement of bacterial growth. *Di dalam Grundpraktikum Mikrobiol.* 1–11.

172. William, B., and J. A. S. Penfold. 1914. on the Nature of Bacterial Lag . *Journal of Hygiene*. 14(2):215-241.

173. Wong, P., S. Gladney, and J. D. Keasling. 1997. Mathematical model of the *lac* operon: Inducer exclusion, catabolite repression, and diauxic growth on glucose and lactose. *Biotechnol. Prog.* 13:132–143.

174. Wu, Y., M. W. Griffiths, and R. C. McKellar. 2000. A comparison of the bioscreen method and microscopy for the determination of lag times of individual cells of *Listeria monocytogenes*. *Lett. Appl. Microbiol.* 30:468–72.

175. Yamashino, T., C. Ueguchi, and T. Mizuno. 1995. Quantitative control of the stationary phase-specific sigma factor, sigma S, in *Escherichia coli*: involvement of the nucleoid protein H-NS. *EMBO J.* 14:594–602.

176. Zwietering, M. H., I. Jongenburger, F. M. Rombouts, and K. van 't Riet. 1990. Modeling of the bacterial growth curve. *Appl. Environ. Microbiol.* 56:1875–1881.

177. Zwietering, M. H., J. T. D. E. Koos, B. E. Hasenack, J. C. D. E. Wit, and K. V. A. N. T. Riet. 1991. Modeling of Bacterial Growth Function of Temperature. *Appl Environ Microbiol.* 57(4):1094–1101.